Technical Report (DLR Contract 50EE0507) TN-IUP-SCIACO2CH7-001

Initial study on CO_2 column density retrieval using SCIAMACHY channel 7 nadir measurements

Final version (25th April 2006)

Institute of Environmental Physics (IUP)
University of Bremen, FB1

Bremen, Germany

Authors:

Dr. Michael Buchwitz	IUP-Bremen	Michael.Buchwitz@iup.physik.uni-bremen.de
Dr. Rüdiger de Beek	IUP-Bremen	Ruediger.de_Beek@iup.physik.uni-bremen.de
Dr. Marco Bruns	IUP-Bremen	Marco.Bruns@iup.physik.uni-bremen.de
Dipl. Phys. Oliver Schneising	IUP-Bremen	Oliver.Schneising@iup.physik.uni-bremen.de

Inmitten von Schwierigkeiten liegen günstige Gelegenheiten.

Albert Einstein (1879 – 1955)

Contents

1 Executive summary

1.1 Extended abstract

Atmospheric concentrations of carbon dioxide (CO_2) are increasing since the beginning of the industrial revolution mostly due to burning of fossil fuels. As CO_2 is a radiatively active gas (a so called greenhouse gas) this results in an increase of the average temperature of the lower atmosphere and associated change of other climate parameters. In order to make reliable predictions of the future climate it is important to have a good understanding of the sources and sinks of CO_2. Whereas the anthropogenic part of the CO_2 fluxes (emissions) is relatively well known from economic statistical data (within about 10%) the uncertainties of regional (continents, ocean basins) natural fluxes are very large (typically 100%). The natural fluxes are typically much larger (by about one order of magnitude) than the anthropogenic fluxes and show a large variability from year to year. Currently about half of the CO_2 emitted by mankind every year is taken up by natural sinks: about 50% is stored in the oceans and about 50% is taken up by terrestrial vegetation. It is expected that this may change in the future because sinks can saturate and because CO_2 uptake and release depends on the climatic conditions. As the natural fluxes are large, a small change of the natural fluxes can result in an effective emission that is larger than the emitted anthropogenic CO_2. What is needed is a better understanding of regional (e.g., 1000×1000 km^2) natural carbon sources and sinks globally: Where are they? What are their characteristics (strength, seasonal dependence, response to climate change, etc.)?

To address these important questions dedicated CO_2 satellite missions are planed for the near future: OCO/USA and GOSAT/Japan. Both are foreseen for launch at the end of 2008. OCO and GOSAT will perform nadir measurements of spectra in the near-infrared spectral region covering absorption bands of CO_2 and O_2 also covered by SCIAMACHY. SCIAMACHY is not a dedicated CO_2 mission but performs similar measurements as planned for OCO and GOSAT which are optimized for CO_2 in terms of, e.g., better spectral and spatial resolution. For example, the spatial resolution of OCO is 1×1.5 km^2 to obtain high probability for cloud free pixels. According to OCO studies it is necessary to simultaneously record spectra in three bands in order to get the desired accuracy and precision for the main OCO data product which is the dry air column averaged mixing ratio of CO_2, denoted XCO_2 (basically the ratio of the CO_2 column and the dry air column obtained from O_2): around 760 nm for O_2 (corresponding to SCIAMACHY channel 4), and at 1.6 μm and 2.0 μm for CO_2 (corresponding to SCIAMACHY channels 6 and 7). Because SCIAMACHY is the first instrument that performs these type of measurements SCIAMACHY plays a pioneering role in this new area of satellite remote sensing. The retrieval of CO_2 from satellites is however a challenging task because of demanding accuracy and precision requirements.

SCIAMACHY channel 7 was designed to be the main channel for CO_2 retrieval. After launch it was found out that channel 7 suffers from two unexpected problems that significantly add to the complexity of high precision and low bias CO_2 retrieval: a varying ice-layer on the detector which increases the noise and changes the slit function and a light-leak that adds a variable signal to the spectral measurements. Because of these problems prior to this study no detailed attempts have been undertaken to retrieved CO_2 from channel 7. Instead it was considered more promising with the limited resources available for CO_2 retrieval to retrieve CO_2 from channel 6 although the spectral resolution of channel 6 is quite low and does not permit a very accurate retrieval. For example, channel 7 enables (at least theoretically) to separate between CO_2 and aerosol effects due to its mixture of strong and weak CO_2 lines and its quite high spectral resolution. This is not possible for channel 6. Nevertheless, quite promising initial results of CO_2 from SCIAMACHY channel 6 have been published, indicating, for example, that SCIAMACHY can detect broad scale features of uptake and release of CO_2 due to vegetation. Comparisons with global model simulations have shown reasonable agreement for example with respect to the time dependence of the seasonal cycle of CO_2. The measured spatio-temporal variability of CO_2 is however significantly larger (about a factor of 2–6) than the variability of the model field. The reason for this is under investigation. Because of the limited number of ground stations that measure column averaged CO_2 it was not possible to clarify this until now. From the error analysis of the SCIAMACHY measurements it is estimated that the error of the currently used initial retrieval algorithm based on channel 6 is about several percent, i.e., larger that the requirement of about 1%. This means that the estimated error is on the order of or even larger than the weak CO_2 signal that needs to be detected. This makes the interpretation of the measurements difficult. A large number of error sources contribute to the overall error and algorithm improvements are needed in order to generate a CO_2 data product with better accuracy and precision.

This study permitted for the first time to investigate SCIAMACHY channel 7 CO_2 retrieval in some detail. The main question to be answered after six months (i.e., after stage 1 of this study) is: Is channel 7 useful for CO_2 retrieval? If yes: Is it possible to specify an operational retrieval algorithm in a (not yet approved) stage 2 of the study? This report summarizes the work performed during stage 1 of this study.

To answer the main question within the time constraints of the study the following tasks were performed:

Requirements for the CO_2 column measurements had been defined based on the IGOS/IGACO report: Threshold single pixel measurements precision: 3% (goal: 1%). Threshold accuracy: 2% (goal: 1%). For verification the SCIAMACHY channel 7 CO_2 columns were compared with reference data: global model simulations, the WFM-DOAS version 0.4 CO_2 data product derived from channel 6, and ground based FTS measurements. An existing retrieval algorithm (WFM–DOAS version 0.4) had been adjusted for SCIAMACHY channel 7 CO_2 retrievals. An initial error budget for this algorithm has been established. The spectral fitting window to be investigated was defined to be the (pre-launch) recommended operational window 2030-2040 nm (detailed fitting window studies were not possible within the time constraints of the study). A literature survey has been performed to get an overview about known channel 7 issues. For each issue an estimate of the corresponding CO_2 error has been derived. The retrieval algorithm has been applied to real SCIAMACHY channel 7 data. The results have been compared with the reference data. Focus was on identifying the individual error components in the retrieved CO_2 and to verify if the errors have the expected magnitude and characteristics. The main results of this error analysis are given in Tab. 1. Column "Existing initial algorithm / Channel 7" lists the individual channel 7 specific and non-specific errors for CO_2 retrieval for cloud free measurements over land.

As can be seen, the three dominating channel 7 specific error sources are: light-leak (7%), ice-layer (20%), and undetected dead/bad pixel (8%). The errors given for the light-leak and the ice-layer are to be understood as the maximum errors that can occur if no special means are implemented for correction. The 20% error due to the ice-layer has been observed in 2003 during a time period when a large ice-layer was formed on the channel 7 detector using a retrieval algorithm without any correction for ice. On the other hand, during the entire year 2005, for example, the channel 7 throughput is close to 1.0, i.e., there is no detectable ice-layer and therefore no or only a very small error due to the ice-layer. The 8% error for undetected dead/bad pixels is a rough estimate. It still needs to be verified if the existing algorithms for detecting dead/bad pixels are able to reliably detect all dead/bad pixels in the spectral regions used for CO_2 retrieval or if these algorithms need optimization. It is expected that this error can be reduced to well below 1% after careful optimization. The issue is the following: Channel 7 contains a significant amount if dead/bad pixels (several hundred) that need to be reliably identified in order to make sure that they are not used for retrieval. Even a single undetected dead/bad pixel can result in a large error. Several algorithms have been developed or are under development to identify dead/bad pixels, most notably the algorithm developed by SRON which provides a pixel mask for each orbit based on analyzing the orbital dark signal measurements. If the existing algorithms that generate pixel masks are appropriate for accurate CO_2 retrieval from channel 7 still needs to be assessed. The pixel mask issue is complex because the number of dead/bad pixels changes with time (on average the number of dead/bad pixels in channel 7 increases by about 60 pixels per year), a single undetected pixel can introduce a large errors, and a new dead/bad pixel can occur during an orbit and may not be flagged as dead/bad in the pixel mask file of this orbit.

SCIAMACHY CO2 column retrieval error budget for cloud free scenes over land

Error source	Error type*) (random/system.) fraction random	CO2 error [%] Existing initial algorithm		Improved algo. (estimate)		Comments / proposed improvements
		Channel 6	Channel 7	Best case	Worst case	
Instrument noise	1,0	1,0	0,5	0,5	1,0	Purely random; determined by fitting window
Light leak	0,5	0,0	**7,0**	1,0	3,0	(i) Determine light leak from saturated CO2 lines
Ice layer	0,1	0,0	**20,0**	0,5	2,0	(i) Determine slit function (solar, line lamp, nadir) (ii) Use correction based on throughput analysis (iii) Use only ice free time periodes
Undetected dead/bad pixel	0,9	**4,0**	**8,0**	0,5	2,0	(i) Verify time dependent pixel masks (e.g. SRON) if not appropriate for CO2 (ii) optimize existing algorithm
Non-linearity (residual error)	0,9	0,5	0,5	0,5	0,5	Residual error after non-linearity correction (probably difficult to improve)
Dark signal (residual error)	0,1	0,1	0,2	0,1	0,2	Residual error after dark signal correction (probably difficult to improve)
Albedo	0,2	**4,0**	**4,0**	0,5	1,0	(i) Estimation of (effective) albedo from spectrum & e.g. extended look-up table
Aerosols	0,5	**6,0**	**6,0**	1,0	3,0	(i) Better consideration of aerosols in retrieval (e.g. add aerosol w/f to fit - potential solution for chan. 7) (ii) Via effective albedo
Subvisual cirrus	0,2	2,0	2,0	1,0	2,0	(i) See aerosols (ii) Improved detection and rejection
Temperature & humidity	0,5	2,0	2,0	0,5	1,0	(i) Use of meteorological data (ECMWF)
Surface pressure	0,5	**3,0**	**3,0**	0,5	1,0	(i) Use of meteorological data (ECMWF)
Scan	0,2	1,0	1,0	0,2	0,5	(i) Better consideration in radiative transfer
Total random error [%]:		5,2	9,0	**1,1**	**3,1**	Required precision: Threshold < 3%; Target < 1%
Total system. error [%]:		5,1	19,0	**1,3**	**3,4**	Required accuracy: Threshold < 2%; Target < 1%

**) value X means: fraction X of error is random (precision) and 1-X systematic (accuracy), 0.2 means: 20% random and 80% systematic*

Maximum error & without any correction
Rough estimate, to be assessed in detail
Maximum error, currently only first order corrections

Table 1: Initial SCIAMACHY CO_2 error budget. The different error sources investigated are listed in the first column. The second column specifies an estimate of the type of each error in terms of the fraction of the random component of this error and 1 minus this fraction is assumed to be systematic (example: if "fraction random" is X = 0.2 this means that 20% of the errors listed in columns 3–6 is assumed to be the random component of this error and the fraction 1-X, in this case 80%, is assumed to be systematic contributing to the measurement accuracy). It is assumed that the individual errors can be summed up in root-sum-square manner to given the overall error (listed in the two bottom rows where they are compared with the requirements). Column 3 lists the errors for current channel 6 CO_2 retrievals using WFM–DOAS version 0.4. Column 4 lists the errors for the initial channel 7 CO_2 retrievals performed during this study. Note that the channel 7 error for the ice-layer is the maximum error that occurs under certain conditions and if no correction is performed. The channel 7 error for undetected dead/bad pixels is a rough estimate. It still needs to be verified if the existing algorithms for detecting dead/bad pixels are appropriate for CO_2 retrieval. "Improved algo. (estimate)" lists a range of errors (best case, worse case) that most likely can be achieved after implementing the proposed improvements listed in the last column.

Table 1 shows that the existing initial algorithm applied to channel 7 results in CO_2 errors which are significantly larger than the requirements. As already described, the errors for the light-leak and the ice-layer are maximum values that occur under certain conditions and if NO correction is performed - the initial algorithm does not contain any special means to correct for these channel 7 specific errors. Correction procedures are under development but not yet implemented and finally assessed.

Although the errors obtained using channel 6 - which does not suffer from a light leak and an ice layer - are significantly smaller, they exceed the required threshold precision and accuracy. Also for channel 6 the reliable detection of dead/bad pixels needs to be verified and the sensitivity of the algorithm with respect to albedo, aerosols, etc., needs to be reduced.

Several of the errors can be reduced by extending the currently used look-up table scheme or by using on-line radiative transfer simulations (which would be the most flexible and accurate approach). One of the most important challenges in improving the retrieval algorithm is to improve the accuracy and precision without significantly reducing its speed. Currently the algorithm is very fast, significantly faster than real time. But using for example on-line radiative transfer simulations including line absorption and multiple scattering will increase the time needed for retrieval by many orders of magnitude and can easily reach several minutes per spectrum which is barely acceptable with more than 1000 measurements per hour.

This study indicates that accurate and precise satellite CO_2 retrieval is a challenging task which is further complicated by various issues related to SCIAMACHY's near infrared channels, especially issues related to channel 7. Several error sources have been investigated and quantified. The development of solutions especially for the channel 7 specific problems is however in its early stage. With the currently existing algorithm it is not possible to achieve the required accuracy and precision. Solutions for all error sources have been proposed and initial work on solutions for channel 7 specific problems has been performed during this study. Despite the progress a significant amount of work is still needed in order to achieve a precision and accuracy better than the threshold requirements. It is highly unlikely that all problems can be solved within a couple of month or even within one year. This means that in the near future (e.g., next year) it will not be possible to specify an operational algorithm that is capable of producing a CO_2 data product that fulfills user needs.

There is significant room for improvement of the currently existing initial (rather simple) algorithm. Some of the errors (e.g., due to albedo and surface pressure) are due to a rather simplified treatment in the current look-up table scheme and can be reduced for example by extending the look-up table in combination with appropriate interpolation schemes. There is however significant uncertainty of what can finally be achieved. This is reflected by the best case / worse case range in Tab. 1. Of course, the more time one can spend on improvements, the better the results. The time available is however limited by the launch of the dedicated CO_2 satellite missions OCO and GOSAT which are supposed to be launched end of 2008. Concerning satellite CO_2 retrieval SCIAMACHY would be a great success if a multi-year data set can be generated prior to the launch of OCO and GOSAT with a quality high enough for initial inverse modeling, if not globally than at least for certain interesting regions such as the boreal forests or the tropics. The error estimates for the improved algorithm given in Tab. 1 are based on assuming that two persons are working in parallel on improving the existing algorithm during a time period of about two years. A very useful CO_2 data set would be a multi-year CO_2 data available in two years (beginning of 2008) with globally or at least regionally precisions and accuracies better that the worse case values given in Tab. 1.

In summary:

In this study the first detailed investigation of CO_2 retrieval from SCIAMACHY channel 7 has been performed. Although channel 7 has been designed to be the main CO_2 channel, investigations prior to this study focussed on channel 6 because of a number of channel 7 issues (e.g., light leak, ice layer). The following tasks have been performed in this study: An existing retrieval algorithm has been adjusted to channel 7, a large data set has been processed with this algorithm, the results have been analyzed and errors have been quantified. Several main problems have been iden-

tified and their impact on the CO_2 retrieval has been estimated. The three most important error sources are: (i) light leak, (ii) changing slit function due to varying ice layer, and (iii) increasing number of dead and bad detector pixels. At least one solution per problem has been proposed and initial studies on solutions have been performed. The issues are however quite complex and the development of reliable solutions time consuming. Therefore, the development of solutions for the channel 7 issues is still in its early stage. A significant amount of further study is needed before an accurate CO_2 retrieval from channel 7 is possible. Even if these channel 7 specific problems can be solved there still exists a significant number of relatively minor but still significant errors that need to be minimized, e.g., errors due to atmospheric temperature, pressure and aerosol variability and second order albedo effects. Currently, the most promising CO_2 is retrieved from channel 6 which does not suffer from the problems that currently prevent accurate retrieval of CO_2 from channel 7. As long as it has not been demonstrated that the channel 7 problems have been solved by verifying that the proposed solutions are good enough for accurate CO_2 retrieval it is recommended to focus on the currently much more promising channel 6.

1.2 Background information

Carbon dioxide (CO_2) is the most important anthropogenic greenhouse gas and increasing atmospheric concentrations - mainly due to burning of fossil fuels - are expected to result in a warmer climate with adverse consequences such as rising sea levels and an increase of extreme weather conditions.

Atmospheric CO_2 has increased from about 280 ppmv at pre-industrial times to more than 370 ppmv today mostly due to burning of fossil fuels but also due to cement production and land use changes. In order to reliably predict future concentrations of CO_2 and associated climate change it is necessary, among many other aspects (e.g., reliable projection of economical developments), to have a good understanding of the natural carbon cycle, especially of the (natural) carbon fluxes into and out of the atmosphere. The natural terrestrial and marine carbon exchange with the atmosphere is significantly larger than anthropogenic CO_2 emissions (by about one order of magnitude) and shows a large year-to-year variability due to a complex and not well understood dependence on climate (temperature, humidity, etc.). A small perturbation, e.g. due to changing climatic conditions, may result in changes of the natural fluxes which are larger than the direct anthropogenic CO_2 emissions. Currently, the marine and terrestrial carbon “reservoirs” are a net sink for anthropogenic CO_2 emissions: on average they take up about 50% of the emitted CO_2. It is however expected that these sinks will show saturation effects in the future and may even change to a net source at some point (depending on the future climate). Currently there are large uncertainties in our understanding of the natural CO_2 sources and sinks: Where are the sources and sinks? What are their characteristics? How do they respond to a changing climate?

SCIAMACHY onboard ENVISAT is the first satellite instrument that has the potential to significantly improve our understanding of (terrestrial) CO_2 surface sources and sinks. This is because SCIAMACHYs near-infrared nadir observations are highly sensitive to CO_2 concentration changes at all atmospheric altitude levels including the important boundary layer where the CO_2 source/sink signal is largest. This is a clear advantage of SCIAMACHY compared to other nadir sensors such as AIRS/AQUA (or IASI/Metop) which measure (or will measure) in the thermal infrared part of the spectrum which has intrinsically low sensitivity for the lower part of the troposphere and therefore can contribute only little to better constraining regional source/sink uncertainties.

SCIAMACHY is not a dedicated CO_2 mission such as the planned OCO (NASA) and GOSAT (Japan) missions (both to be launched in late 2008) but performs similar measurements as proposed for OCO and GOSAT (albeit with worse spatial and somewhat worse spectral resolution). Therefore, SCIAMACHY plays an important pioneering role in this new area of satellite remote sensing of CO_2.

Currently, our information on CO_2 surface sources and sinks on the global scale is obtained by inverting ("inverse modeling") the highly precise but sparse measurements of networks (e.g. NOAA/CMDL) of (mainly flask sampling) ground stations (complemented by ships and aircraft). From these measurements net surface fluxes for very large regions (entire continents and ocean basins) with large uncertainties (typically 100%) can be derived. For many regions it is currently not clear if they are a net sink or a net source.

Satellite measurements have the potential to overcome the limitations of the ground based networks. This however requires high precision and low bias CO_2 (column) measurements. It has been shown that SCIAMACHY can significantly improve our knowledge concerning CO_2 sources and sinks if a measurement precision close to the theoretical limit ($\sim$1%) can be reached and no significant biases are introduced. These are very challenging requirements for both Level 0–1 processing (calibration) and Level 1–2 processing (inversion of the spectra to obtain CO_2 information).

1.3 Study overview

SCIAMACHY channel 7 was planned to be the main CO_2 channel. Channel 7 covers two strong absorption bands of CO_2 with a quite high spectral resolution of 0.23 nm or 0.6 cm^{-1} (resolving power 10000) such that some fine structure of the CO_2 bands are resolved. Channel 6 covers three relatively week CO_2 bands. This study is the first study where CO_2 retrieval from channel 7 has been investigated in detail. Prior to this study CO_2 retrieval focused on SCIAMACHY channel 6. Because of limited resources priorities had to be established and channel 6 was considered more promising to provide first interesting results compared to channel 7. Channel 7 was considered much more challenging because of a number of channel 7 specific problems that were expected to complicate accurate CO_2 retrieval. Channel 7 suffers from three problems which are not present (or not so severe) in channel 6: (i) a changing ice layer on the detector resulting and signal (throughput) loss with corresponding increase of the noise level and a changing slit function introducing systematic errors, (ii) a light leak resulting in a variable spectral offset, and (iii) a large number of dead and bad pixels (also present in the part of channel 6 called channel 6+) which increases with time. All these issues further complicate the accurate retrieval of CO_2 columns from the SCIAMACHY nadir spectra. A task that would even be a challenge without these complications because of the high precision/accuracy requirements but also because of the characteristics of the near-infrared detectors (high and variable dark signals, inhomogeneous and time dependent detector characteristics, etc.).

The goal of this study is to perform an initial assessment of CO_2 retrieval using SCIAMACHY channel 7. The main question to be answered by this study is: To what extent is it possible to retrieve CO_2 information from channel 7? This question shall be answered after the first six month of this study, i.e., end of February 2006 (the study started beginning of September 2005).

To answer this question requirements need to be formulated and the achieved quality of the retrieved CO_2 has to be compared with the requirements in order to judge if a useful CO_2 retrieval is possible at some stage. The requirements are: The to be achieved single pixel measurements threshold precision is **3%** (target precision: 1%) and the to be achieved threshold accuracy is **2%** (target accuracy: 1%).

In order to judge which quality has been achieved the retrieved CO_2 needs to be compared with reference data of known and good quality. This however is not a trivial task because CO_2 column measurements are sparse. For this study the CO_2 retrieved from channel 7 has been compared with three different types of reference data: (i) with global model simulations, (ii) with the initial (= latest)

WFM-DOAS version 0.4 CO_2 data product derived from SCIAMACHY channel 6, and (iii) with ground based FTS CO_2 measurements.

Because of the time constraints priorities had to be established. Out of the scope of this study was the development of a new retrieval algorithm (e.g., Optimal Estimation with on-line radiative transfer simulations) nor detailed spectral fitting window studies. It was decided to perform the channel 7 CO_2 retrievals with an existing retrieval algorithm (WFM-DOAS version 0.4) adjusted to channel 7. The fitting window to be investigated is the spectral region 2030–2040 nm, a spectral region that has been recommended pre-flight. The corresponding "cluster" has an integration time of typically 0.5 s corresponding to a ground pixel size of 30$\times$120 km^2. Selecting a different (e.g., larger) fitting window would mean doubling the size of the ground pixel which would result in, for example, a reduced number of cloud free ground pixels.

The following tasks have been performed in this study:

- A literature survey on channel 7 issues has been performed to get an overview about the work that has been performed prior to this study.
- The relationship between errors on the spectrum ("signal errors", "radiance errors") and CO_2 column errors has been established to transform spectral radiance errors into CO_2 column errors. A simple formula has been derived that translates signal errors which are typically specified in binary units (BU) into a percentage CO_2 column retrieval error.
- Based on the literature survey several radiance error sources have been identified and the resulting CO_2 errors have been quantified and characterized. The magnitudes of the individual CO_2 errors have been used to define priorities for the development of solutions. A good estimate of the typical characteristics of the various errors (e.g., characteristic time dependence) is important in order to be able to identify the individual error caused by the individual error sources in the retrieved CO_2 (i.e., to "see" the individual errors in the retrieved CO_2). After a solution has been developed it has to be verified by how much a solution of a given problem reduces the corresponding CO_2 error.

- The WFM-DOAS retrieval program has been adjusted to perform channel 7 CO_2 retrievals. This comprises the following main tasks: generation of a channel 7 look-up table of radiances and derivatives (= weighting functions), adjustment of the configuration file of the retrieval program, definition of an initial pixel mask.

- Initial channel 7 CO_2 retrieval and comparison with reference data (global model simulations, WFM-DOAS v0.4 CO_2 product from channel 6, ground based FTS).

- Initial error budget of existing WFM-DOAS algorithm for channel 7 CO_2 retrieval to quantify retrieval errors originating from Level 1–2 processing (e.g., due to simplified radiative transfer). These are sources for CO_2 errors that would be present even if the calibration of the spectra would be perfect.

- Investigation of solutions for major channel 7 issues:
  - Light-leak issue
  - Ice-layer issue
  - Dead/bad pixel mask issue

1.4 Summary of main results

1.4.1 Error analysis

Radiance errors (Level 0–1 processing): Errors on the channel 7 spectra, i.e. on the spectral radiance, result in errors on the retrieved CO_2 columns, if uncorrected. Five channel 7 radiance error sources have been identified and quantified: Light-leak, ice-layer, undetected dead/bad pixel, residual errors of the dark signal calibration, and residual errors of the non-linearity correction. Three of these error sources can result in major (i.e., significantly larger than 1%) CO_2 errors (at least under certain circumstances): Light-leak, ice-layer, and undetected dead/bad pixel. Two of the error sources can be classified as minor errors: residual errors of the dark signal calibration and of the non-linearity correction. An overview about these channel 7 related radiance error sources is given here:

- **Light-leak issue:** This is a channel 7 specific issue which has not been observed for the other channels. The light-leak issue has initially been identified by analyzing limb measurements at high tangent heights looking at deep space on the Earths day side. The only signal that should be recorded under these circumstances is the dark signal. With the exception of channel 7 this is what has been observed. In channel 7, however, a signal significantly higher than the dark signal has been measured which varies along the orbit in a relatively "smooth" way. This indicates that light leaks into channel 7. The origin and the light path is not known but somehow light enters the instrument that originates from the scene below the satellite plus a possible contribution of direct solar radiation. The light-leak adds a time dependent (spectrally smoothly varying) offset to the spectrum which is on the order of 100 BU/s (values of up to 300 BU/s have been reported). The corresponding CO_2 retrieval error depends primarily on the relative offset not on its absolute value (relative offset: offset in terms of fraction of the background; a 100 BU offset on a 1000 BU background signal is a 10% relative offset). The background signal, and therefore the CO_2 retrieval error for a given offset depends on, e.g., surface albedo and solar zenith angle. The lower the albedo the potentially more critical is the error due to the light-leak. If only measurements over land are considered (more precisely: if scenes with very low albedo such as over water are excluded), the CO_2 error is estimated to be less than about 7%. If also measurements over water (oceans) are included (i.e., very low albedo / low signal scenes) the expected error can be as large as 40% (low bias), if no correction for the light-leak is applied. In order to verify if the uncorrected channel 7 CO_2 columns are affected by the light-leak in a way that is consistent with the expectations described above several orbits have been analyzed. It has been found that the retrieved CO_2 shows a variability that is consistent with the expected error due to the light-leak. For example, a low bias of up to 30% of the retrieved CO_2 columns over water relative to measurements over land has been observed. There is, however, large variability from orbit to orbit and not all orbits show a clear land/ocean CO_2 bias. This is consistent with the expectation that the land/ocean bias not only depends on the observed scenes (its albedos) but (of course) primarily on the magnitude of the light-leak signal which is basically independent of the observed scenes as it originates mainly (if not entirely) from its "surroundings". In summary: The CO_2 error caused by the light-leak has been quantified and characterized: For measurements over land the error can be as large as about **7%**. The retrieved uncorrected channel 7 CO_2 has been analyzed and it has been found that the variability of the uncorrected CO_2 shows pattern that are consistent with the assumed error caused by the light-leak.

- **Ice-layer issue:** The coldest detectors are the detectors of channels 7 and 8. Water vapor condenses on these detectors which therefore suffer from a (varying) ice-layer. The ice-layer affects the channel throughput and therefore the signal and the signal-to-noise ratio which both decrease with increasing ice-layer thickness resulting in a degraded precision (the thicker the ice-layer the larger the throughput loss, i.e., the less signal is recorded for a given input radiance). A second and more critical effect is that the ice-layer results in changes of the instrument slit function. This causes a bias of the retrieved CO_2, if uncorrected. Prior to this study it was not clear by how much the channel 7 ice-layer affects the CO_2 retrieval, especially how large the bias would be. Based on channel 8 methane retrieval it was expected that this is a potentially very critical error source for CO_2. For methane retrieved from channel 8 a time dependent bias of up to about 20% has been found and an error of a similar magnitude was expected for CO_2. In order to determine by how much the retrieved CO_2 is affected by the ice-layer, CO_2 columns have been retrieved from channel 7 by processing all year 2003 SCIAMACHY orbits over the Sahara. For each day an average CO_2 column has been computed. These daily CO_2 columns over the Sahara have been compared with the channel 7 throughput (provided by the SCIAMACHY Operations Support Team (SOST)) determined from ratios of solar spectra. The comparison yields similar results as have been found for channel 8 methane retrieval: The uncorrected channel 7 CO_2 columns show a high correlation with throughput which varies with time because of the changing ice-layer. This shows that the uncorrected CO_2 column is adversely affected by the ice-layer. The maximum CO_2 error is about **20%**.

- **Dead/bad pixel mask issue:** Depending on how “bad” a pixel is, the CO_2 error can essentially be arbitrarily large. Dead/bad pixels typically result in (permanent or temporary) “spikes” in the spectrum which need to be identified and excluded from the retrieval. This is a potentially very critical error source as the error can be 100% or even results in unphysical (negative) radiance values in the spectrum (in this case a retrieval is not possible at all). It is very important to detect and reject all the dead/bad pixels in the spectral fitting window as even a single undetected dead/bad pixels can introduce a large error. For WFM-DOAS retrievals so far mostly static pixel masks have been used, mainly pixel masks valid for a given year, e.g., 2003. For initial channel 7 CO_2 retrievals we defined a static pixel mask for 2003 (optimized for October 2003). As has been found out, however, this pixel mask is not appropriate for later time periods (e.g., 2005), because the number of dead/bad pixels increases with time. Several groups have developed algorithms to detect dead and bad pixels. The most advanced algorithm is probably the one developed by SRON. Other (similar) algorithms have been developed by University of Heidelberg and Bremen. These pixel masks are determined by analyzing the (orbital) dark signal measurements contained in the Level 1 orbit files (mean value, standard deviation, linearity, etc.). These algorithms generate a pixel mask for each orbit. It has however been shown that pixels get worse during an orbit and, therefore, might not be flagged as not useful in the pixel mask of the corresponding orbit. As even one undetected single bad pixel can have a large negative impact on the retrieved CO_2, it is mandatory to carefully investigate the dead/bad pixels mask issue and to find out if the existing algorithms are appropriate for channel 7 CO_2 retrieval. In order to point out that this is a critical error source that needs careful attention we assign an error of **8%** to this error source (note that for orbits where the existing algorithms are appropriate to identify all dead/bad pixels the error is essentially 0% but for measurements where this is not the case the error can be (much) larger than 8%).

- **Dark signal issue:** A good dark signal calibration is mandatory for channel 7 as the dark signal is high and variable. Using Level 1 products generated with the latest version of the operational Level 0–1 processor (i.e., Level 1 version 5.04 products) results in a good dark signal calibration (this means that there seems to be no need any more for “patching” the darks signals as was necessary for Level 1 version 4.0x spectra). The orbital variation of the dark signal has been estimated to about 5 BU/s. A good dark signal calibration is mandatory and the initial Level 1 products suffered from a good calibration. It is assumed that most of the problems have been solved now and that the dark signal issue is only a minor (about **0.2%**) issue now (to be confirmed).

- **Detector non-linearity issue:** After non-linearity correction the residual error is assumed to be in the range 12-18 BU (mostly a random error). The estimated CO_2 error is about **0.5%**.

Inversion errors (Level 1–2 processing): Not only the errors on the spectrum as discussed above contribute to errors on the measured CO_2. There are other error sources originating from Level 1–2 processing. These errors may be called "inversion errors", as they originate from the inversion (or retrieval) step that converts a radiance into a CO_2 column. They are also called retrieval errors. The most important errors have been identified and quantified. The CO_2 errors given here are based on an error analysis performed with simulated measurements using the existing WFM-DOAS algorithm as applied to SCIAMACHY channel 7 measurements but also on published values using different algorithms and spectral intervals. The results can be summarized as follows:

- The surface albedo largely determines the overall level of the radiance observed by SCIAMACHY in nadir mode. To a good approximation the radiance is proportional to albedo. If there would be strict proportionality and if the albedo would have a sufficiently smooth spectral dependence in the spectral fitting window used for CO_2 retrieval, no CO_2 retrieval error would occur because of the polynomial included in the WFM–DOAS fit. There are, however, second order effects which result in errors on the order of a few percent if not carefully accounted for. Due to scattering in the atmosphere not all light rays are reflected at the Earth surface and there is even a probability for a light ray to be reflected more than once before the ray leaves the top of the atmosphere and is detected by SCIAMACHY. One can imagine an average light path representing light coming from the the sun which enters the atmosphere, is reflected at some altitude (the effective scattering height which can be at or near the Earth surface), and is leaving the atmosphere in the direction of the satellite. The altitude of the effective scattering layer depends on the surface albedo (strictly speaking on the absorption and reflection properties of the surface) and on the scattering and absorption properties of the atmosphere. Depending on the altitude of the scattering layer more or less CO_2 molecules contribute to the measured signal. As a result, an error on the retrieved CO_2 column is introduced if the scattering and absorption properties of the surface and of the atmosphere are not known precisely, which is typically not the case. The existing retrieval algorithm assumes a constant albedo of 0.1 for CO_2 retrieval and considers first order albedo effects by the polynomial included in the WFM–DOAS fit. The CO_2 error of the existing retrieval algorithm due to surface albedo variability has been estimated using simulated channel 7 CO_2 retrievals to be less than **4%** for measurements over land (more precisely: for albedos larger than about 2%).

- As described above aerosols also influence the light path and, therefore, the number of CO_2 molecules "seen" by SCIAMACHY which results in an error on the retrieved CO_2 if not properly accounted for. We have estimated the retrieval error due to aerosols by applying the currently existing retrieval algorithm to simulated channel 6 and 7 CO_2 measurements and found errors less than 1%. When analysing real SCIAMACHY measurements we found the largest error of several percent over the Sahara correlated with the strength of dust storms. Houweling et al. (2005) analyzed a large number of SCIAMACHY CO_2 measurements and found the largest errors due to aerosol of up to 10% over the Sahara. Currently only first order effects of aerosols are considered in WFM-DOAS by including a polynomial. We conclude that CO_2 errors due to aerosol of the currently existing algorithm is typically less than **6%** but may reach 10% under extreme conditions.

- Similar as aerosols thin undetected clouds influence the light path and therefore may result in errors on the retrieved CO_2. The CO_2 error due to (undetected) sub-visual cirrus clouds has been estimated to be less than **2%** (for cirrus scattering optical depth less than 3%).

- Atmospheric temperature profile variability affects the CO_2 retrieval because, for example, the strength of molecular absorption lines depends on temperature. Water vapor absorption needs to be considered in every spectral fitting window. Temperature variability is considered in WFM–DOAS by including a weighting function for a temperature shift. Water vapor variability is considered by including a water vapor weighting function in the fit. Nevertheless, some errors remain, because the profile shapes are fixed. The CO_2 error due to variability of vertical profiles of temperature and humidity has been estimated to be about **2%**.

- In the existing algorithm the variation of surface elevation (pressure) is considered using a relatively simple scheme based a a surface elevation data bases. The look-up table of radiances and derivatives is computed for a rather coarse 1 km elevation grid. The actual surface pressure is currently not considered. The CO_2 error due to variability of surface pressure has been estimated to be about **3%**.
- Currently the look-up table is limited to direct nadir observation neglecting the details of the nadir scan. The retrieved column is a-posteriori corrected using a simple geometrical scheme. The error caused by not properly taking into account the details of the scan is estimated to about **1%**.

1.4.2 Development of solutions for major issues

The current status can be summarized as follows:

- **Light-leak issue:** Cloud free measurements of CO_2 over land (moderate to high albedo) and ocean (low albedo) have been compared to see if the expected underestimation of the retrieved CO_2 over water of about up to 25% compared to measurements over land is visible in the retrieved CO_2. Two orbits have been analyzed and the retrieved CO_2 is in fact consistent with the expected estimated light leak induced error. In order to correct for the light leak a (spectrally smoothly varying) offset has to be subtracted from the measurements (note that the offset will be different for every ground pixel). It has been investigated if this offset can be determined from spectral regions with very strong (saturated) CO_2 absorption lines. This approach requires analysis of spectral regions outside of the initial fitting window (2030–2040 nm) which does not contain strongly absorbing lines (this means that clusters with longer exposure times need to be used and that it needs to be shown that the results obtained using these clusters can be interpolated to the time resolution of the 2030–2040 nm cluster / fitting window). Radiative transfer simulations have been performed to determine the degree of saturation. They show that the saturation is far from perfect. For example, for ground pixels with relatively high surface elevation and relatively low solar zenith angle the amount of CO_2 along the light path is not high enough for perfect saturation. This is line with what has been found by analyzing the SCIAMACHY measurements: The signal at the saturated CO_2 lines is too high, higher than the expected light leak signal. This means these measurements do not give the light leak signal directly. Instead a correction is needed. Radiative transfer simulations have been used to compute the signal at the saturated CO_2 lines that SCIAMACHY should measure in case of no light leak. One day of SCIAMACHY data have been processed to produce a global map of the light leak signal estimated as described. This signal is mostly in the expected range of 0–300 BU butu with some exceptions, where negative values have been found (over a scene with high albedo and high surface elevation). These negative values show that at least under certain conditions the radiative transfer simulations overestimate the measured signal indicating that the light leak detection algorithm is not yet perfect (it also needs to be verified that the programms to calculate the light leak signal are free of errors). Within the time available for this study it was not possible to perform additional investigations, e.g., to correct the spectra using the estimated light leak signal and estimate how this improves the CO_2 retrieval.

- **Ice-layer issue:** The expected correlation of channel 7 throughput and retrieved CO_2 column has been found by analyzing year 2003 CO_2 measurements over the Sahara thus confirming that the ice layer results in errors on the retrieved CO_2 column. The maximum error is about **20%** which is in good agreement with what was expected. It is assumed that this error is due to changes of the instrument slit function. The best solution would therefore be to determine a time dependent slit function (or slit function parameters) directly from the nadir spectra, the solar measurements and/or the line lamp spectra. The best approach would be to determine the slit function directly from the nadir spectra. Initial investigations however show that a changing slit function only results in very small changes of the RMS of the fit residuum.

More studies are needed using different types of slit functions. In addition, solar spectra have been analysed. The idea is to determine the slit function by convolution of a high resolution solar spectrum. A high resolution solar spectrum (from Livingston and Wallace) has been compiled covering the relevant parts of the near-infrared spectrum and promising initial fits have been performed but so far only for a few solar spectra. More spectra need to be analyzed and also the fitting algorithm needs substantial refinement to consider different slit function types, spectral and radiometric adjustments, etc. Another approach would be to use the throughput information of channel 7 assuming that a reliable relationship between throughput and CO_2 error can be established e.g. using measurements at one ground station. This would be a similar approach as has been used or is still used to correct methane retrieved from channel 8 for the ice-layer induced time dependent bias. The disadvantage of this approach is that the computation of the CO_2 error requires additional information (e.g., using a ground station or a model) and the assumption that the correction procedure is valid globally. Using this approach it should be possible relatively easily to reduce the error from 20% to about 2–4% (this is approximately what has been achieved for channel 8 methane retrieval using a relatively simple correction scheme) but it is currently unclear if it is possible to reduce the error below say 1%. The prefered solution is however to determine the changing slit function (preferably from the solar spectra) because this causes the CO_2 retrieval problems.

- **Dead/bad pixels issue:** The year 2003 spectra in the spectral region 2030–2040 nm have been processed using an initial (static) pixel mask optimized for October 2003. As expected it has been found that the number of dead/bad pixels increases with time. It is mandatory to have an algorithm that reliably detects dead/bad pixels in the spectra. These pixels need to be avoided during retrieval. Several groups, e.g. SRON, have developed algorithms that produce a dynamical pixel mask. It has however not yet been assessed if any of these algorithms are able to produce a time dependent pixels mask that is suitable to the spectral regions used to retrieve CO_2. A first comparison between the SRON mask and the IUP generated mask has been performed resulting in a 5% difference of the CO_2 but more studies are needed. As long as it has has not been verified that a reliable pixel mask for channel 7 CO_2 esists one must assume that significant errors are introduced. It is however assumed that after careful optimization a reliable detection of dead/bad pixels will be possible for CO_2 retrieval.

2 Study overview

2.1 Background information

SCIAMACHY on ENVISAT is currently the only satellite instrument which globally measures atmospheric carbon dioxide (CO_2) with high sensitivity down to the Earth surface including the important boundary layer. There are other satellite instruments that measure CO_2 in nadir viewing geometry, e.g., AIRS on AQUA. These instruments measure in the thermal infrared (TIR) part of the spectrum and, therefore, have only low sensitivity for the boundary layer (TIR nadir measurements have their maximum sensitivity in the middle/upper troposphere with low sensitivity above and below this region). High sensitivity for the boundary layer is important for the main application of these measurements which is the detection (and, if possible, quantification) of CO_2 surface sources and sinks. Highly precise and accurate column averaged CO_2 measurements can be inverted (using inverse modeling) to better constrain surface fluxes of CO_2. Accurate global measurements of surface fluxes of CO_2 is important to improve our knowledge about the global carbon cycle and is also required by the Kyoto protocol.

SCIAMACHY measures reflected and scattered solar radiation in the near-infrared (NIR) spectral region (Buchwitz et al., 2000, 2005a). For the near future dedicated satellite mission are planned to get information on CO_2 surface sources and sinks such as OCO/USA (launch late 2008) and GOSAT/Japan (launch late 2008). OCO and GOSAT will perform similar measurements as SCIAMACHY but with higher spectral and spatial resolution. SCIAMACHY plays an important pioneering role in this new area of satellite remote sensing. Because the CO_2 sources and sinks only result in a small modulation (about 1% or less) on top of a large background, the precision and accuracy requirements of the atmospheric CO_2 measurements are challenging. This translates into challenging requirements on the quality of the spectra (Level 0-1 algorithms) and on the Level 1-2 retrieval algorithm.

Our current knowledge about the CO_2 fluxes on the global scale mainly stems from networks of highly precise but rather sparse ground stations (e.g., NOAA CMDL). The spatial resolution of these measurements is on the order of continents and ocean basins. Uncertainties are large ($\sim$ 100%) so that for many regions it is even unclear if they are a net source or a net sink.

Rayner and O'Brian (2001) have shown that satellite measurements have the potential to improve this situation if a precision of 2.5 ppmv (0.7%) can be reached for monthly column averaged CO_2 (denoted XCO2) within regions of 8$\times$10 degrees.

Theoretical pre-launch studies performed for SCIAMACHY have shown that a precision of 1% is possible for a single measurement if only instrument noise contributes to the CO_2 measurement error and if the entire channel 7 is used for retrieval (Buchwitz et al., 2000). Instrument noise is an important error source but not the only one. Many other error sources contribute to the overall random error (precision) and to biases (systematic errors), such as aerosols, albedo varaibility, temperature profile variability and interferences from other gases. A good retrieval algorithm has to minimize the sensitivity for these disturbing parameters as much as possbile.

Originally (pre-launch) channel 7 was considered to be the main CO_2 channel because it covers two strong CO_2 bands with many CO_2 absorption lines. Due to a number of problems with this channel (Lichtenberg et al., 2005; Houweling et al., 2005; Gloudemans et al., 2005; Kleipool, 2004; Lichtenberg, 2003) which have been partially detected after launch (e.g., the growth of an ice layer on the cold detector and a light leak resulting in a scene dependent offset) on top of a significant number of other problems known already before launch (large dark signal, large number of dead/bad detector pixels, etc.) CO_2 retrieval from SCIAMACHY has so far focused on channel 6 and first encouraging papers have been published showing the potential of the SCIAMACHY CO_2 measurements (Buchwitz et al., 2005a,b; de Beek et al., 2006). The estimated errors are currently on the order of a few percent, i.e., the challenging accuracy and precision requirements have not yet been met. Currently the channel 6 based retrieval algorithms is being improved which will result in an improved CO_2 data set from SCIAMACHY. In parallel to (or in combination with) this activity it is important to also have a detailed look at channel 7 to improve the precision and to reduce biases. This includes working on solutions for the channel 7 (Level 1 and Level 2) problems listed above. This study is supposed to significantly contribute to this important topic.

2.2 Study goals

The main goal of this study is to investigate to what extent SCIAMACHY channel 7 can contribute to (an improved) CO_2 retrieval. This includes the development of solutions for known channel 7 problems (ice issue, light leak issue, dead/bad pixel issue, etc.). As the main goal is an accurate CO_2 data product this study will focus on the quality of the CO_2 end product and not (only) on certain calibration aspects.

The study has been initiated by DLR-Bonn because it was unclear to what extent channel 7 is useful for CO_2 retrieval. This study is supposed to contribute to clarifying this. This includes the development of solutions for identified problems. There are, however, boundary conditions (from e.g. financial limitations) limiting the efforts that can be spend on developing the solutions. A boundary condition is that after six months a decision should be made if or not it is possible (in the very near future) to generate a usful CO_2 product from channel 7. To answer this question (at the end of this six months study) the achieved accuracy/precision needs to be compared with the requirements. If the results of this study indicate that channel 7 is needed for CO_2 retrieval - and if at least an outline of an algorithm exists how to achieve this - this study will be extended (phase 2) with the goal to give clear recommendations for operational generation of a CO_2 product in terms of an ATBD (algorithm specification document).

2.3 Boundary conditions and implications

In order to achieve the study goal taking into account the boundary condtions this study is split into two phases. Phase 1 (the current phase) last six months (September 2005 to February 2006).
The goals of phase 1 are:

- To have a first detailed look at channel 7 nadir CO_2 retrievals.
- To quantify CO_2 retrieval errors due to channel 7 specific and non-specific errors.
- To develop initial solutions for the identified problems.
- To compare the channel 7 CO_2 with reference data to determine the quality of the retrieved CO_2.
- To give a quality statement at the end of phase 1 with the focus on adressing the question how useful channel 7 is for CO_2 retrieval.

The goals of a possible phase 2 are:

- If not all problems have been solved the development of final solutions.
- Final implementation of the best retrieval approach(es) in the scientific data processor.
- Final comparison with reference data and, if possible, publication of the algorithm and its results.
- Preparation for the implementation in the operational processor (implementation of a "clean" scientific prototype processor, generation of reference input/output, ATBD).
- Assistence during the implementation in operational processing.

In order to meet the tight time schedule it is important to note that there are clear limitations on what can be done and what cannot be done:

- It is not possible to develop a new retrieval algorithm (e.g., an optimal estimation type of algorithm). This study will be based on a existing algorithm (WFM-DOAS) which needs to be adjusted to channel 7. Focus is the analysis of channel 7 spectra and the development of solutions for channel 7 specific problems. The existing WFM-DOAS algorithm is however not perfect and various errors have been identified that contribute (individually) to the CO_2 error on the order of 1% or more (aerosols, residual clouds, albedo variability, temperature profile variability, etc.). It is out of the scope of this study to solve all these problems. Instead an error analysis will be used to quantify these (Level 1–2 processing related) errors to make sure that errors resulting from channel 7 specific issues can be separated from other error sources.
- The WFM-DOAS v0.4 channel 6 CO_2 product is not the absolute CO_2 column but the dry air column averaged mixing ratio XCO_2 which is basically the ratio of the CO_2 column divided by the O_2 column (obtained from the O_2 A band around 760 nm). Because of the demanding accuracy and precision requirements the O_2 retrieval is also not unproblematic. Improving the O_2 retrieval is however outside the scope of this study which will therefore focus on absolute CO_2 columns retrieved from channel 7 (only).
- The time schedule does not permit comprehensive fitting window studies. The fitting window that will be investigated in this study is the window 2030–2040 nm (cluster 52, typical integration time 0.5 s, ground pixel size typically 30×120 km^2) which has been recommended pre-flight. Only if it turns out that this spectral region is not suitable (e.g., due to too many dead/bad pixel) other spectral regions will be investigated.

The final goal is to give recommendations for operational processing. Therefore, there are some additional boundary conditions that need to be taken into account:

- All information needs to be provided by the current orbit file, i.e., the retrieval algorithm shall not be based on past/future orbits.
- Level 0–1 algorithms should be independent of Level 1–2 processing. Especially there should not be any iteration between these major processing steps.

2.4 Accuracy and precision requirements

Requirements for CO_2 column measurements can be found in, e.g., the IGOS/IGACO report:

Threshold requirements (minimum that should be achieved):
Precision: 1% for 500$\times$500 km^2 / daily mean
Accuracy: 2%

Target requirements:
Precision: 0.5% for 50$\times$50 km^2 / daily mean
Accuracy: 1%

For this study it is important to translate this into precision requirements for single SCIAMACHY single measurement: The target requirement is already appropriate for a single measurement as 50 km corresponds to size of a single ground pixel. The threshold requirement can be relaxed using the usually made assumption that the precision improves with $\sqrt{n}$ where n is the number of (sufficient cloud free) SCIAMACHY measurements per day within an area of 500$\times$500 km^2. This area roughly corresponds to one half of a full nadir state which lasts typically 65 s. For an integration time of 0.5 s (e.g., cluster 52 (2030-2040 nm) in channel 7) this corresponds to 2$\times$32.5 = 65 single measurements. Assuming that only 10% of these measurements are useful (e.g., only cloud free forward pixels) results in 7 single measurements. The threshold precision for a single measurement is therefore about 1%$\times\sqrt{7}\sim$ 1% $\times$3=3%.

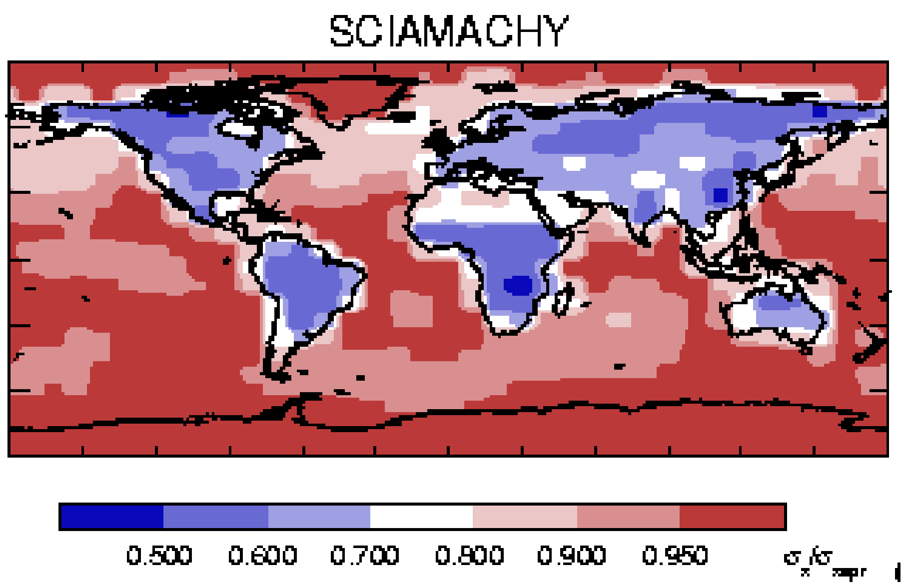

Figure 1: Carbon dioxide surface flux uncertainty reduction (relative to a-priori uncertainty) using SCIAMACHY measurements over land computed using simulated measurements with a single pixel CO_2 measurement precision of 1% and no (systematic) biases (from Houweling et al. (2004)).

To summarize, the requirements for the CO_2 measurements for this study are:

Required precision: $<$3% (ideally $\sim$1.0% or better)
Required accuracy: $<$2% (ideally $\sim$1.0% or better)

These requirements are valid for measurements over land. Because of the low albedo of water (oceans, lakes) in the NIR spectral region measurements over water are more difficult and therefore typically of lower quality compared to measurements over land. Therefore this study will focus on (cloud free) measurements over land. However, all measurements will be processed including measurements over water.

2.5 Verification approach

Goal of this study is an algorithm for CO_2 column retrieval using channel 7. To assess the quality of channel 7 CO_2 retrievals the CO_2 columns need to be compared with reference data. This is however not trivial because the CO_2 variability is small and the number of CO_2 column reference data is very limited.

For this study three different types of reference data will be used: (i) Global model simulations, (ii) the WFM-DOAS Version 0.4 CO_2 data product retrieved from channel 6 (Buchwitz et al., 2005a,b; de Beek et al., 2006), and (iii) ground based FTS measurements, if available.

2.6 Work package overview

The structure of this document is based on the work packages presented in Fig. 2. Details are given in each of the following sections and subsection. There are two main work packages (WP): WP 1000 focuses on Level 0–1 aspects and WP 2000 on Level 1–2 aspects. Main deliverable of this study is a technical report (i.e., the final version of this document) describing the investigations that have been performed, a description of the algorithms, a CO_2 column data set derived from the SCIAMACHY channel 7 nadir spectra (for a set of reference orbits called REFORBITS), the comparison of this data set with CO_2 reference data (called REFCO2), and, finally, an assessment of the quality of the obtained CO_2 results based on a comparison of the estimated achieved accuracy and precision with the CO_2 requirements listed in subsection 2.4.

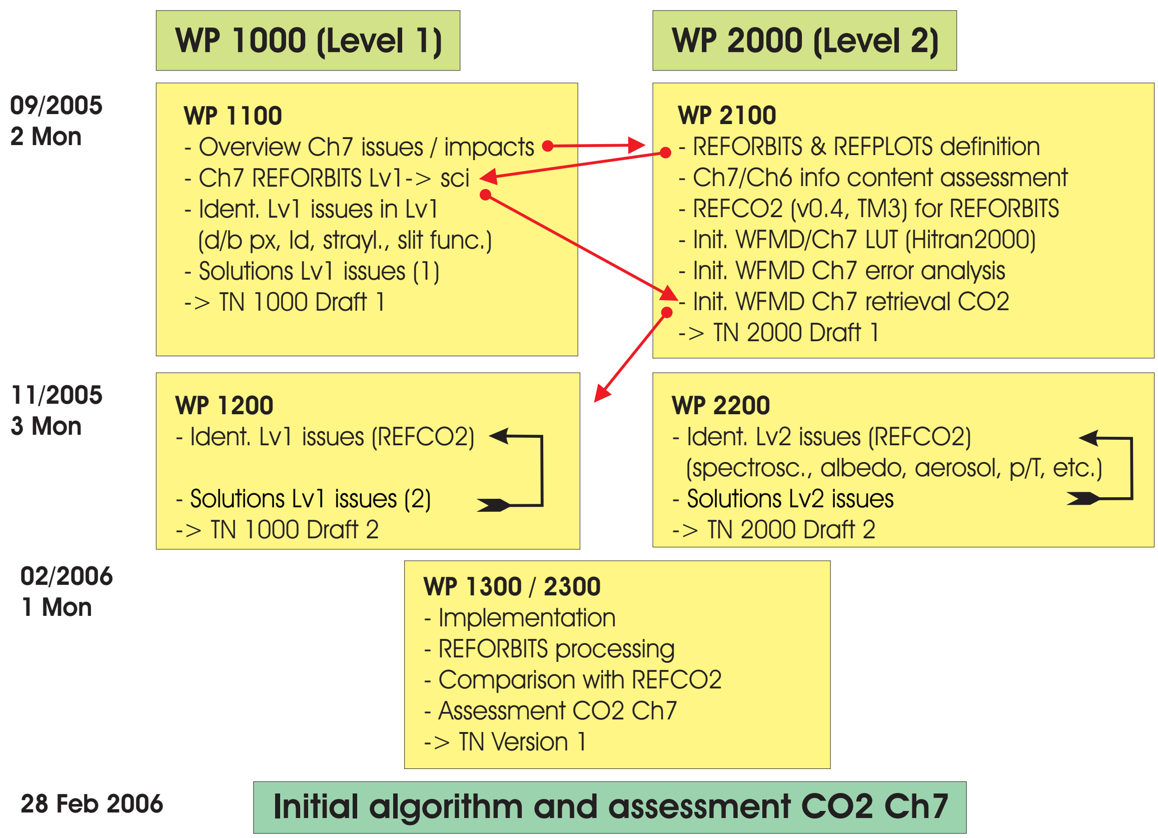

Figure 2: Work package overview.

3 Why channel 7 ?

3.1 General

Channel 7 contains many weak and strong CO_2 absorption lines as shown in Fig. 3. In contrast, channel 6 only contains relatively weak bands of CO_2 without resolved absorption lines (see Fig. 4). Only one of the channel 6 bands is useful (the one at 1585 nm), because the other bands overlap with strong water vapor absorption or are located in channel 6+ which has many dead and bad pixels. Because of more and better resolved CO_2 absorption lines in channel 7 compared to channel 6, channel 7 was planned to be the main CO_2 channel of SCIAMACHY. It can be shown that the precision of the channel 7 CO_2 measurements (defined as CO_2 measurement error due to instrument noise) is significantly better than the precision using only channel 6. It also has to be pointed out that one of the two CO_2 bands in channel 6 is located in the so called channel 6+ which has a lot of dead and bad pixels. Therefore, the CO_2 band located in channel 6+ has not yet been used for CO_2 retrieval.

The best approach is, of course, to use both channels. This is actually the approach on which the OCO measurement concept is based on. According to OCO studies both spectral regions have to be used in order to get the desired performance.

We have not yet done any studies on the simultaneous use of channels 6 and 7 of SCIAMACHY. However, in the following section we give one example to show the potential of channel 7 to improve the accuracy of the CO_2 measurements, in this case the potential for reducing path length errors related to aerosols (the results are probably also valid to reduce the sensitivity to albedo variability and thin cirrus clouds). We show that using only channel 6 measurements one cannot distinguish between CO_2 variability and aerosol variability because the resolution of channel 6 is too low. We show that channel 7 (at least in theory) enables a much better discrimination between aerosol and CO_2 effects because aerosols and CO_2 typically produce somewhat different spectral “fingerprints” at channel 7 (i.e., high enough) resolution.

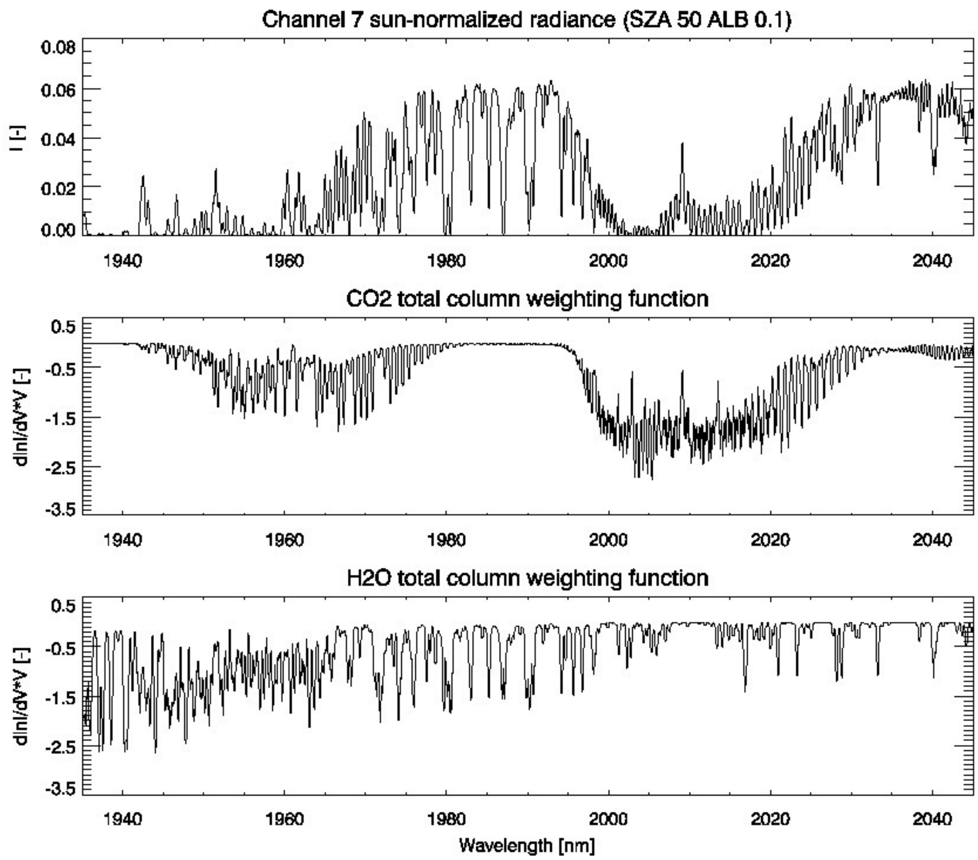

Figure 3: Simulated SCIAMACHY channel 7 nadir spectrum and derivatives (weighting functions) of CO_2 and interfering gases.

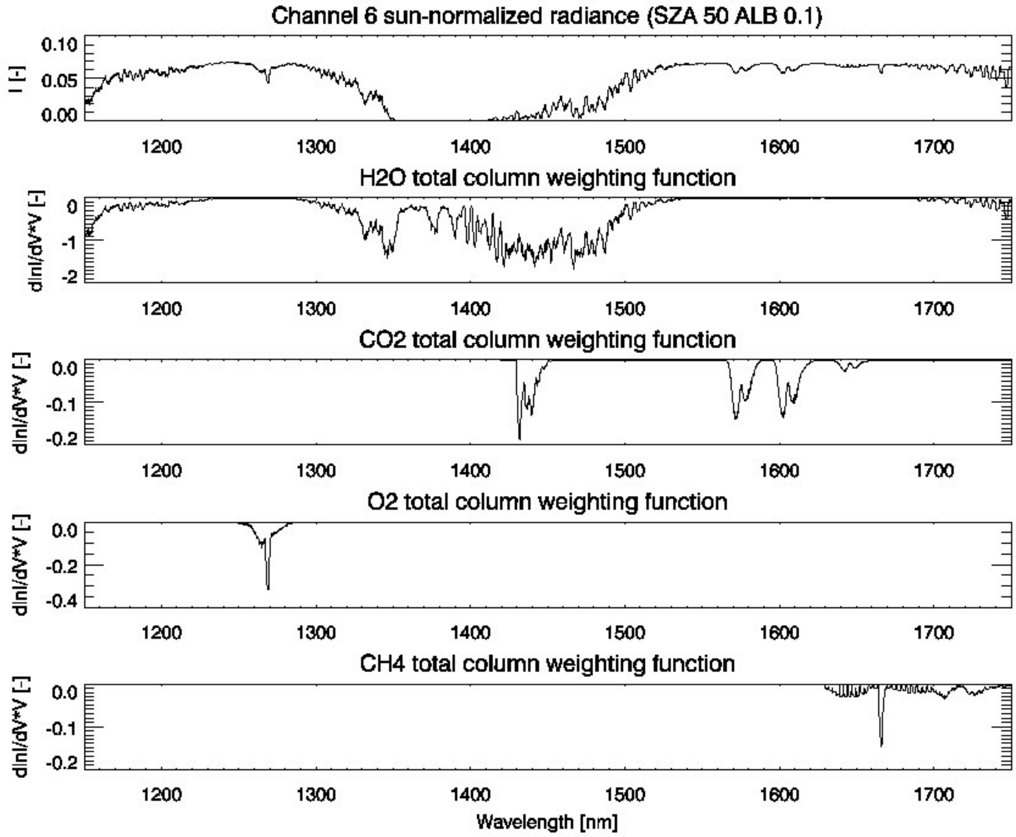

Figure 4: Simulated SCIAMACHY channel 6 nadir spectrum and derivatives (weighting functions) of CO_2 and interfering gases.

3.2 Towards a reduced sensitivity to aerosols

3.2.1 Introduction

One error source in retrieving CO_2 from SCIAMACHY data is the non-proper treatment of aerosols in the retrieval algorithm, which can lead to an overestimation of CO_2 of up to 10% in regions with very large atmospheric aerosol loading as shown by Houweling et al. (2005) over the Sahara desert. The sensitivity to aerosols is also discussed by Buchwitz and Burrows (2004) and in this report in Section 6.1.2.

In order to include an aerosol weighting function in the retrieval at least two conditions should be fulfilled: The aerosol-derivatives of intensity $\frac{dI}{dA}$ for different aerosol-scenarios have to be highly correlated ensuring that all aerosol types can be considered in maximal generality in only one additional weighting function. Moreover the correlation between $\frac{dI}{dA}$ and $\frac{dI}{dCO_2}$ should be as small as possible to have the ability of distinguishing CO_2 from aerosols reliably.

Therefore, spectra with and without pertubations in the boundary layer ($<$3 km) of CO_2 (+1%) and aerosols (+10%), respectively, are simulated using SCIATRAN to calculate these derivatives for different aerosol scenarios. This is done in the spectral interval of the fitting window of the WFM-DOAS v0.4 CO_2-retrieval algorithm in channel 6 (1558-1594 nm) and for comparison in the intervals 1990-2040 nm and 2030 - 2040 nm of channel 7.

3.2.2 Correlation of aerosol-derivatives for different scenarios

To represent the different aerosol scenarios in the SCIATRAN simulation the LOWTRAN aerosol model is used. The default scenario with which the other scenarios are compared can be characterized as follows: Fall/Winter, maritime aerosol in the boundary layer, visibility and humidity in the boundary layer and the troposphere 23 km and 80%, respectively. The different scenarios are coded with numbers as can be seen in Table 2, for example the mentioned default scenario is 132323.

Season	Boundary layer aerosol type	Boundary layer visibility	Boundary layer humidity	Tropospheric visibility	Tropospheric humidity
1 = Fall/Winter	1 = rural	1 = 50km	1 = 0%	1 = 50km	1 = 0%
2 = Spring/Summer	2 = urban	2 = 23km	2 = 70%	2 = 23km	2 = 70%
	3 = maritime	3 = 10km	3 = 80%		3 = 80%
	4 = tropospheric	4 = 5km	4 = 99%		4 = 99%
		5 = 2km			

Table 2: LOWTRAN aerosol scenarios.

The aerosol-derivatives calculated using convolved spectra are shown in Figures 5, 6 and 7 in the spectral intervals 1558-1594 nm, 1990-2040 nm and additionally in the subinterval 2030-2040 nm, assuming Gaussian slit functions with Full Width at Half Maximum of 1.4 nm and 0.23 nm, respectively. For better comparison the spectra are fitted to the default scenario allowing a scaling factor and an additive offset ($\tilde{f} = c_1 + c_2 f$).

Since this fitting procedure does not alter the corresponding correlations these plots are in agreement with the calculated correlation coefficients which can be seen in Table 3 where also the values for the unconvolved case are listed. It turns out that almost all aerosol-derivatives are highly correlated with coefficients near 1 in both spectral intervals as required. The only exceptions are the scenarios with rural aerosol type (1**1**3222 and 2**1**4111) as can be seen in both, the figures and the table.

3.2.3 Correlation between aerosol- and CO_2-derivatives

As a second step the correlation between $\frac{dI}{dA}$ and $\frac{dI}{dCO_2}$ is examined for all scenarios which should be as small as possible as mentioned in the introduction. The correlation coefficients for the three intervals are shown in Table 4 where, again, also the values for the unconvolved case are listed.

Unfortunately these derivatives are in general highly correlated in the spectral in-

Scenario	Spectral interval 1558-1594 nm	Spectral interval 1990-2040 nm	Spectral interval 2030-2040 nm
132323	1.00 (1.00)	1.00 (1.00)	1.00 (1.00)
224424	1.00 (1.00)	0.99 (0.99)	0.99 (0.99)
113222	-0.89 (-0.97)	0.19 (0.16)	-0.43 (-0.01)
245121	0.99 (0.99)	0.99 (0.99)	0.99 (0.98)
231414	1.00 (1.00)	1.00 (1.00)	1.00 (1.00)
123322	-0.99 (-1.00)	-1.00 (-0.99)	-1.00 (-0.99)
142223	1.00 (0.99)	0.94 (0.91)	0.85 (0.85)
214111	-0.22 (-0.05)	0.71 (0.66)	-0.44 (0.25)

Table 3: Correlation between the derivatives $\frac{dI}{dA}$ for different aerosol-scenarios and the derivative of the default 132323. The values are calculated using a convolution with a Gaussian slit function with typical Full Width at Half Maximum of SCIAMACHY channel 6 (fwhm=1.4 nm) and channel 7 (fwhm=0.23 nm), respectively. In brackets are the correlations for unconvolved high-resolution spectra.

terval of the fitting window of the WFM-DOAS v0.4 CO_2-retrieval algorithm (1558-1594 nm) especially for convolved spectra where correlation coefficients near 1 are reached. Therefore it seems impossible to distinguish properly between CO_2 and aerosols using the current retrieval scheme, because the aerosol- and CO_2-derivatives are nearly identical in this interval resulting in potential errors in the CO_2-retrieval.

Nevertheless the situation is different in the spectral interval 1990-2040 nm which is covered by SCIAMACHY channel 7 where the correlation coefficients never exceed 0.2 even in the case of convolved spectra potentially allowing to better distinguish between CO_2 and aerosols resulting in a potential possibility of reducing systematic errors in retrieved CO_2 due to aerosols. In the selected subinterval 2030-2040 nm correlations are higher but still significantly smaller than 1.

Scenario	Spectral interval 1558-1594 nm	Spectral interval 1990-2040 nm	Spectral interval 2030-2040 nm
132323	0.99 (0.77)	0.14 (-0.02)	0.36 (0.46)
224424	0.97 (0.74)	0.12 (-0.06)	0.41 (0.50)
113222	-0.92 (-0.70)	0.19 (-0.05)	0.32 (0.51)
245121	0.96 (0.70)	0.12 (-0.07)	0.37 (0.46)
231414	0.98 (0.78)	0.15 (-0.01)	0.40 (0.50)
123322	-0.99 (-0.75)	-0.13 (0.02)	-0.31 (-0.39)
142223	0.99 (0.81)	0.11 (-0.14)	0.65 (0.64)
214111	-0.34 (-0.42)	0.12 (-0.14)	0.28 (0.56)

Table 4: Correlation between $\frac{dI}{dA}$ and $\frac{dI}{dCO_2}$ for different aerosol-scenarios. The values are calculated using a convolution with a Gaussian slit function with typical Full Width at Half Maximum of SCIAMACHY channel 6 (FWHM=1.4 nm) and channel 7 (FWHM=0.23 nm), respectively. In brackets are the correlations for unconvolved high-resolution spectra.

3.2.4 Conclusions

It has been shown in a theoretical study using simulated spectra that for SCIAMACHY channel 7 the potential exists to distinguish between spectral CO_2 and aerosol features (= high frequency part of radiance derivatives). The existence of different (i.e., low correlation) weighting functions is a prerequisite to reduce aerosol induced errors on the CO_2 column retrieved using a DOAS type algorithm. For channel 6 this seems not to be possible because of the high correlation of the CO_2 weighting function with typical aerosol weighting functions. This is very promising but more studies are needed, e.g., detailed retrieval studies taking into account instrument noise, systematic errors and a more complete consideration of atmospheric variability (aerosol, temperature, water vapor, etc.). Besides this some other factors have to be taken into consideration: In principle the CO_2 band used in the WFM-DOAS v0.4 retrieval algorithm (located in channel 6) is well suited for retrieving column CO_2 and should therefore be maintained. The problems that occur in situations of very large atmospheric aerosol loading show, however, that this band alone cannot yield CO_2 with sufficient precision for all situations. Therefore it seems desirable to use additional information from channel

7 in order to reduce systematic errors due to aerosols and thus increase retrieval precision. The final strategy of doing this needs further investigation.

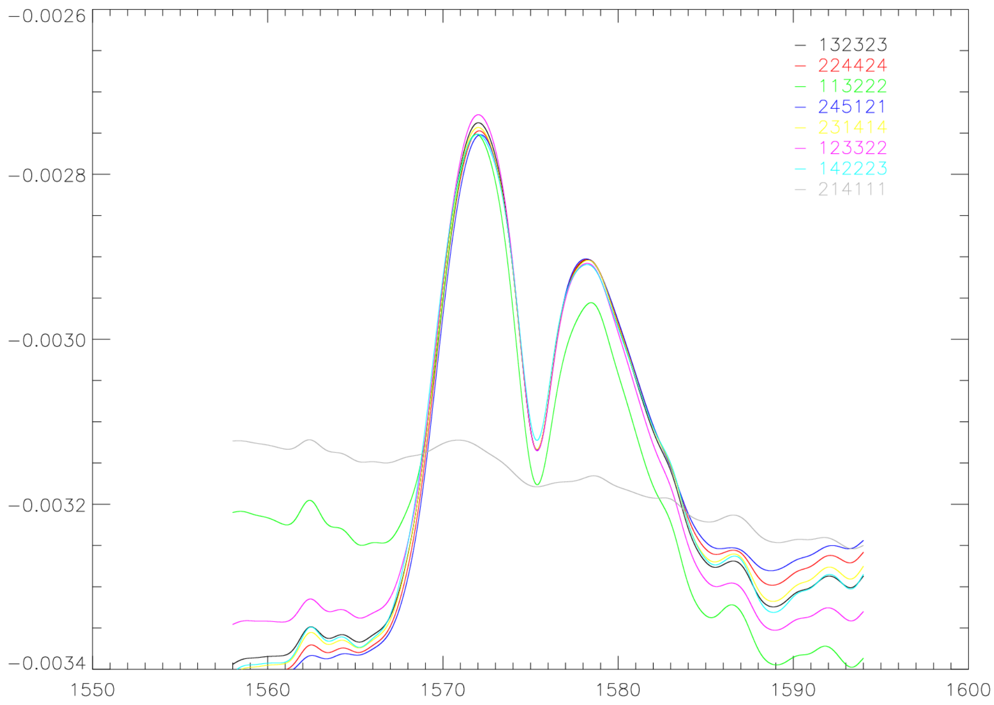

Figure 5: $\frac{dI}{dA}$ for different aerosol-scenarios derived using convolution with a Gaussian slit function with FWHM 1.4 nm fitted to the default 132323 in the spectral interval 1558-1594 nm by scaling and offset.

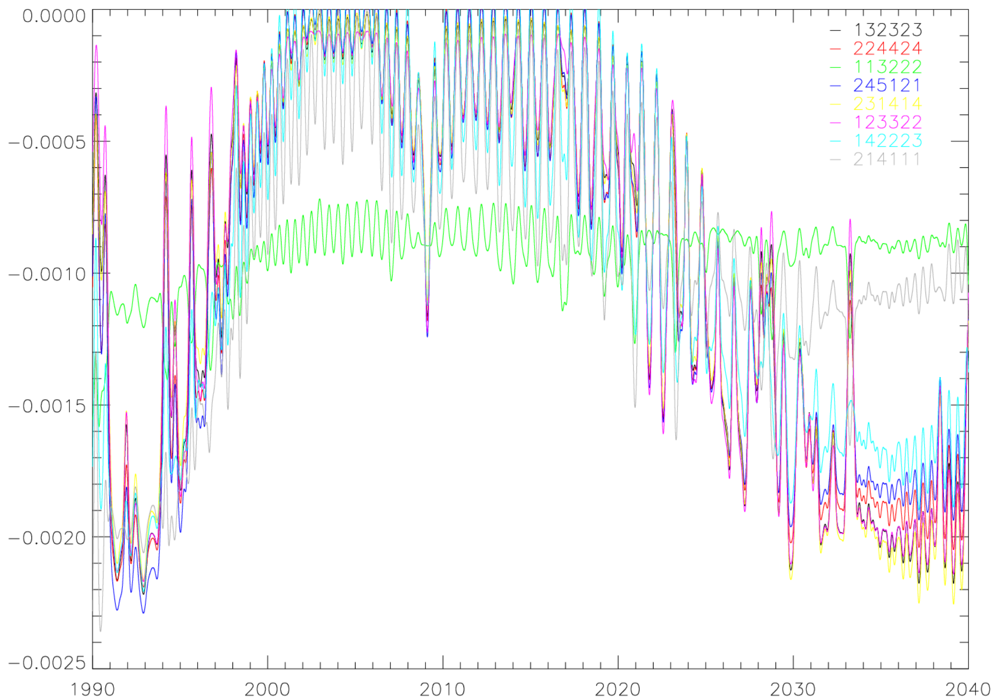

Figure 6: As Figure 5 but in the spectral interval 1990-2040 nm and with FWHM 0.23 nm.

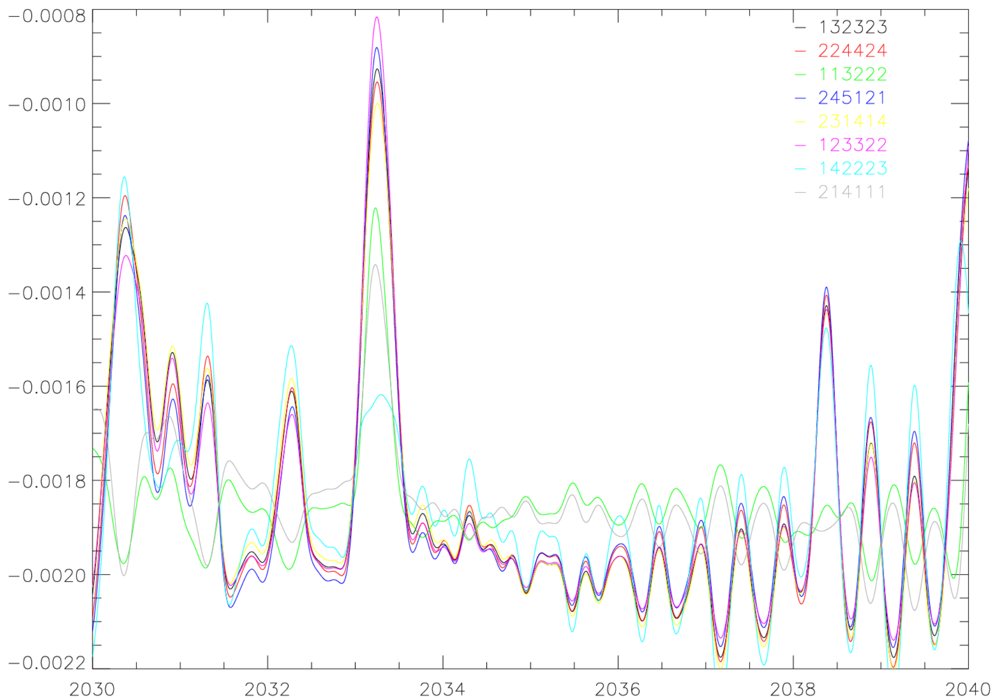

Figure 7: As Figures 5 and 6 but in the spectral interval 2030-2040 nm with FWHM 0.23 nm.

4 Overview channel 7 issues (WP 1100)

Start of WP 1100: Beginning of September 2005
End of WP 1100: End of October 2005

4.1 Relationship between calibration offsets and CO_2 errors

In the following sections an overview is given about known channel 7 (radiometric) calibration issues using existing literature (mostly technical reports which existed at the beginning of this study). For each error source an estimate is given how the corresponding calibration error / issue affects the CO_2 retrieval (what is the magnitude of the CO_2 error and what are its characteristics?).

In most of these (previous) studies calibration errors are given in binary units (BU). For this study it is important to estimate the (potential) impact of these errors on the retrieved CO_2 column.

In this section we provide a simple estimate of the relationship between calibration errors (in BU) and corresponding CO_2 column retrieval errors (in percent). This relationship can be derived as follows:

Based on the standard DOAS approach the relation between the differential optical depth of CO_2, τ (= $VA\sigma$), and the measured signal a is given by $a = b\,\exp(-\tau)$. Here, a is the measured (absorption) signal at the center wavelength of a CO_2 absorption line, b is the "background" signal next to the absorption line (the signal one would measure if σ, the differential absorption cross-section of CO_2, is zero). V is the vertical column of CO_2 and A is the airmass factor. Assuming that τ is small compared to 1, i.e., for relatively weak absorption lines, the relation between a and V is: $a = b\,(1 - VA\sigma)$.

In this case the only unknown V is given by $V = (1 - a/b)/(A\sigma)$ (this is equal to the true column V^t in case of no calibration errors). In case of a systematic calibration error (i.e., for an offset o on the nadir spectrum) the following column will be retrieved: $\hat{V} = (1 - (a+o)/(b+o)/(A\sigma)$.

From these formulas one can derive a simple relationship between the percentage CO_2 retrieval error ϵ, the measured signal b in, e.g., in BU (strictly speaking, only a is measured; b is basically the continuum signal next to the absorption line), and the signal offset o given in the same unit as b:

$$\epsilon = 100 \times (\frac{1}{1+\frac{o}{b}} - 1). \tag{1}$$

It is interesting to note that the CO_2 error does not depend on τ (for small τ, i.e., weak absorption).

The signal b as a function of solar zenith angle θ and surface albedo A can be estimated as follows:

The measured radiance R for a nadir observation is approximately given by

$$R(\theta, A) = I_o(A/\pi)T_{eff}(\theta). \tag{2}$$

Here I_o is the solar irradiance and T_{eff} is the effective slant path atmospheric transmission, which is approximately given by $T_{eff} = T \exp(-(-\ln(T)/\cos(\theta))$, where T is the vertical path (background or broadband) atmospheric transmission. The solar irradiance I_o at 2μm is about 10^{14} photons/s/nm/cm^2 and T is about 0.8.

The corresponding signal b (in BU) measured for exposure time t is given by:

$$b = R\ F_{mir}\ Ap\ \Omega\ Tr\ \Delta\lambda\ QE\ (1/ADC)\ t = R\ F. \tag{3}$$

Here, R is the measured nadir radiance. The other variables have the following meaning (typical channel 7 values for each parameter are given in brackets):

F_{mir} is the scan mirror reflectivity (0.9), Ap is the aperture (1.53 cm^2), Ω is the instantaneous field-of-view (2.5 10^{-5} sr corresponding to 1.8^o $\times$ 0.045^o), Tr is the channel 7 throughput (0.28), $\Delta\lambda$ is the spectral width of a channel 7 detector pixel (0.1 nm), QE is the quantum efficiency (0.5), and ADC is the conversion factor for the conversion of electrons in (digital) binary units (153 electrons/BU). For an exposure time t of 0.5 s this gives the following conversion factor F for the conversion of radiance R (in photons/s/nm/cm^2/sr) into a signal b in BU: F = 1.3$\times$10^{-9} BU/(photons/s/nm/cm^2/sr).

Typical land albedos (Buchwitz and Burrows, 2004) at 2μm are in the range 0.1 (vegetation) - 0.4 (desert). For oceans the albedo is about 0.01 (probably even less). The albedo of snow/ice is also very low (about 0.02).

Using the above given formulas the CO_2 retrieval errors listed in Tab. 5 can be computed (the number are valid for a solar zenith angle θ of 50^o where T_{eff}=0.56).

Table 5 shows that the CO_2 retrieval error is to a good approximation inversely proportional to albedo and proportional to the offset error.

Albedo (-)	Radiance R (phot/s/nm/cm^2/sr)	Signal b (BU)	Offset o (BU)	CO_2 error ϵ (%)
0.01	1.8e11	283	5	-1.73
0.1	1.8e12	2834	5	-0.18
0.2	3.6e12	5669	5	-0.09
0.3	5.4e12	8503	5	-0.06
0.4	7.2e12	11337	5	-0.05
0.01	1.8e11	283	100	-26.1
0.1	1.8e12	2834	100	-3.4
0.2	3.6e12	5669	100	-1.7
0.3	5.4e12	8503	100	-1.2
0.4	7.2e12	11337	100	-0.9
0.01	1.8e11	283	200	-41.4
0.1	1.8e12	2834	200	-6.6
0.2	3.6e12	5669	200	-3.4
0.3	5.4e12	8503	200	-2.3
0.4	7.2e12	11337	200	-1.7

Table 5: Relative CO_2 column retrieval error for different surface albedos and calibration errors (constant additive offsets).

4.2 Known channel 7 issues and impact on CO_2

This section summarizes the existing literature on channel 7 issues. For each identified channel 7 issue an estimation is given concerning how the issue affects the CO_2 retrieval:

- Estimate of magnitude of CO_2 retrieval error for each error source. This is important as due to the time constraints for this study a priority list needs to be established and work has to be prioritized to start developing solutions for the most important problems first.
- The characteristics of CO_2 retrieval error (e.g., dependence on season, orbital position, scene brightness (albedo, clouds), etc.) needs to be determined/described. The main question here is: What needs to be done to identify this error source in the retrieved CO_2 columns? The philosophy of this study is: Before algorithms will be developed to solve a problem it first needs to be established that the particular error has been detected using the retrieved channel 7 CO_2. After it has been demonstrated that the error is "visible" in the retrieved CO_2 solutions shall be developed. A successful solution is a solution for which it has been demonstrated that the error is no longer "visible" in the CO_2 or that at least the magnitude of the error has been significantly reduced.

This chapter is based on the description of the calibration status in December 2003 reported by Lichtenberg (2003). More recent developments in the calibration status are also taken into account. In the following a description of every issue is given along with an estimate how this issue affects the CO_2 retrieval.

The set of orbits that will be processed and analyzed in this study is called REFORBITS (reference orbits). The REFORBITS need to be defined such that the corresponding CO_2 data set is suitable to detect the individual CO_2 errors for each error source separately, if possible. The goal is: we want to make the individual errors visible in the retrieved CO_2. For each error source a recommendation concerning suitable REFORBITS is given.

4.2.1 Light leak issue

Description of the issue:

A light leak was detected in channel 7 leading to a high, diffuse, and spectrally not resolved background in the spectra of up to 80 BU/s (300 BU/s according to Kleipool (2004)). Lichtenberg et al. (2005) suggested that the signal caused by the light leak is not only a function of orbital phase (Fig. 8 shows an example for one orbit) but more likely a function of viewing geometry combined with the presence of regions with high albedo (e.g., clouds). The spectral dependence of the light leak signal is shown in Fig. 9 (from Skupin (2003)).

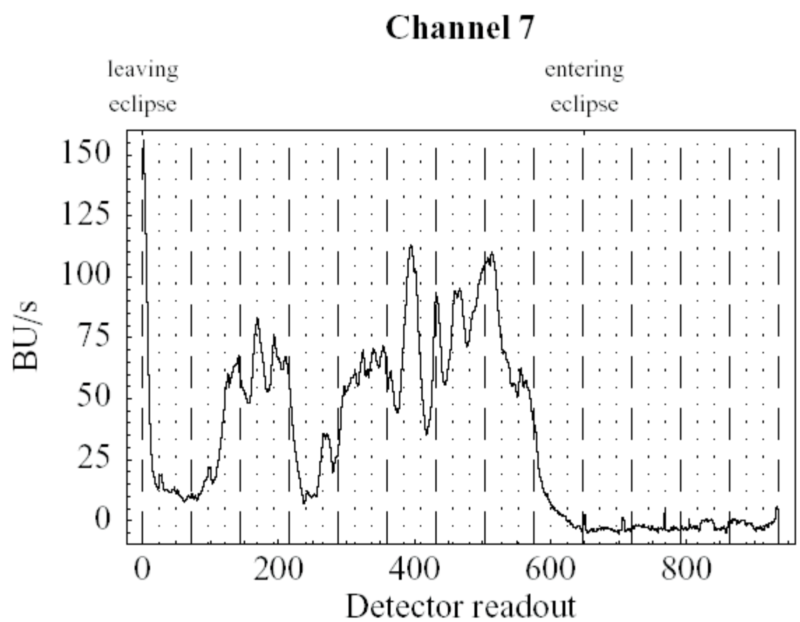

Figure 8: Channel 7 light leak signal measured during a special dark orbit on the Earth's dayside (from Skupin (2003)). "Detector readout" basically means orbital position (see annotation for terminator position).

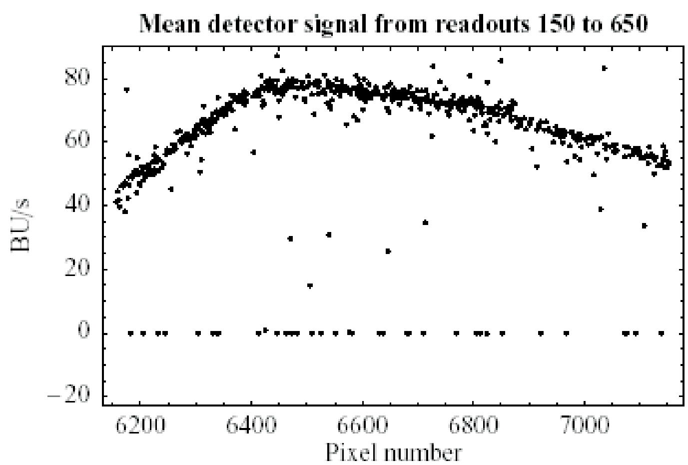

Figure 10: Mean detector signals in channel 7 from readouts 150 to 650 of orbit 3959. Dead/Bad pixels are deleted.

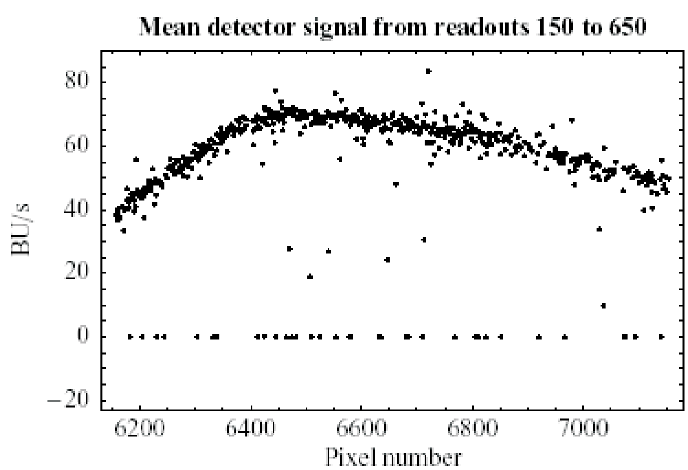

Figure 11: Mean detector signals in channel 7 from readouts 150 to 650 of orbit 3960. Dead/Bad pixels are deleted.

Figure 9: Figures 10 and 11 from Skupin (2003) showing the spectral characteristics of the channel 7 light leak signal.

Estimate of resulting CO_2 error and its characteristics:

If the light leak causes a constant scene-independent offset of, say 100 BU, than the CO_2 errors listed in Tab. 5 are relevant. In this case a downward jump of about 25% in the retrieved CO_2 should be visible between land (moderate to high albedo) and ocean (very low albedo).

If the light leak will cause an offset that is proportional to scene brightness than a constant, ground scene independent, relative CO_2 error will result as can be seen from Eq. 1. This type of error will be difficult to detect (note that this requires an accurate measurement of the absolute level of CO_2 which is not yet possible for channel 6 version 0.4 retrievals). This however assumes strict proportionality of the offset and the background radiance. This is not to be expected because the light leak is not restricted to originate from the ground pixel observed in nadir mode but will also be influenced by its surroundings. This means that good proportionality might be expected for very homogeneous scenes (e.g., cloud free Sahara, cloud free ocean, or totally overcast situations) but not for inhomogeneous scenes.

REFORBITS requirements:

Several orbits covering land and ocean (with a sufficiently large number of cloud free pixels) need to be analyzed to see the expected drop in CO_2 when going from land to water (e.g., orbits 4714 (24 Jan 2003, western Africa), 4757 (27 Jan 2003, western Africa), and/or 8663 (27 Oct 2003, eastern Africa). In addition, the Park Falls 2003-2005 orbits data set, or a subset of this, could be used as well.

4.2.2 Detector ice-layer issue

Description of the issue:

Channel 7 shows a loss in transmission due to an ice layer on top of the detector. The ice is (partially) removed during so-called decontamination phases, but growth with time as along as the detector is at its nominal (cold) temperature of about 150 K.

Depending on the thickness of the ice-layer, the channel throughput decreases, the noise increases and it also has been observed that the slit function changes (Gloudemans et al., 2005). All this impacts the CO_2 retrieval.

Estimate of resulting CO_2 error and its characteristics:

It is expected that the channel 7 ice-layer induced throughput loss results in lower signal-to-noise ratios and therefore lower CO_2 precision. As a rough estimate this means a degradation of a precision from about 1% to about 1.4% if the transmission decreases from its nominal value (no ice) to 50% of the nominal value (this estimate assumes a square root (of the signal) dependence of the precision). This is an error one has to accept because there are no means to correct for additional noise in the spectra (a compensation is possible however, e.g., the use of a larger fitting window).

Figures 10 and 11 show the time dependence of the channel 7 and 8 channel-averaged throughput.

The more systematic CO_2 errors due to the slitfunction change are expected to be similar in time dependence and magnitude as observed for channel 8 WFM-DOAS version 0.4 methane retrievals. For methane retrieval the following has been observed (Buchwitz et al., 2005b): As shown in Fig. 12 the observed error was $\sim$10% (low bias) a couple of weeks or months after the last decontamination period. The methane bias is correlated very well with the (independently) observed throughput loss. For CO_2 a similar behavior is expected. Therefore, this is a potentially very critical error.

In Lichtenberg (2003b) it is shown that the thickness of the ice-layer in channel 7 is about 5 times smaller (thinner) than the ice-layer in channel 8 probably due to different amounts of water in the two channels. This could mean that the slit function change and corresponding CO_2 retrieval error is a factor of 5 smaller compared to the methane bias observed in channel 8. If this turns out to be true, than the maximum systematic error on the CO_2 column due to the ice issues is "only" about 2% compared to the 10% error that has been observed for (version 0.4 channel 8) methane.

REFORBITS requirements:

A long time series needs to processed and analyzed to detect the expected correlation with the channel 7 throughput loss. The Park Falls 2003-2005 orbits data set, or a subset of this, would be sufficient.

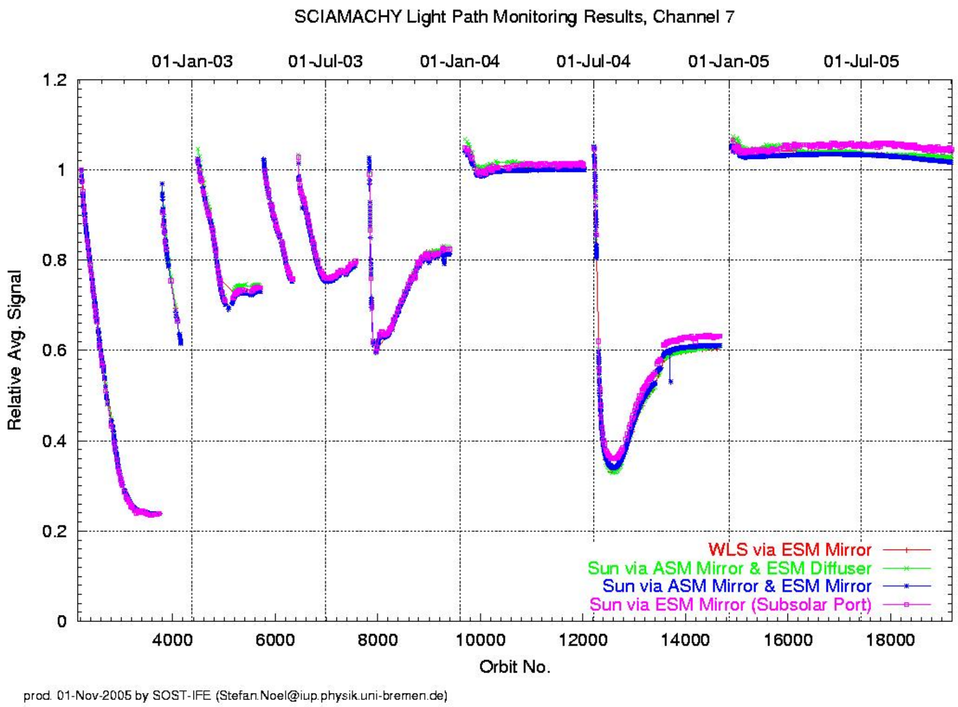

Figure 10: Channel 7 throughput loss from SOST light path analysis (from: SOST web page).

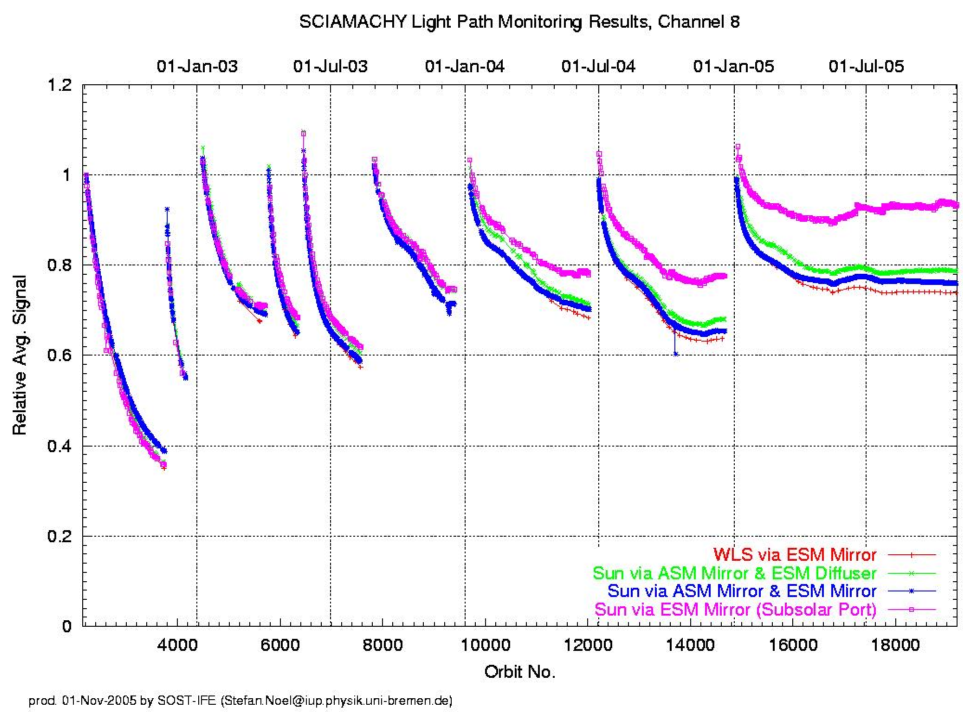

Figure 11: Channel 8 throughput loss from SOST light path analysis (from: SOST web page).

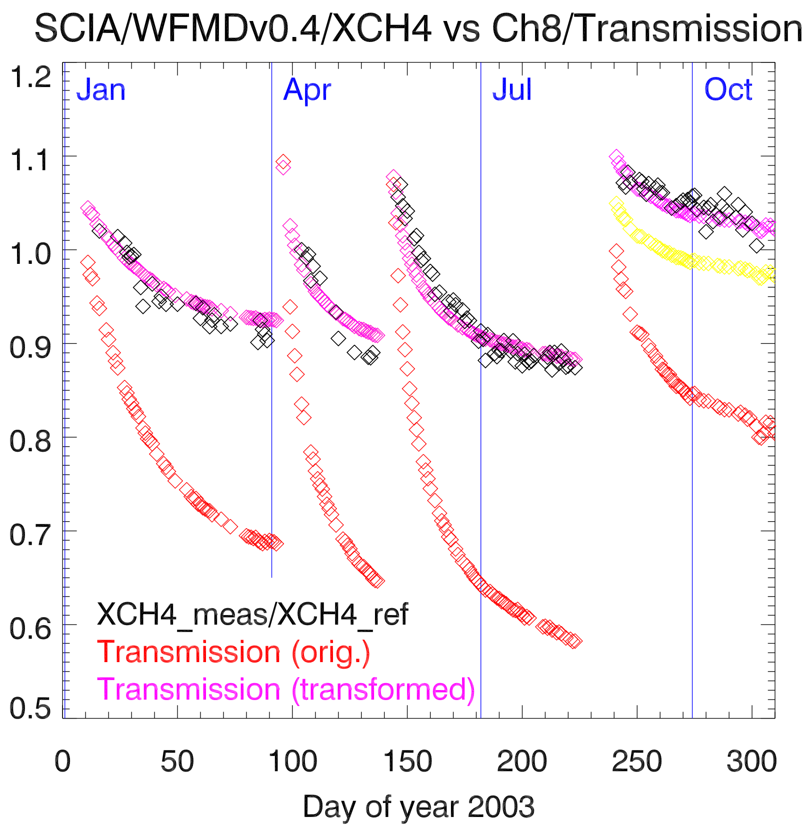

Figure 12: Relative bias of WFM-DOAS version 0.4 methane (black symbols) due to the varying channel 8 ice-layer. The bias is clearly correlated with the channel 8 average throughput (red and magenta symbols) (from: Buchwitz et al. (2005b)).

4.2.3 Dead/bad pixel mask issue

Description of the issue:

The NIR channel 6–8 detector arrays of SCIAMACHY are quite inhomogeneous in terms of detector pixel characteristics such as dark signal and quantum efficiency. Several pixels need to be mask our for retrieval, i.e., should not be used for retrieval. For this purpose a so called "dead and bad pixels mask" has been defined (already pre-launch). A dead pixel is a pixel that should not / cannot be used at all. A bad pixel is a pixel with bad performance such as high dark signal.

Estimate of resulting CO_2 error and its characteristics:

Dead/bad pixels result in obvious spikes in the spectrum and in the fit residuum (dead/bad pixels can, therefore, be detected by inspection of spectra and fit residuals). The radiance at the position of a dead/bad pixel can even be negative, i.e. can have unphysical values. In this case the measurement cannot be processed by WFM-DOAS (the WFM-DOAS algorithm skips the corresponding ground pixel because it computes the logarithm of the spectrum which requires positive values; this mostly happens over water resulting in large CO_2 data gaps). Dead/bad pixels can also be identified by analyzing the dark spectra contained in the Level 1 product files.

If a bad pixel is in the fitting window it will result in errors of the retrieved CO_2 column. The error can be "arbitrarily" large or small depending on how bad a pixel is. Even a single bad pixel can significantly degrade the retrieval (Gloudemans et al., 2005).

It has been found that the dead/bad pixels are not static, i.e., the number of dead/bad pixels increases with time (Gloudemans et al., 2005).

REFORBITS requirements:

A long time series needs to be processed in order to detect any time dependencies in the characteristics of the detector pixels, e.g., an increasing number of dead/bad pixels with negative consequences for CO_2 retrieval.

4.2.4 Dark signal calibration issue

Description of the issue:

In channel 7 the changing ice layer on the detector results in a changing dark signal (because the detected thermal radiation of the instrument is absorbed/scattered in the ice-layer). To correct for this, dark currents need to be measured frequently, e.g., every orbit.

This is done since beginning of 2003 (“orbital darks”). The orbital darks are part of the Level 1b data product. The initial versions of the Level 0 to 1c processor were not able to use the improved dark signal measurements. At IUP a method has been developed to circumvent this problem. The binary Level 1b files have been modified (“patched”) such that the improved dark signals are applied during Level 1b to 1c conversion using EnviView. Using this procedure it was possible to get much better spectral fits and more accurate columns (especially important for channel 8 CO retrieval). It is assumed that the latest version of the Level 0 to 1c processor makes use of the improved dark signal measurements and that this issue has been solved (this will be verified by WFM-DOAS analysis of channel 7 year 2003-2005 spectra).

Another issue is the variation of the dark signal during each single orbit, i.e., the dark signal dependence on orbital phase. Kleipool (2004) has estimated that the orbital variation of the dark signal for channel 7 is less than about 5 BU/s. This is much smaller than the signal caused by the channel 7 light leak which is on the order of 100 BU (for details see Sect. 4.2.1).

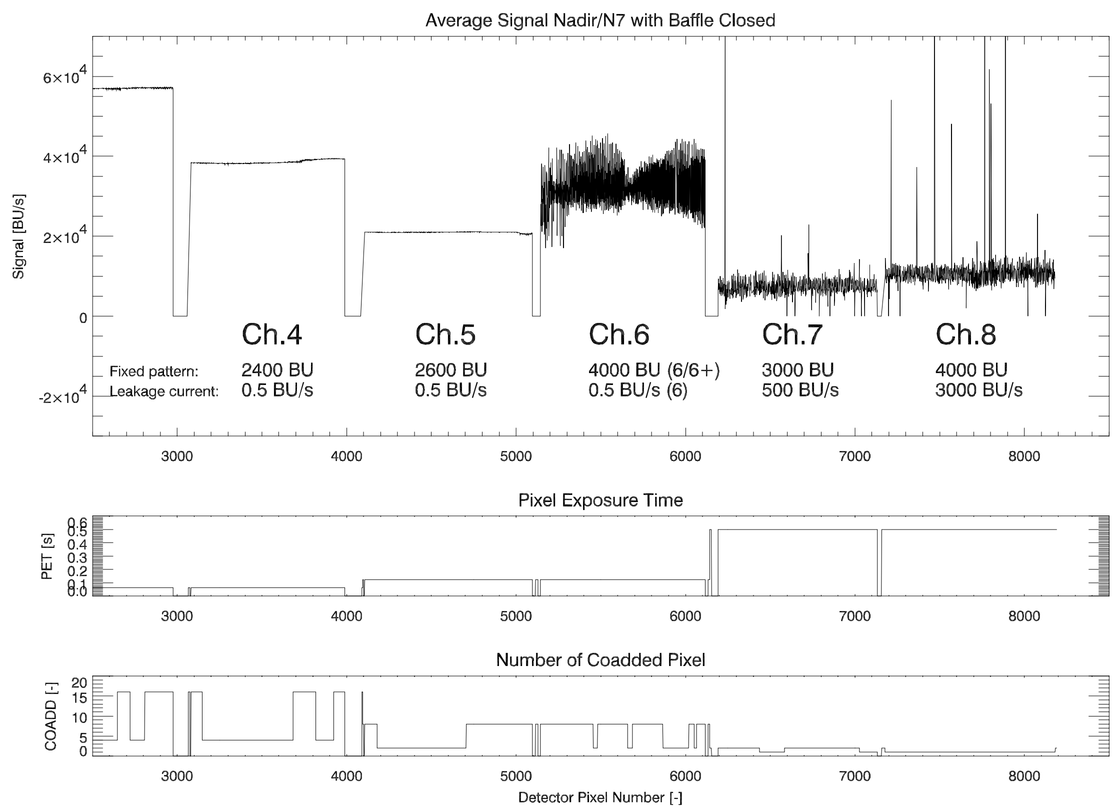

Figure 13: Typical SCIAMACHY dark signals in channels 4–8. The total dark signal consists of an exposure time independent part (in BU) and an exposure time dependent part (in BU/s). Typical values for the different channels are given in the top panel.

Estimate of resulting CO_2 error and its characteristics:

As can be seen from Tab. 5 an offset of 5 BU over a scene with not too low albedo (i.e., outside water or snow/ice covered surfaces) is expected to cause a CO_2 retrieval error of well below 1%, typically 0.1%. Even for very low albedo the error is “only” about 2% at maximum. This means that the orbital variation of the dark signal is expected to result in a CO_2 retrieval error that is correlated (on average) with the orbital phase and has an amplitude of less than 2%.

The impact of this error on the quality of a future channel 7 CO_2 column data product is small because good measurements will be restricted to moderate to high albedo scenes (for which the error is only about 0.1%). Measurements over very low albedo scenes (water, snow/ice covered surfaces) will suffer from many additional problems such as low signal-to-noise ratios and correspondingly a low precision of the CO_2 columns.

REFORBITS requirements:

The dark signal varies over an orbit, i.e., there is an orbital phase dependence of the dark signal. This orbit dependence is currently not / not good enough taken into account in the calibration (to be confirmed).

Therefore, at least one orbits needs to be analyzed as a starting point. The particular choice of the orbit is not critical. Orbit 8663 from October 27, 2003, could be used. This orbit has also been used for CO verification. It passes over eastern Africa with a large number of sufficiently cloud free pixels.

The calibration of the Level 1 spectra has improved over time (different versions). Initial channel 6 processing of year 2003 spectra by WFM-DOAS revealed significant errors due to non-optimal dark signal calibration. Therefore, the binary Level 1 files had been "patched" to improve the dark signal calibration. Dark signal calibration was and is the most important/critical step during the radiometric calibration. Recent channel 6 year 2004/2005 processing by WFM-DOAS yields much better results using the standard Level 1 products (without "patching"). This indicates that the calibration of the operational products has been improved. It is still to be investigated, however, if this is also true for channel 7.

Therefore, several orbits should be analyzed covering the time period 2003–2005. A good data set would be all available orbits over Park Falls, Wisconsin, USA, because of the Park Falls ground-based FTS measurements (2004-2005). Comparison with TM3 model simulations (2003) and channel 6 WFM-DOAS v0.4 (2003-2005) is also possible for this data set.

4.2.5 Detector non-linearity issue

Description of the issue:

The maximum error due to detector non-linearity (NL) is about 250 BU. Kleipool (2003) has presented an algorithm to correct for NL. After the correction the total noise due to NL ranges from 12 to 18 BU (1 σ) at 10 kBU and 40 kBU respectively.

Estimate of resulting CO_2 error and its characteristics:

A 12-18 BU error will result in a CO_2 retrieval error of well below 1% for most land surfaces as can be concluded from Tab. 5. Depending on the homogeneity of the the ground scene the error adds to the total random and systematic error. The characterization of the error e.g. in terms of ground scene dependence is extremely difficult. Because the error is relatively small and difficult to characterize it will be difficult to clearly identify this error component in the retrieved CO_2. Even if this would be possible it would be difficult to correct for it.

REFORBITS requirements:

The corresponding error will be difficult to detect. Analysis of the Park Falls 2003-2005 orbits data set, or a subset of this, will probably confirm this.

4.2.6 Summary channel 7 issues

Three important issues have been identified which can result in CO_2 errors on the order of 1–10% (or larger), namely (i) the light leak issues which might result in errors of the retrieved CO_2 over land of several percent (over low surface albedo scenes such as oceans and snow/ice covered surfaces the error might be as large as 30%), the ice-issue which results in changes of the instrument slit function and might cause a time dependent bias up to about 20% (estimate from channel 8 methane retrieval), and (iii) the dead/bad pixel mask issue.

5 Preparation and initial channel 7 CO_2 retrieval (WP 2100)

Start of WP 2100: Beginning of September 2005
End of WP 2100: End of October 2005

5.1 Adjusting WFM-DOAS for channel 7 retrieval

In order to perform WFM-DOAS retrieval the following steps have been performed: The generation of a look-up table of channel 7 radiances and derivatives computed with the SCIATRAN radiative transfer model, the adjustment of the configuration file of the retrieval program, and the compilation of an initial pixel mask.

The look-up table of channel 7 radiances and derivatives has been generated analog to the tables used for WFM–DOAS version 0.4 channel 6 CO_2 retrieval (Buchwitz and Burrows, 2004; Buchwitz et al., 2005a,b). The tables depend on: solar zenith angle, surface elevation, and water vapor column. WFM–DOAS uses a solar zenith angle interpolation scheme, a surface elevation next neighbor scheme, and an iterative scheme for water vapor. A a-posteriori correction is made for the scan angle dependence of the retrieved column.

5.2 Initial results

Here we present initial channel 7 CO_2 retrieval results. Figure 15 shows a comparison of channel 7 CO_2 columns retrieved from a single orbit (eastern Africa) with TM3 model simulations and WFM-DOAS version 0.4 CO_2 columns (retrieved from channel 6).

Figure 16 shows one year (2003) of channel 7 CO_2 measurements over Park Falls, Wisconsin, USA. For comparison, Figure 17 shows the year 2003 CO_2 columns of the WFM-DOAS version 0.4 data product.

Figure 18 shows a direct comparison of channel 7 CO_2 columns (shown as anomaly, i.e., the mean value has been subtracted) with WFM-DOAS version 0.4 XCO_2, TM3 model simulations, and preliminary XCO_2 ground-based FTS measurements. As can be seen, the scatter of the channel 7 measurements is significantly larger compared to channel 6 and also significant (few percent) biases (compared to channel 6) are visible especially during the first half of the year.

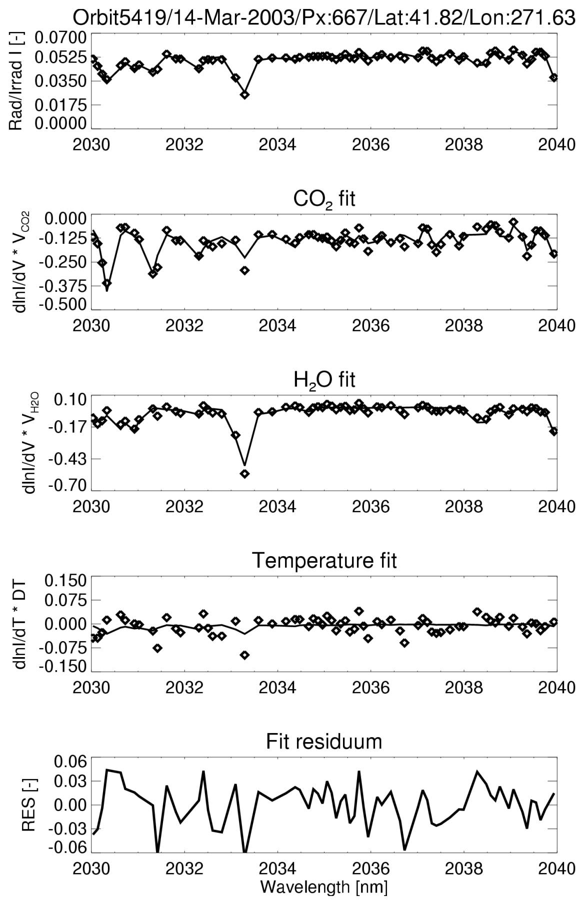

Figure 14: SCIAMACHY channel 7 WFM-DOAS example fit for the CO_2 fitting window from 2030 to 2040 nm. WFM-DOAS has been applied to a patched Level 1b/1c data of Orbit 05419 from 3 Mar 2003. The presented fit belongs to a spectrum recorded near Park Falls, Wisconsin (USA). Situation: cloud free, surface type soil, SZA 51 deg, LOS scan angle 20 deg. Fit: Gaussian slit function 0.23 nm, degree of polynomial: 2, shift and squeeze of earthshine spectrum (MODE SINGLE). Retrieved CO_2 column: 7.9e21$\pm$12%, RMS of fit residuum: 2.4%. The RMS is not noise limited but determined by systematic features. Subtracting the mean residuum (determined from a number of next-by ground pixels) reduces the RMS to 0.9%.

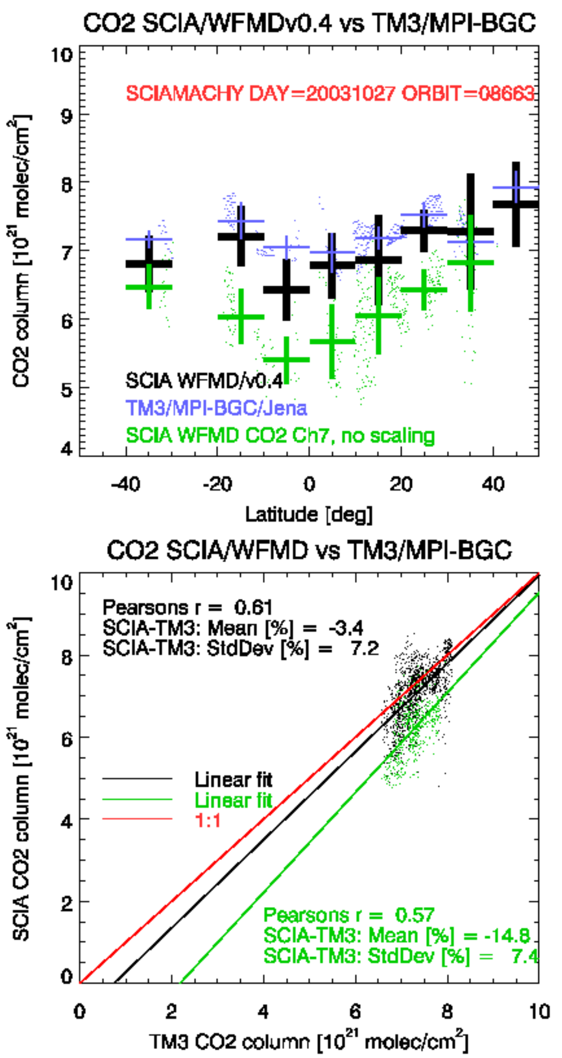

Figure 15: Initial channel 7 CO_2 columns (retrieved from orbit 8663, October 27, 2003) shown in green compared to TM3 model results (blue) and WFM-DOAS CO_2 version 0.4 (black). Top: CO_2 column versus 10 degree latitude mean and standard deviation (1-σ). Bottom: Correlation plot of channel 7 CO_2 (green) and v0.4 CO_2 (black) with TM3 CO_2 columns.

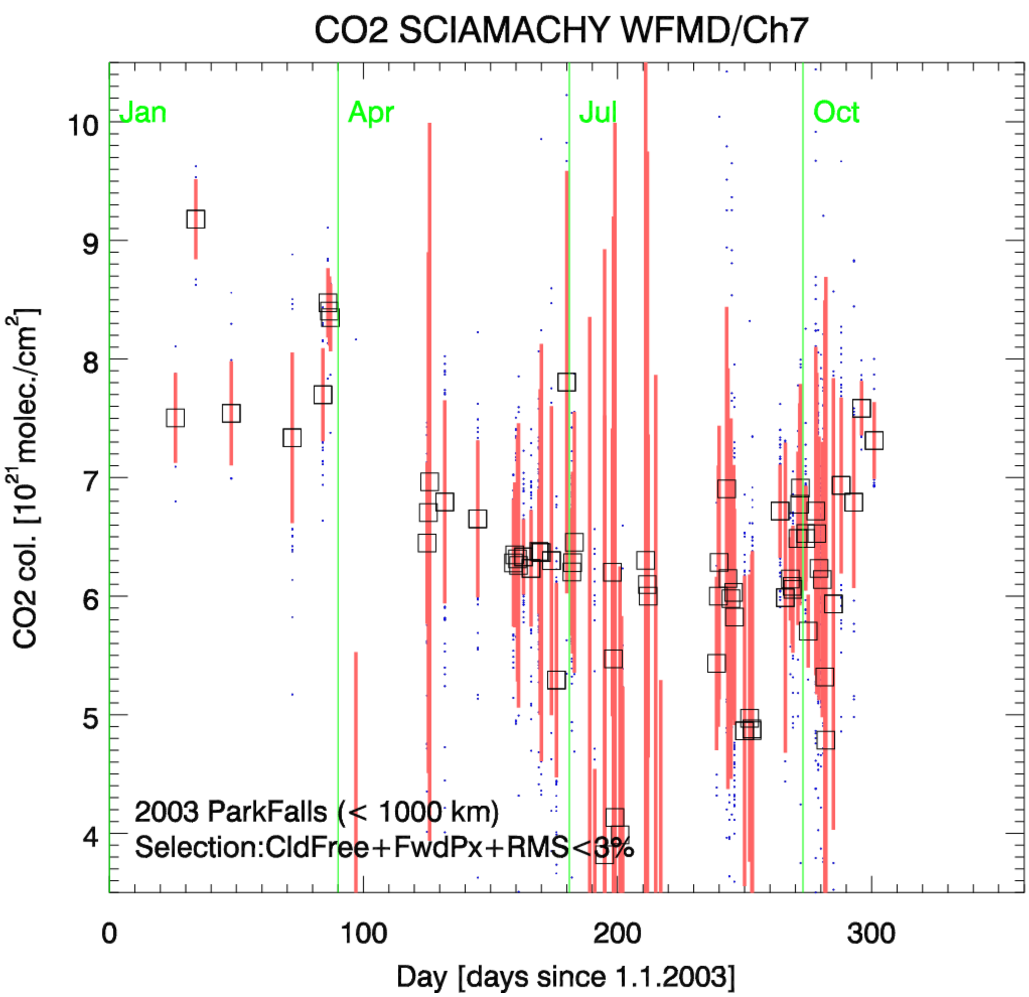

Figure 16: Year 2003 time series of channel 7 CO_2 columns over Park Falls, Wisconsin, USA. The individual measurements are shown as blue points. The symbols and vertical lines denote the daily mean and standard deviation. Selection criteria: Cloud free forward pixels, RMS of fit residuum less than 3%.

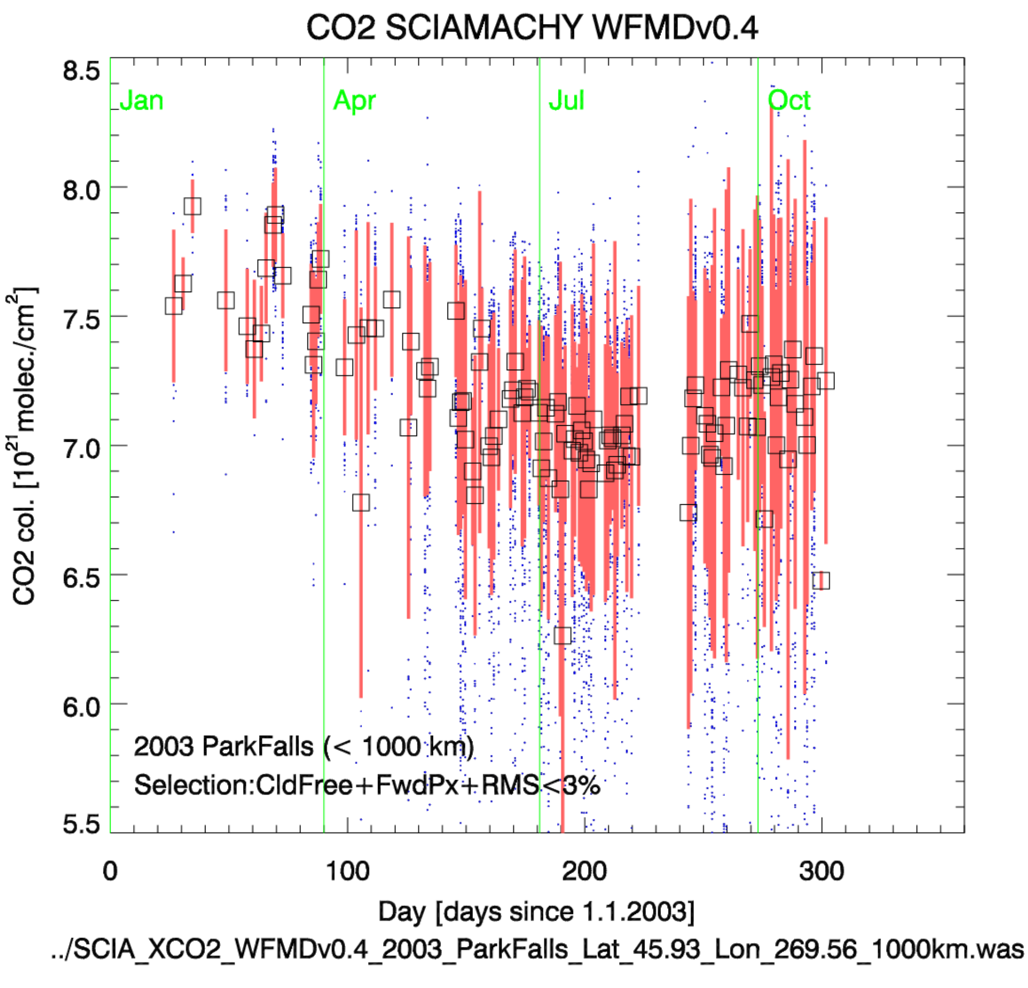

Figure 17: As Fig. 16 but for WFM-DOAS v0.4 CO_2 columns retrieved from channel 6 (using the same selection criteria as used for channel 7 CO_2).

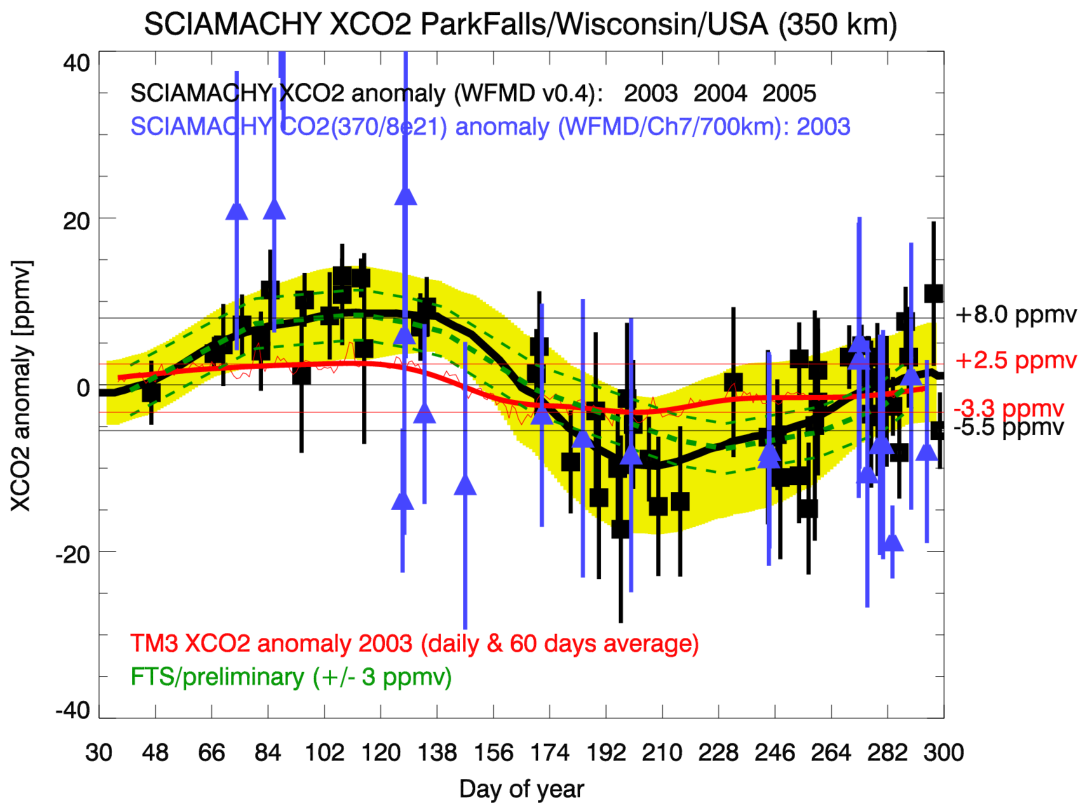

Figure 18: Comparison of channel 7 CO_2 (blue) with channel 6 CO_2 (black). The channel 7 CO_2 columns have been converted to a mixing ratio in ppmv by dividing the retrieved columns by 8e21 molecules/cm^2 (= assumed average CO_2 column for a ground pixel at sea level) and multiplication by 370 ppmv (the assumed mean column averaged mixing ratio). Because of the larger ground pixel size of the channel 7 measurements a selection radius of 700 km around Park Falls has been used for channel 7 CO_2 (350 km has been used for channel 6). Only cloud free forward pixels are shown for which the CO_2 column is within $\pm$20% of 8e21 molecules/cm^2 (for channel 7 and channel 6 CO_2). Additional criteria: fiterror less than 15% (channel 6: less than 8%), RMS of fit residdum less than 3% (channel 6: 0.65%). The green curved are the approximate values of the XCO_2 (anomaly) of the Park Falls ground-based FTS (preliminary analysis, not yet published, not yet available).

6 Estimation of Level 1–2 processing related CO_2 errors (WP 2100)

This section summarizes the existing literature on SCIAMACHY channel 6 CO_2 retrieval issues. For each identified issue an overview should be given how this issue affects the CO_2 retrieval:

- Estimate of magnitude of CO_2 retrieval error for each error source. This is important because due to the time constraints a priority lists needs to be established and work has to be prioritized to start developing solutions for the most important problems first.
- The characteristics of CO_2 retrieval error (e.g., dependence on season, orbital position, scene brightness (albedo, clouds), etc.) needs to be determined/described. The main question here is: What needs to be done to identify this error source in the retrieved CO_2 columns? The philosophy of this study is: Before algorithms will be developed to solve a problem it first needs to be established that the particular error has been detected using the retrieved channel 7 CO_2. After it has been demonstrated that the error is "visible" in the retrieved CO_2 solutions shall be developed. A successful solution is a solution for which it has been demonstrated that the error is no longer "visible" in the CO_2 or that at least the magnitude of the error has been significantly reduced.

WFM-DOAS version 0.4 carbon dioxide (XCO_2) is overestimated over scenes with high albedo (deserts, e.g., Sahara). The main reason is that WFM-DOAS version 0.4 assumes a constant albedo of 0.1. First order effects of albedo variability are taken into account by including a low-order polynomial in the WFM-DOAS fit. Second order effects, however, which result in differential structures in the derivative of the satellite observed radiance with respect to albedo changes are not considered. As a results errors on the order of a few percent occure (Buchwitz and Burrows, 2004; Buchwitz et al., 2005a,b).

Second errors due to aerosol (and sub-visual clouds) variability occure for similar reasons as for albedo variability (see also Houweling et al. (2005)). All errors occure, of course, in general simultaneously. For example over the Sahara (high albedo) in case of a large mineral dust storm (high aerosol load) (Buchwitz et al., 2005b; Houweling et al., 2005).

In Buchwitz and Burrows (2004); Buchwitz et al. (2005b) the aerosol-induced error is estimated to be on the order of 1% (if the albedo is 0.1). The error due to subvisual cirrus clouds may be as large as a few percent.

In Houweling et al. (2005) the aerosol-induced error over the Sahara of the CO_2 column is estimated to $\sim$10%. This value is believed to be a an upper limit for the error (worst case scenario). Averaged over all continents the CO_2 error is estiamted to be $\sim$3 ppmv ($\sim$1%).

At present no detailed studies have been performed how albedo, aerosol, and cloud variability can be better taken into accout in the CO_2 retrieval. Fundamental studies are needed to investigate several possibilities using SCIAMACHY measurements only (the is the preferred approach) and/or using additional information (e.g., from other satellites).

There exist a large number of other error sources, e.g., errors due to temperature and pressure profile variability, errors in the spectroscopic data, etc. Details are given in Sect. 6.1.

6.1 Initial WFM-DOAS channel 7 CO_2 error analysis

Here we present an error analysis for WFM-DOAS channel 7 (and 6) CO_2 retrieval using simulated SCIAMACHY measurements. Details are also given in Buchwitz and Burrows (2004) and Buchwitz et al. (2005a).

Table 6 gives a short overview about the two fitting windows analysed in this study located in channel 6 (WFM-DOAS version 0.4) and channel 7.

Channel	Spectral interval [nm]	Add. fit parameter	S/N [-]	CO_2 precision [%]
Ch6	1558 - 1594	H_2O, T	0.25: 670, 0.5: 1100	0.25: 1.0, 0.5: 0.6
Ch7	2030 - 2040	H_2O, T	0.50: 260, 1.0: 390	0.50: 1.4, 1.0: 0.9

Table 6: Overview of the spectral fitting windows and main retrieval parameters used in this study (first three columns). The last two columns indicate the performance of these channels in terms of signal-to-noise ratios and retrieval precisions. S/N is the average signal-to-noise-ratio (valid for a solar zenith angle of 50° and an albedo of 0.1) given for two integration times (value before colon, unit is seconds). Precision is the 1-sigma CO_2 column retrieval precision for the given S/N performance.

6.1.1 Sensitivity to surface albedo

To a first approximation albedo affects the overall (i.e., spectrally broadband) level of backscattered solar radiation. This effect is taken into account by the WFM–DOAS polynomial. Table 7 shows that the retrieval errors are less than 1–2% except for very low albedo scenes. Note that the WFM–DOAS look-up table used in this study has been generated assuming a constant (Lambertian) albedo of 0.1.

Albedo scenario	Ch6: CO_2 error [%]	Ch7: CO_2 error [%]
0.30	1.4	0.9
0.20	0.9	0.6
0.10	0.0	0.0
0.05	-1.3	-1.0
0.03	-2.6	-2.0
0.003	-10.3	-9.0

Table 7: Vertical column retrieval errors as a function of surface albedo. For an albedo of 0.1 the errors are zero because the WFM–DOAS reference spectra are calculated for albedo 0.1.

6.1.2 Sensitivity to aerosols and subvisual cirrus clouds

Aerosols and clouds mainly scatter but also absorb solar radiation. The bulk of the gases relevant for this study is situated in the lowest kilometers of the atmosphere, i.e., in a region where clouds and aerosols are present in extremely variable type and concentration.

The WFM-DOAS look-up table used in this study has been generated using a single aerosol scenario only. It is based on the aerosol parameterization also implemented in the radiative transfer model MODTRAN based on work done by Shettle and Fenn. This (default) scenario can be characterized as follows: Maritime aerosol in the boundary layer (BL), tropospheric visibility and relative humidity 23 km and 80%, respectively, and background stratospheric and normal mesospheric conditions.

To a first approximation aerosols increase or decrease the overall (i.e., spectrally broadband) level of solar radiation scattered back to space. This effect is taken into account by the polynomial included in Eq. (1). However, aerosols also determine the relative depth of absorption lines by influencing the (average) photon path.

The retrieval error due to aerosol has been estimated by defining several (including two rather extreme) aerosol scenarios (see Tables 3 and 4). The "OPAC average continental" aerosol scenario and radiative transfer simulations differ from the default scenario used for the reference spectra in various aspects (Mie phase function instead of Henyey-Greenstein approximation, scattering and extinction profiles). "OPAC average continental" aerosol consists of a mixture of "water soluble aerosol" (small particles mainly originating from gas-to-particle conversion), soot, and "insoluble aerosol" (dust). The "Enhanced aerosol in boundary layer (BL)" scenario contains urban aerosol in the BL with a visibility as low as 2 km and a high relative humidity of 99%. For the "No aerosol in atmosphere" scenario the aerosols have been entirely "switched off" in the radiative transfer simulation. Table 4 shows that WFM-DOAS as applied to NIR spectra appears to be rather insensitive to aerosols ($<$ 1%). In the visible (O_2 A-band) the sensitivity is, however, significantly larger.

No attempts have been made so far to extend WFM-DOAS by a cloud correction scheme in order to deal with clouds (e.g., partial cloud cover or thin clouds). The current approach is based on identification (and elimination) of cloud contaminated ground pixels. SCIAMACHY offers various possibilities for cloud detection, even on sub-pixel scale. In this study a very simple threshold algorithm is used based on SCIAMACHY's UV PMD (Polarization Measurement Device) measurements. Even with a more sophisticated algorithm it might not be possible to identify all cloud contaminated pixels.

A certain level of cloud contamination might even be tolerated in order to increase the number of useful measurements. In this context it is interesting to estimate the vertical column retrieval error resulting from (undetected) subvisual cirrus clouds. These clouds are predominantly a tropical/subtropical phenomenon. Cirrus clouds have been modeled in this study as a scattering layer of 1 km vertical extent centered at 12 km. The assumed scattering vertical optical depths were 0.01, 0.02, and 0.03 independent of wavelength. This is a reasonable assumption because the particles are much larger than the wavelength considered here. A scattering optical depth of 0.03 roughly corresponds to the maximum optical depth of subvisual cirrus clouds at 500 nm. Table 4 shows that such a scattering layer near the tropopause is expected to lead to an underestimation of the retrieved vertical columns (shielding of the troposphere lying underneath) by more than 1% in most cases. For an optical depth of 0.03 they estimated this error to be -1.0% (here: -1.4%) at 1.6 μm and -2.0% (here: -3.7%) at 2.0 μm. Identical values are not to be expected because of the different spectral resolution and spectral intervals used in both studies. Concerning aerosols they also found similar errors ($<$ 1.5 ppmv (or 0.4%)) as given in Tab. 8 for CO_2.

Aerosol/cloud scenario	Ch6: CO_2 error [%]	Ch7: CO_2 error [%]
Aerosol:		
OPAC average continental	-0.5	-0.2
Enhanced aerosol in BL	-0.9	-0.8
No aerosol in atmosphere	-0.8	-0.1
Clouds:		
Subvisual cirrus (OD 0.01)	-0.4	-1.2
Subvisual cirrus (OD 0.02)	-0.8	-2.4
Subvisual cirrus (OD 0.03)	-1.4	-3.7

Table 8: CO_2 vertical column retrieval errors resulting from aerosol variability and undetected subvisual cirrus clouds at 12 km (OD means scattering optical depth).

6.1.3 Sensitivity to temperature and humidity profiles

The currently implemented look-up table has been generated assuming vertical profiles of pressure, temperature and trace gas volume mixing ratios corresponding to the US Standard Atmosphere (CO_2 concentrations scaled to 370 ppmv). In order to estimate the vertical column retrieval errors resulting from applying WFM-DOAS to different atmospheres, simulated spectra for several model atmospheres have been generated. The results are shown in Tab. 9. The retrieval errors mainly reflect the difference in temperature and water vapor profiles of the various atmospheres compared to the US Standard (USS) reference atmosphere (Temperatures at sea level: USS 288.1 K, SAW 257.2 K, TRO 299.7 K; H_2O columns in g/cm^2: USS 1.43, SAS 0.21, TRO 4.18). As can be seen the CO_2 errors are on the order of 1-2%.

Atmospheric scenario	Ch6: CO_2 error [%]	Ch7: CO_2 error [%]
Sub-arctic summmer (SAS)	0.0	0.6
Sub-arctic winter (SAW)	0.1	-1.7
Mid-latitude summer (MLS)	-0.1	-0.2
Mid-latitude winter (MLW)	0.4	0.0
Tropical (TRO)	-0.4	-2.3

Table 9: CO_2 vertical column retrieval errors resulting from applying WFM-DOAS to spectra generated using various model atmospheres.

7 Investigation of solutions for major channel 7 issues (WP 1200)

Start of WP 1200: Beginning of November 2005
End of WP 1200: End of January 2006

7.1 Light leak issue

7.1.1 Where is the light coming from?

In order to develop a light leak correction algorithm it first needs to be investigated where the light comes from. It could come, for example, exactly from the nominal ground pixel observed in nadir mode or, because this is unlikely, from the scene near the nominal ground pixel, i.e., from its surroundings. It might also come from the entire hemisphere below the satellite. In this case the spatial and temporal dependence (variability) of the light leak signal will be relatively small and not well correlated with the magnitude of the (average or background) channel 7 signal which is typically clearly dominated (at least for moderate to high albedo scenes) by photons originating from the nominally observed ground pixel.

It might be possible to answer this question by comparing the light leak signal with ground scene images obtained from SCIAMACHY (e.g., PMD) or other sources. The light leak has been measured (directly) using special dark states executed during “dark orbits” (orbits 3959 and 3960 from December 2, 2002, during the delta SODAP period) (Skupin, 2003). During the dark states the detector signal in limb geometry at observation tangent height of 150, 200, and 250 km has been measured over the entire orbit to analyze the orbital and tangent height dependence of the straylight.

The dark orbit signals have been compared with the effective top-of-atmosphere (TOA) albedo estimated from US-GOES East and West satellite data. The GOES albedo was estimated using the GOES pixel intensity and assuming that the later is proportional to TOA albedo. In a first approximation this assumption is valid and useful for this case study because clouds are white and reflect radiation quite well. Since the light leak is a problem only for channel 7 one can assume that the light does not enter the optical path at the beginning of this path (i.e., near the front of the spectrometer) but at a later stage relatively close to the end of the channel 7 light path. Otherwise more channels would have been affected. Because only channel 7 is affected by a light leak the leak must originate from a location near the channel 7 detector thereby influencing only channel 7. Not only NIR radiation may enter channel 7 but also radiation at shorter wavelength may contribute to the observed signal as also photons at UV/visible wavelength have an energy larger than the band gap of the channel 7 NIR detector.

For the darks orbits mentioned above co-located images from US-GOES East and West geostationary weather satellites are available. Figure 19 shows the segments of these images used to calculate the albedo equivalent pixel intensities for the corresponding sections of darks orbits 3959 and 3960. The albedo equivalent pixel intensities were calculated by averaging over GOES 20 scan lines and the total width of the segment surrounding the subsatellite point. This segment was shifted along the GOES track in steps of 5 scan lines.

The results of the GOES averaged pixel intensities for orbits 3959 and 3960 compared to the light leak signals of the dedicated SCIAMACHY dark orbits are shown in Figs. 20 and 21.

Figure 20 shows a reasonable correlation between the SCIAMACHY light leak signal of orbit 3959 and the GOES albedo equivalent pixel intensity. It seems that the GOES intensities are slightly shifted to the right. This is probably to some simplifications which have been used when computing the GOES signals (only values near the subsatellite point have been used). The main question to be answered is if the light which causes the light leak signal really originate from this area of the atmosphere. Figure 21 shows a similar comparison but for orbit 3960. Here the correlation between the light leak signal and the GOES intensity is not very good.

From Fig. 20 it can be concluded that there is some evidence that the light that causes the light leak orginates from the sub-satellite scene but it is not possible to say exactly from which part of the atmosphere. More studies are needed before

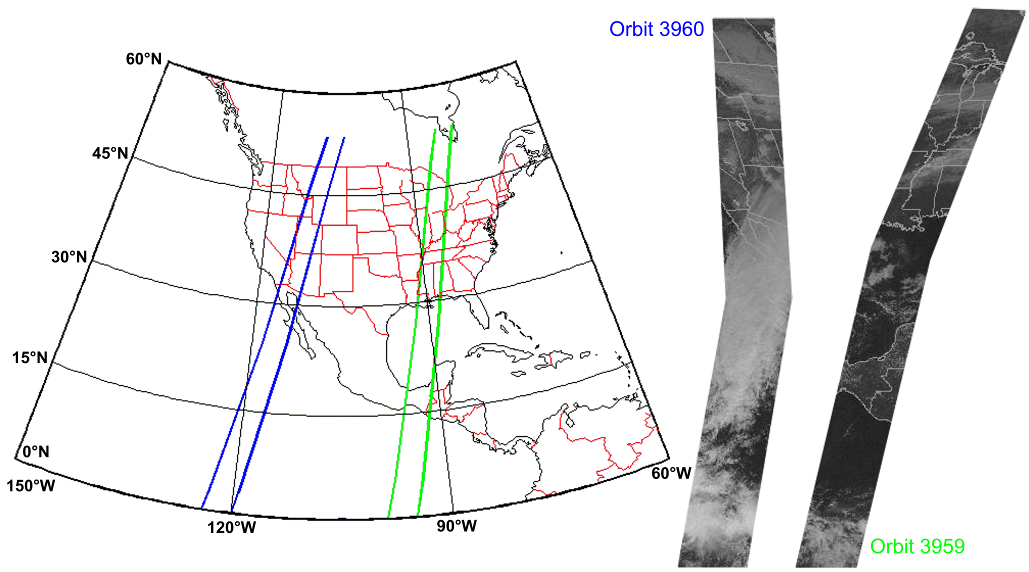

Figure 19: Segments of the US-GOES East and West weather satellite images used for the albedo calculations shown on the right. The corresponding sections of SCIAMACHY dark orbits 3959 and 3960 are shown on the left.

clear conclusions can be drawn.

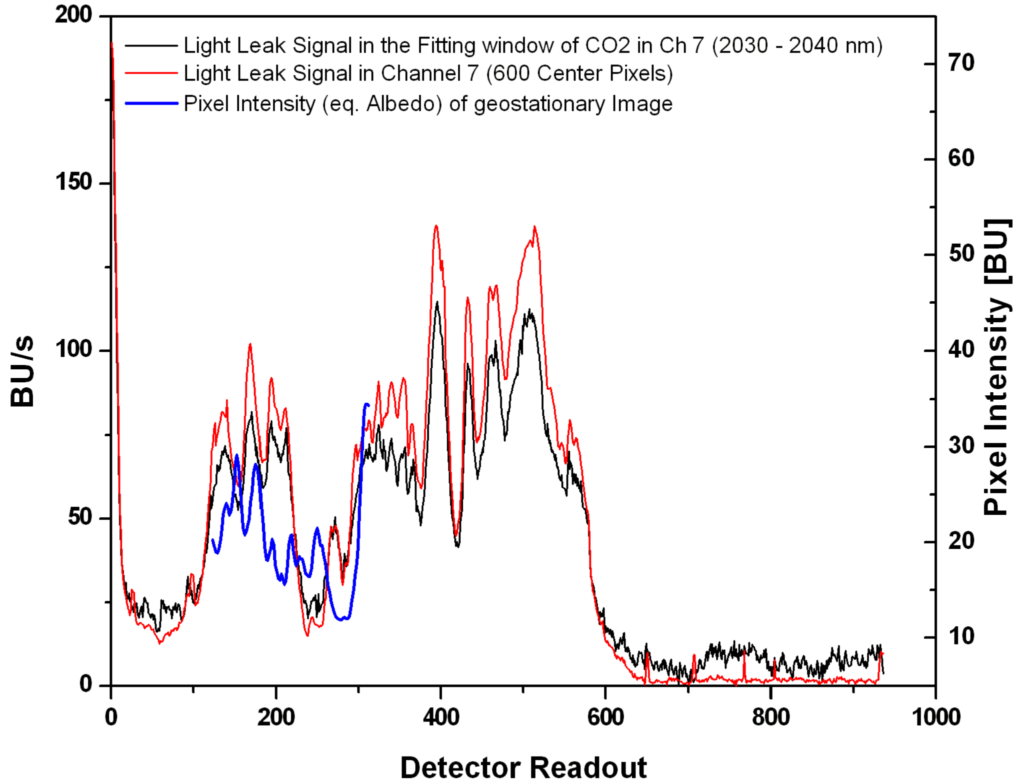

Figure 20: Light leak signal for channel 7 in orbit 3959 averaged over the 600 center pixels (red line) as presented in Skupin (2003) and the 102 pixels of the CO_2 fitting window (black line) compared with pixel intensity (equivalent cloud albedo) measured by the geostationary weather satellite US-GOES-East (blue line). The measurements along the orbit are denoted “Detector readout” (0 = beginning of orbit (roughly when the satellite leaves the eclipse when going from the nightside onto the dayside), 1000 = end of orbit). The high signal around detector readout zero is because the sun is within the total clear field-of-view of SCIAMACHY.

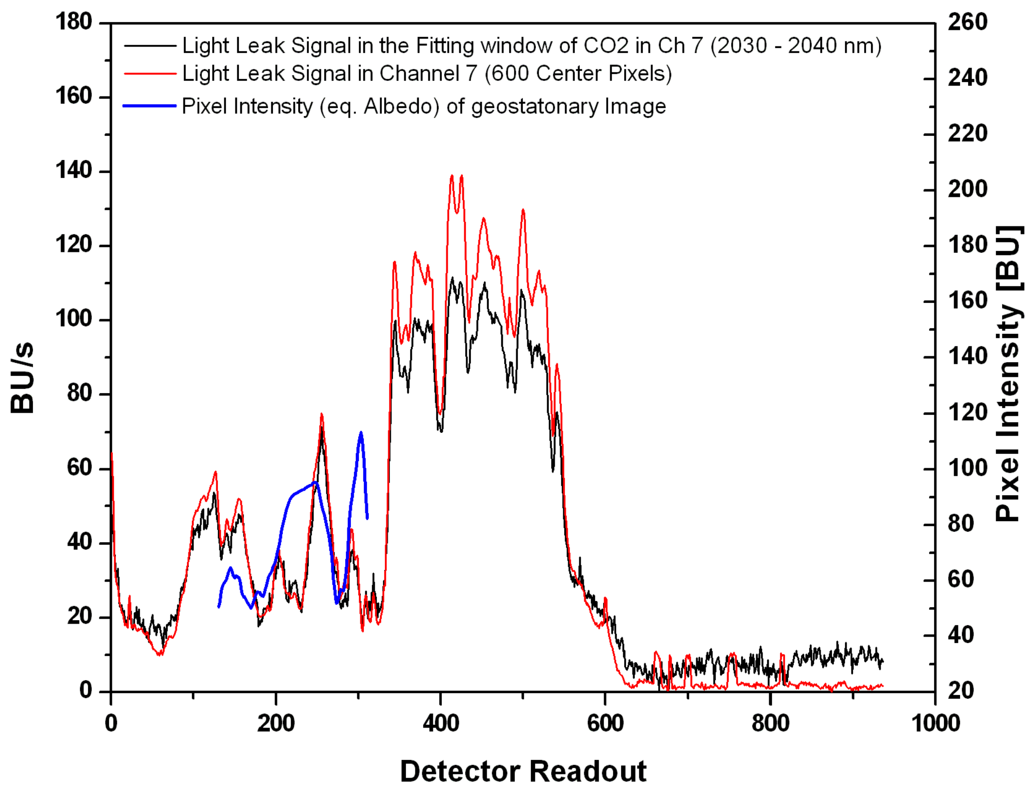

Figure 21: Light leak signal for channel 7 in orbit 3960 averaged over the 600 center pixels (red line) as presented in Skupin (2003) and the 102 pixels of the CO_2 fitting window (black line) compared with pixel intensity (equivalent cloud albedo) measured by the geostationary weather satellite US-GOES-West (blue line).

7.1.2 Spectral dependence

One feature of the light leak signal is the inhomogeneity of the signal across the detector array. Figs. 22 to 25 show the light leak signal averaged over 10 different areas (wavelength regions) of the detector array. Figs. 22 and 24 indicate that the light leak signal is strongest near the center of the detector array (pixel numbers between 200 and 500). This means that the light leak signal is not constant over the channel which further complicates this issue.

This has also been reported in Skupin (2003) (see Fig. 9). This figures shows that the light leak signal has a rather smooth spectral dependence. A correction algorithm is proposed in Skupin (2003): Assuming a stable spectral structure on the dayside (which could be characterized regularly using dark orbits from the monthly calibration sequence) only the amplitude needs to be determined for each measurement (ground pixel) on the dayside. It needs to be investigated if this amplitude can be estimated accurately enough using spectral regions with very strong (saturated) absorption lines (of CO_2 and/or water vapor). One of the issues that complicate this is that different custers are read out with different exposure / integration times. In the 2030-2040 nm baseline spectral fitting window used for this study the integration time is typically 0.5 seconds but most of channel 7 is read out with an integration time of 1 second. The 2030-2040 nm spectral window does not contain very strong absorption lines.

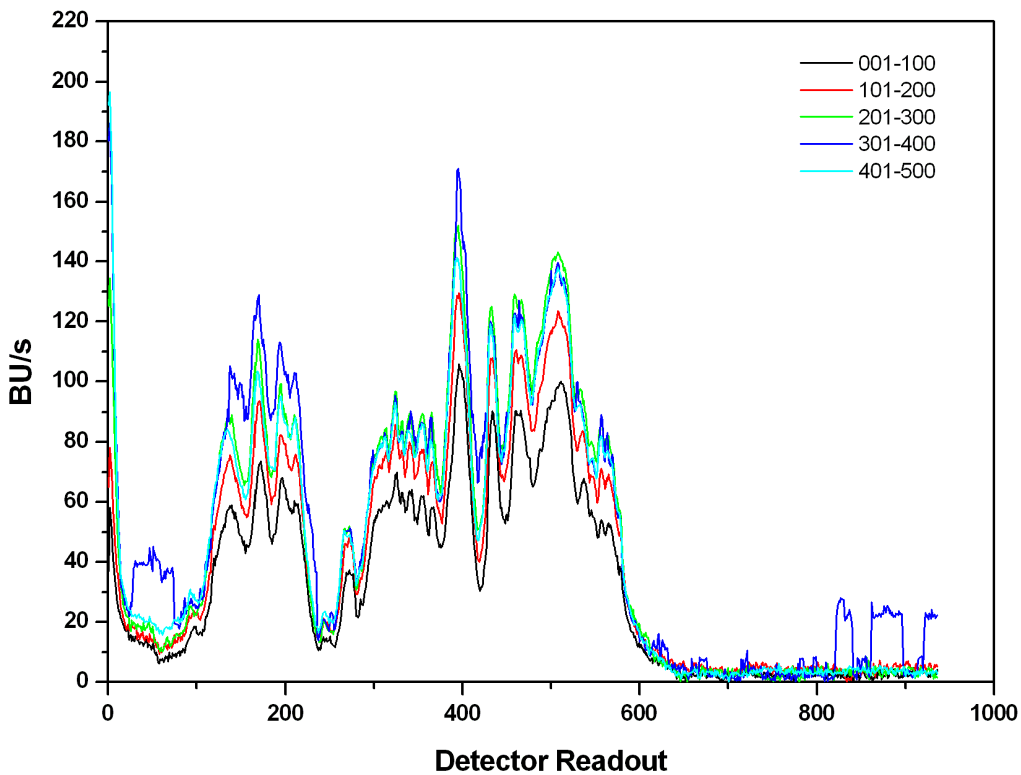

Figure 22: Light leak signal for channel 7 of orbit 3959 as a function of the pixel position on the chip. 5 different areas are shown. The line marked by '001-100', for example, represents the averaged light leak signal over pixel numbers 1 to 100.

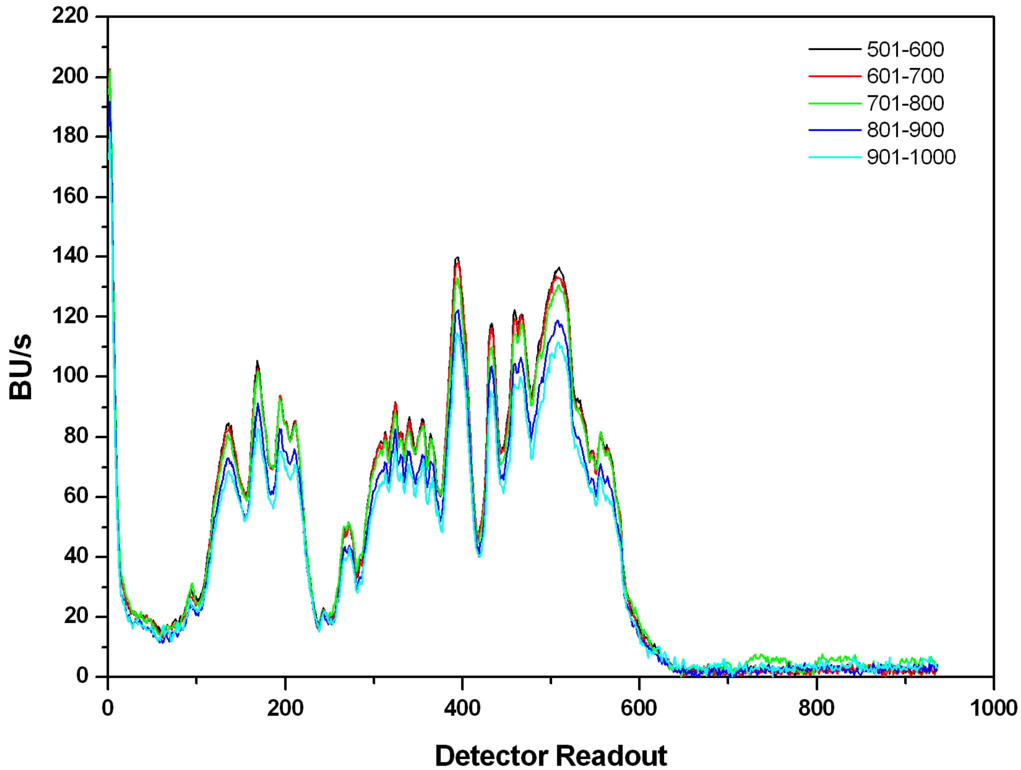

Figure 23: Light leak signal for channel 7 of orbit 3959 as a function of the pixel position on the chip. 5 different areas are shown. The line marked by '501-600', for example, represents the averaged light leak signal over pixel numbers 501 to 600.

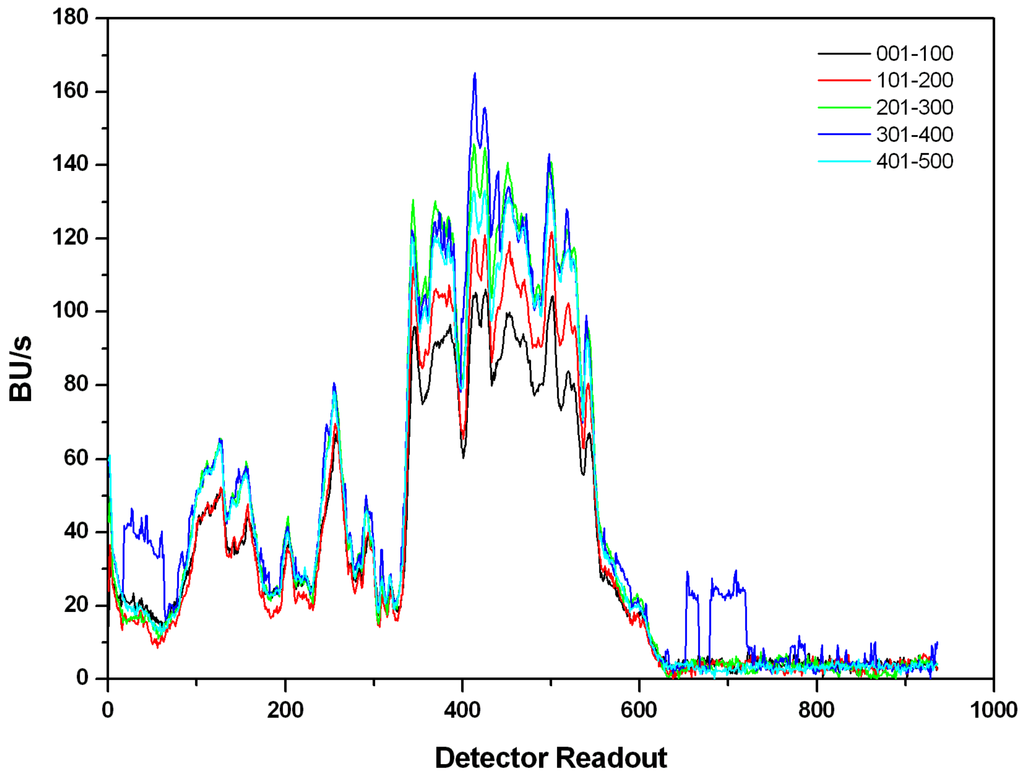

Figure 24: Similar as Fig. 22 but for orbit 3960.

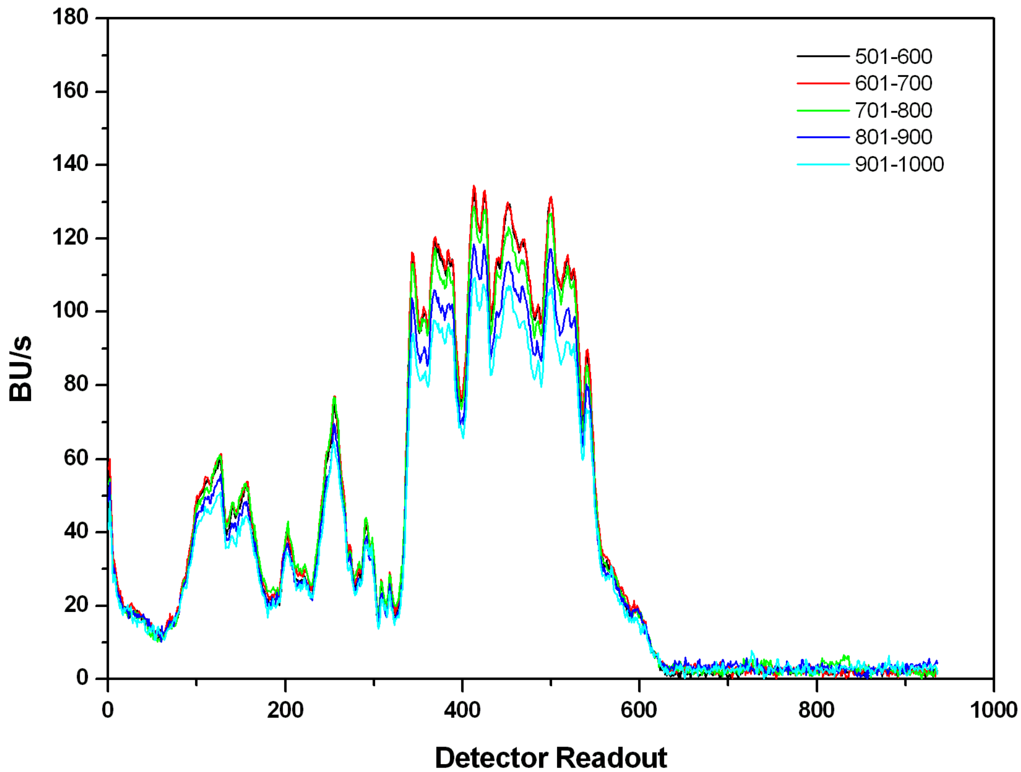

Figure 25: Similar as Fig. 23 but for orbit 3960.

7.1.3 Analysis of retrieved CO_2

Figure 26 shows CO_2 columns retrieved from SCIAMACHY channel 7 from orbit 4757 (January 27, 2003) over Europe, western Africa, and the Atlantic Ocean. Only measurements for cloud free pixels are shown. Measurements over land are shown in black and measurements over water are shown in red. The average CO_2 over land is 7.78 10^{21} molecules/cm^2. The average CO_2 over water is 5.92 10^{21} molecules/cm^2. The mean difference (land - water) is 31%. This is in good agreement with the estimated CO_2 error due to the light leak issue if a constant offset of 100 BU is assumed (see Sect. 4.2.1).

Figure 27 shows the retrieved CO_2 column if 100 BU is subtracted from the nadir signal. As can be seen, the column difference between water and land visible in Fig. 26 nearly vanishes because the effect of subtracting 100 BU leaves the CO_2 columns over land nearly unchanged but results in an increase of the retrieved CO_2 over water of about 30%.

Figure 28 shows the ratio of the uncorrected columns (shown in Fig. 26) and the "corrected" columns (shown in Fig. 27). The effect of subtracting 100 BU from the nadir spectrum is, in line with what has been estimated in Sect. 4.2.1, about 2% over land and 27% over water. The standard deviation of the difference over land is about 1%. Assuming that the light leak causes a constant 100 BU offset on the nadir spectrum over land the resulting error is on the order 1-2% (about 2% systematic underestimation; about 1% ground scene brightness/albedo dependent scatter).

Figures 29 to 31 show similar plots but for orbit 4714 from January 24, 2003. Here the difference of the CO_2 columns over land and water is only about 10%. A 100 BU "correction" of the nadir spectrum results in a significant overestimation of the retrieved columns over water. This shows that a simple offset is not sufficient to correct for the light leak which depends in a complicated way on the ground scene (including the scene outside the nominally observed field-of-view) and its homogeneity/heterogeneity.

Because focus is on the SCIAMACHY CO_2 measurements over land the situation is not that dramatic because the estimated CO_2 light leak induced error is relatively small (about 1-2%) even if no correction is applied. It should be possible with a relatively simple correction (e.g., based on the average channel 7 signal (e.g., assuming that a linear relation exists between the average signal of channel 7 and the light leak signal)) to reduce this error (over land) to below 1%. This however still needs to be investigated and to be confirmed.

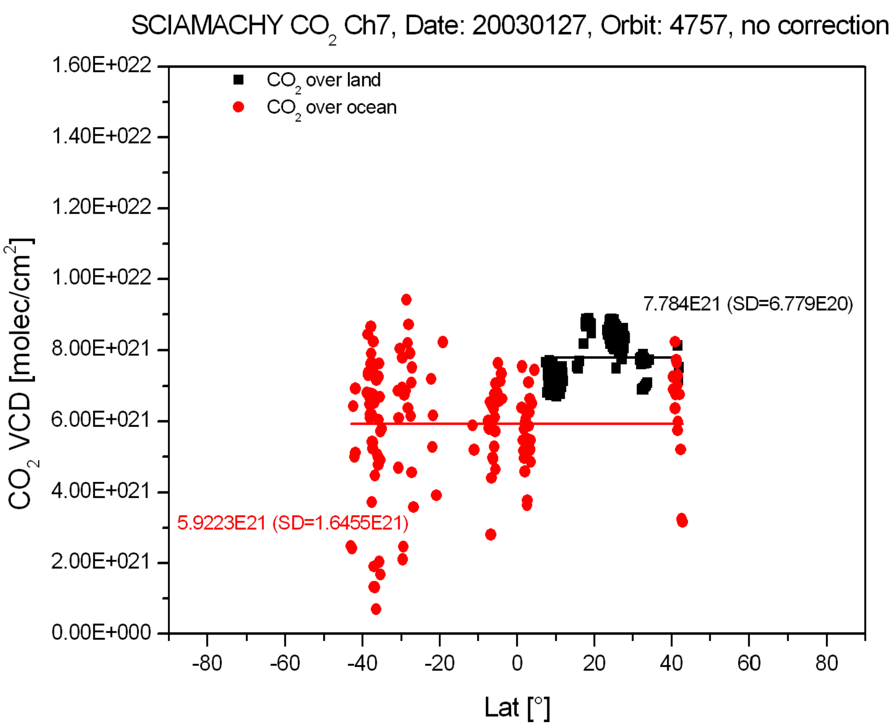

Figure 26: CO_2 vertical columns retrieved from cloud free SCIAMACHY measurements (orbit 4757, January 27, 2003) over land (black) and water (red). The symbols show the individual measurements. The vertical lines show their mean values (the value of the mean and of the standard deviation are also given in the annotation of the figure).

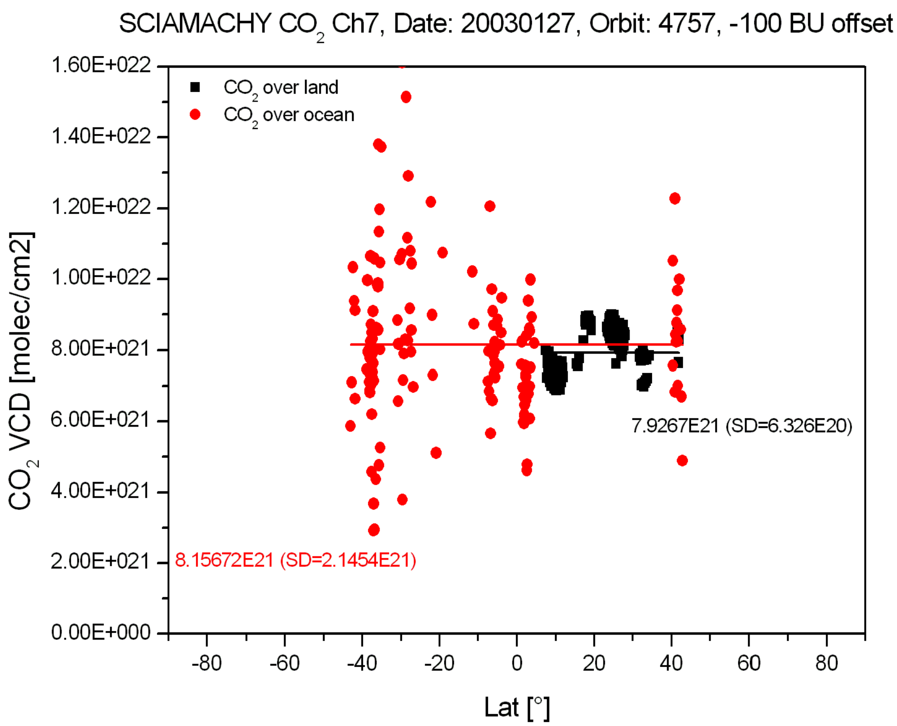

Figure 27: As Fig. 26 except that 100 BU have been subtracted from the nadir signals (corresponding to a first order light leak correction).

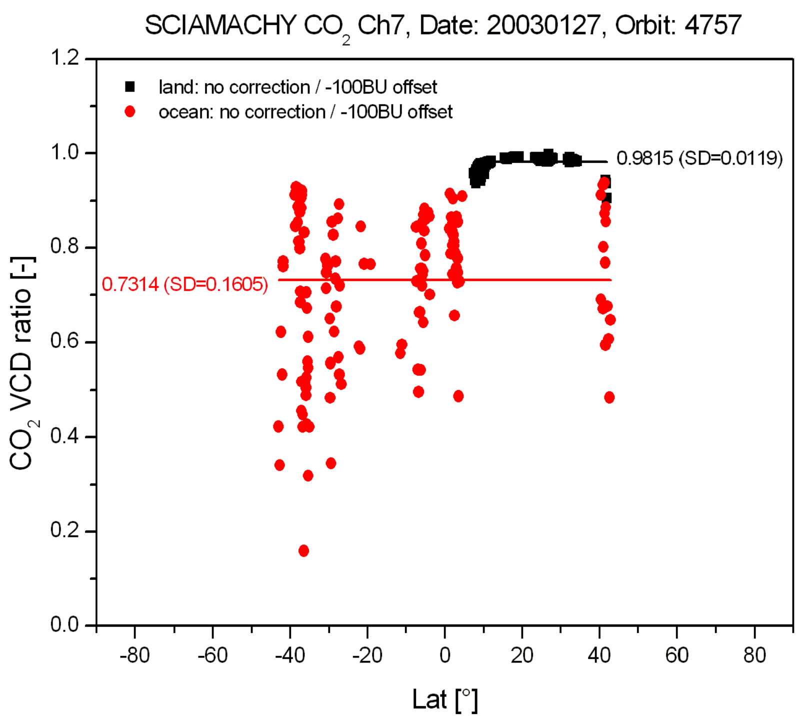

Figure 28: Ratio of the columns shown in Figs. 26 and 27.

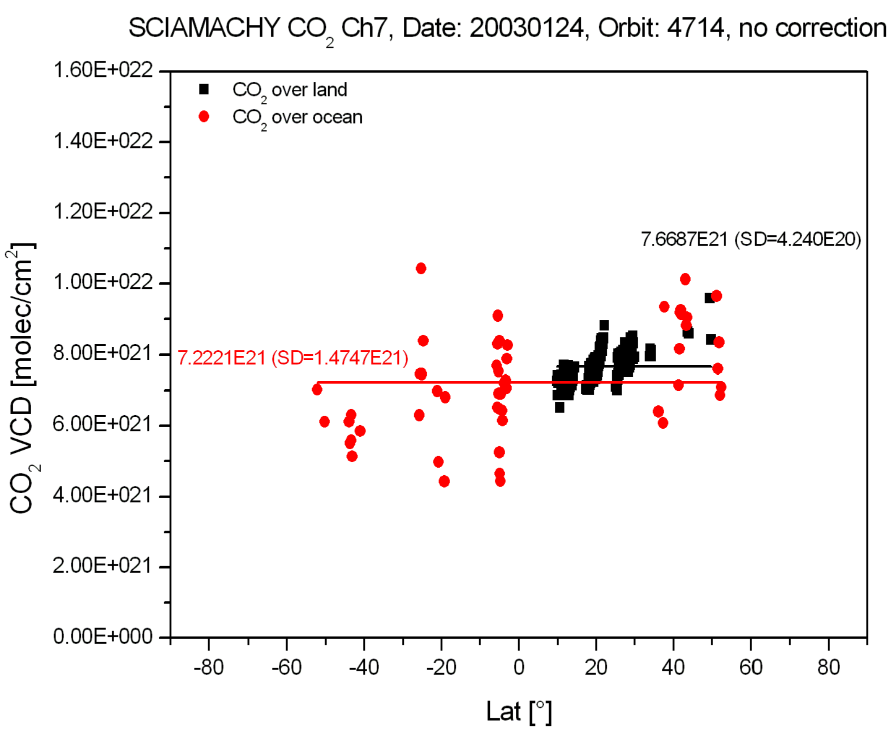

Figure 29: As Fig. 26 but for orbit 4714 (January 24, 2003).

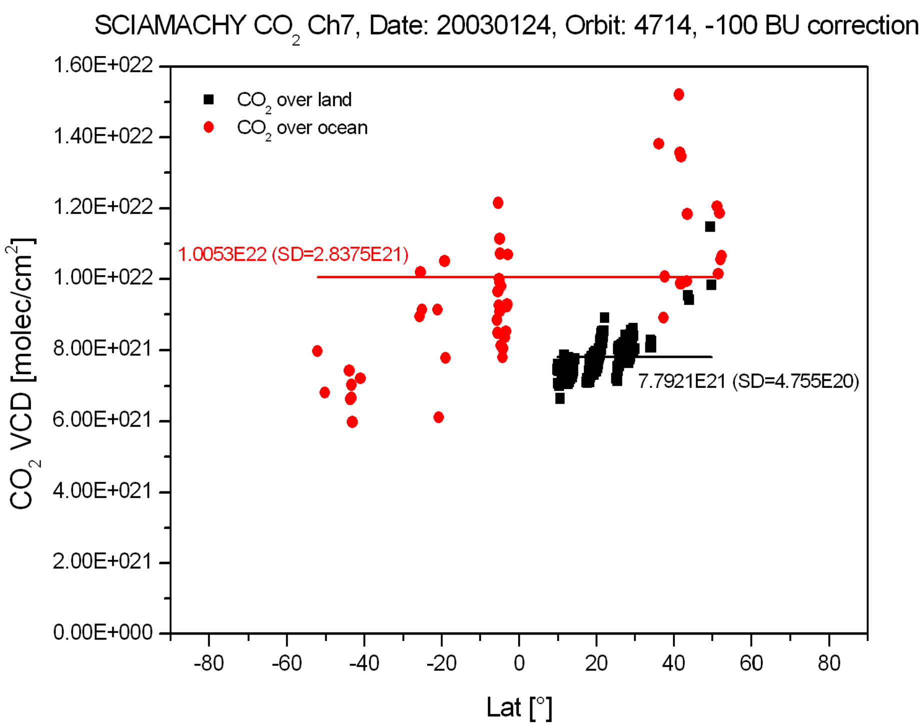

Figure 30: As Fig. 27 but for orbit 4714 (January 24, 2003).

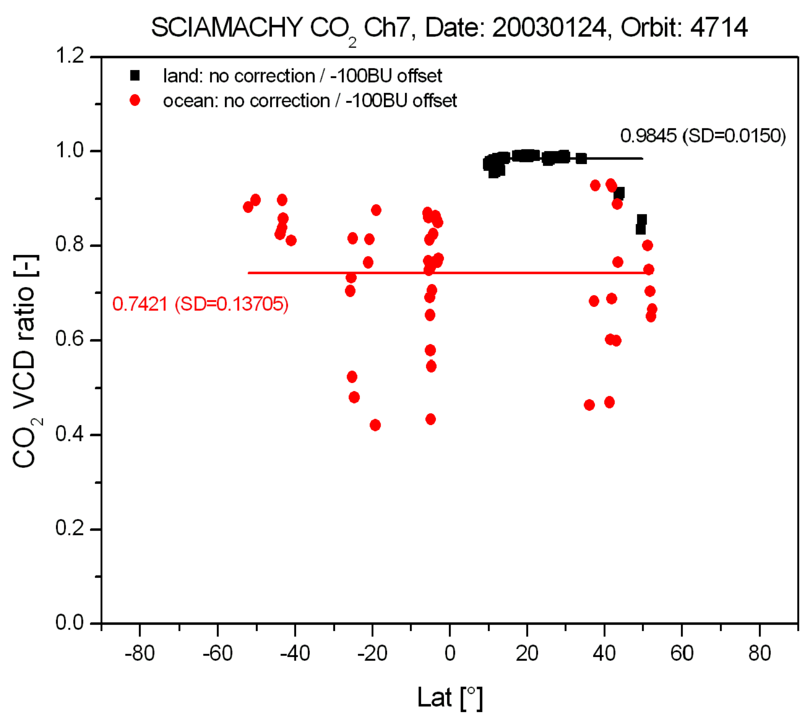

Figure 31: As Fig. 28 but for orbit 4714 (January 24, 2003).

7.1.4 Light leak determination using saturated CO_2 lines

The posposed solution to deal with the light leak in channel 7 is to use saturated CO_2 lines in cluster 51 to determine the offset caused by the light leak due to the fact that at wavelengths of saturated CO_2 lines no atmospheric radiance is registered by the detector pixel. In case radiance is detected by pixels located in the center of saturated CO_2 lines this radiance has to come from other sources (i.e. the light leak). An example for strong CO_2 lines is shown in Fig. 32. To investigate which pixels are the best candidates to determine the light leak signal a histogram is plotted in Fig. 33 identifying those pixels having the most minimum value occurrences in all sprectra of an entire orbit. This procedure identified pixel numbers 634, 639, and 650 as best candicates to determine the light leak signal.

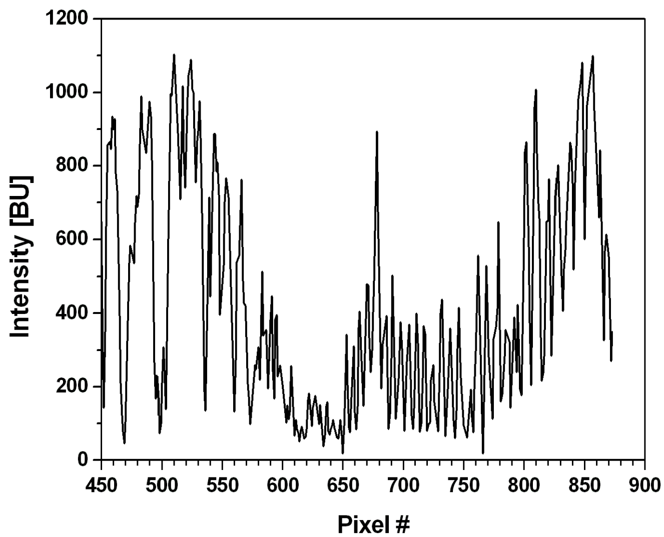

Figure 32: CO_2 spectrum measured by SCIAMACHY in channel 7.

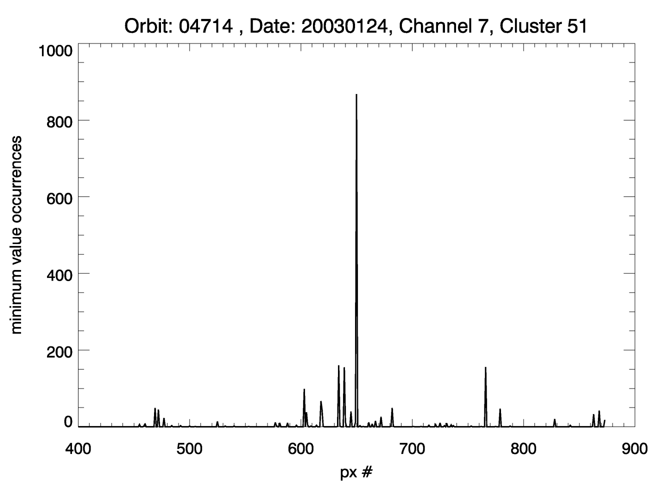

Figure 33: Histogram of minimum value occurrences of SCIAMACHY channel 7 pixels.

The next major question is: are the CO_2 lines really saturated under all circumstances? To answer this question radiative transfer calculations have been performed. Fig. 34 shows the CO_2 lines (the pixel positions are marked by the three magenta colored vertical bars) chosen to determine the light leak signal for various conditions (SZA, surface albedo, and surface elevation). As can be seen in this plot these CO_2 lines are by no means saturated under all conditions. Surface elevation has a large influence on the saturation of the CO_2 absorption lines because the CO_2 over elevated surfaces can be dramatically reduced due to the reduced air pressure. Another large influence is caused by the variation of the SZA because at high SZA the light path through the atmosphere is enhanced as is the CO_2 absorption. Thus the CO_2 lines are more saturated at high SZA as at low SZA. To determine the light leak signal from real SCIAMACHY channel 7 measurements the simulated radiance modelled for the specific SZA, surface albedo and elevation of the ground scene has to be subtracted from the measured signal.

Fig. 35 shows the uncorrected signal averaged over the three pixels (634, 639, and 650) used to determine the signal at the saturated CO_2 absorption lines. This signal is plotted on top of MODIS cloud map for the specific day. The signal is devided by the cosine of the SZA to correct for the SZA dependend reflected cloud top radiance to demonstrate the high correlation of the signal with high clouds. This is expected because the CO_2 column is reduced dramatically over high clouds. Thus the CO_2 lines are by no means saturated any more.

As could be seen in Fig. 35 high clouds falsify the light leak signal determined by saturated CO_2 lines but since cloudfree scenes are being analyzed for the CO_2 column retrieval only this has no effect on the quality of the light leak signal. Fig. 36 shows the same signal as Fig. 35 but for cloudfree scenes only and without devision of the cosine of the SZA. It can be seen that all ground scenes contaminated by an atmospheric signal due to high clouds are eliminated in this plot.

The next step is to determine the surface albedo for each ground scene from SCIAMACHY channel 7 measurements. Therefore a smooth region of the channel 7 spectrum is used without any strong absorptions of CO_2, water, or other trace gases. The wavelength range of 2034.1 to 2035.9 nm including these specific pixels (926, 928, 929, 931, 932, 933, 934, 935, 936, 937, 938, 939, 940, 941, 942, and 944) is used. The albedo is calculated using the following equation:

$$A = \frac{\pi \cdot I/T}{I_0} \cdot \frac{1}{cos(SZA)} \quad (4)$$

where T is the transmission due to the ice layer, I is the measured nadir intensity, I_0 is the measured intensity of the solar spectrum, and SZA is the solar zenith angle. Fig. 37 shows the results of the SCIAMACHY channel 7 albedo for the cloudfree ground scenes. Fig. 38 depicts the surface elevation for each individual ground scene derived from the surface elevation database provided by R. Guzzi. This information is used to select the correct values for the simulated radiance due to unsaturated CO_2 lines from a look up table to calculate the atmospheric contribution due to unsaturated CO_2 lines in the determined light leak signal (see Fig. 39). The signal in Fig. 39 is subtracted from the signal in Fig. 35 to yield the proposed light leak signal (see Fig. 40). It can be seen that the derived light leak signal using the described method is up to 300 BU (300 BU/s taking into account the exposure time of 1 sec for cluster 51) which is consistent with Lichtenberg et al. (2005) who estimate a light leak signal of up to 300 BU/s. But there are still problems with the derived light leak signal, since the signal is negative (minimum values of down to -100 BU) over parts of Nambia's desert. An Investigation has shown that these low values do occurr under special conditions such as low SZA, high surface albedo, and high surface elevation. In this case the radiative transfer model overestimates the atmospheric signal due to unsaturated CO_2 lines. Another critcal parameter (not presented in this work) is the slitfunction used in the radiative transfer model to simulate SCIAMACHY's low spectral resolution. In this work a Gaussian slitfunction with a FWHM of 0.19 nm was used. Using a slitfunction with a larger FWHM yields a larger simulated atmospheric signal due to unsaturated CO_2 lines and therefore even smaller values of the proposed light leak signal over Namibia's desert. This issue still needs further investigation.

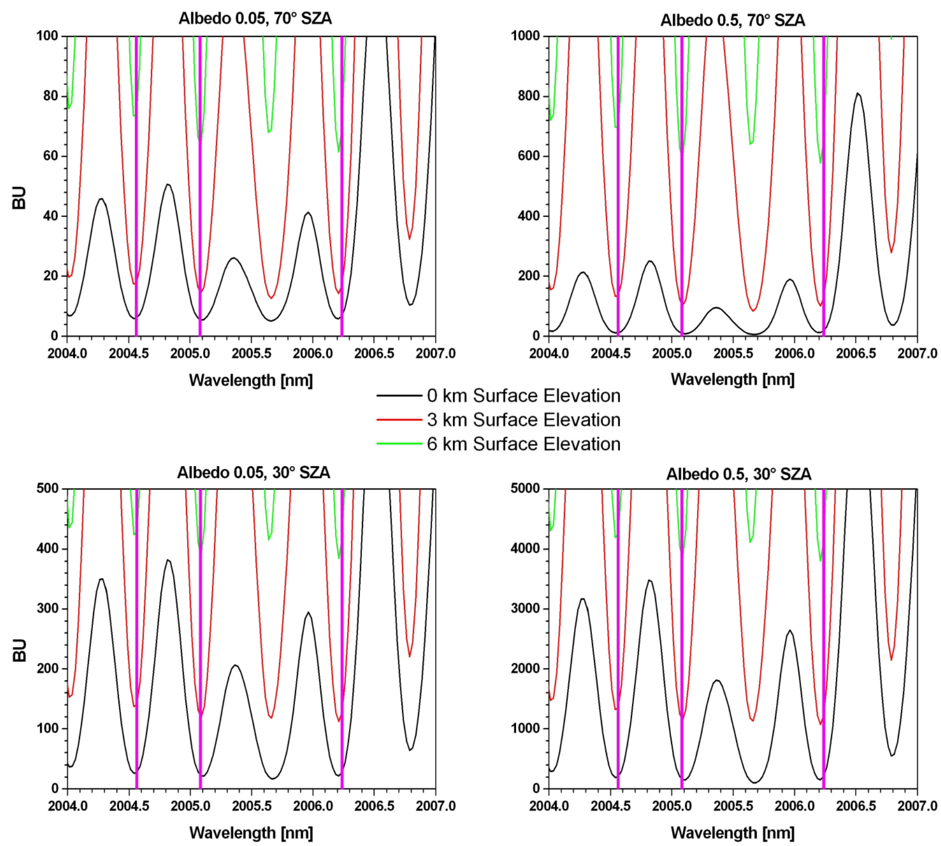

Figure 34: SCIATRAN radiative transfer simulations performed to correct the radiance at saturated CO_2 lines.

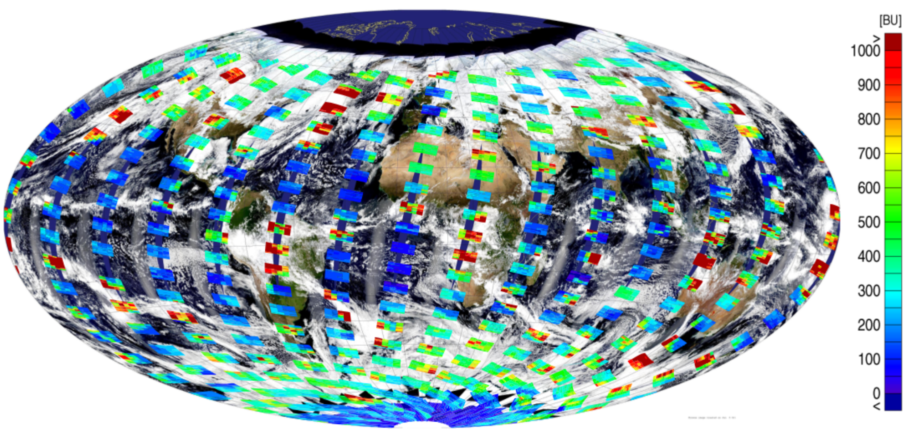

Figure 35: Signal (uncorrected; divided by cos(SZA)) at saturated CO_2 on MODIS map (all orbits from 24 January 2003).

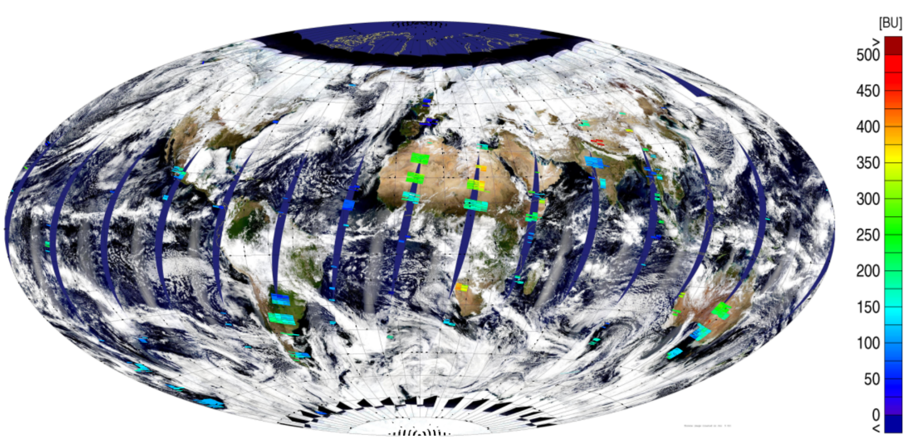

Figure 36: As previous figure but for cloud free scenes (no division by cos(SZA).

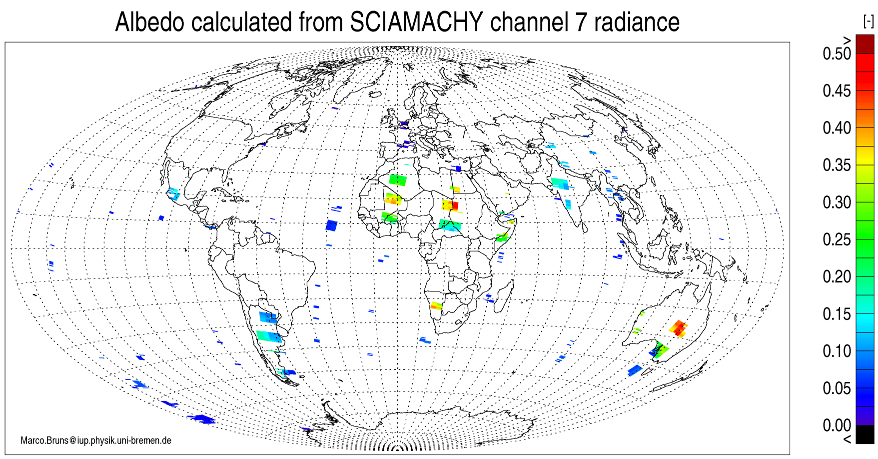

Figure 37: Albedo determined from SCIAMACHY channel 7 radiance.

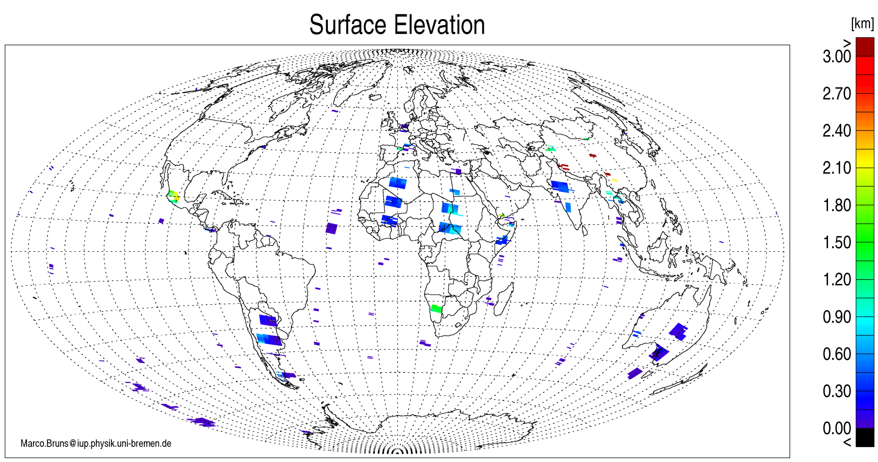

Figure 38: Surface elevation of the cloudfree SCIAMACHY ground scenes.

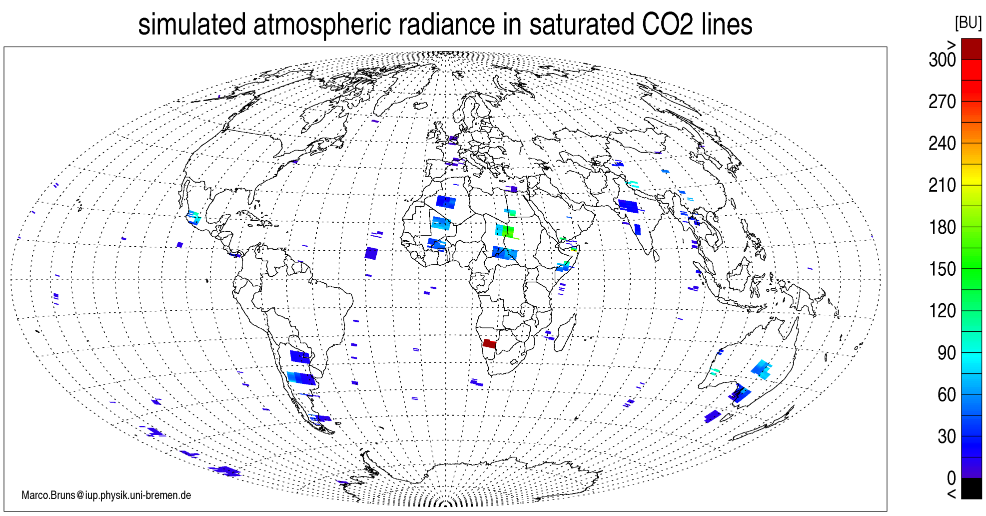

Figure 39: Atmospheric signal due to unsaturated CO_2 lines taking into account the SZA, surface albedo, and surface elevation.

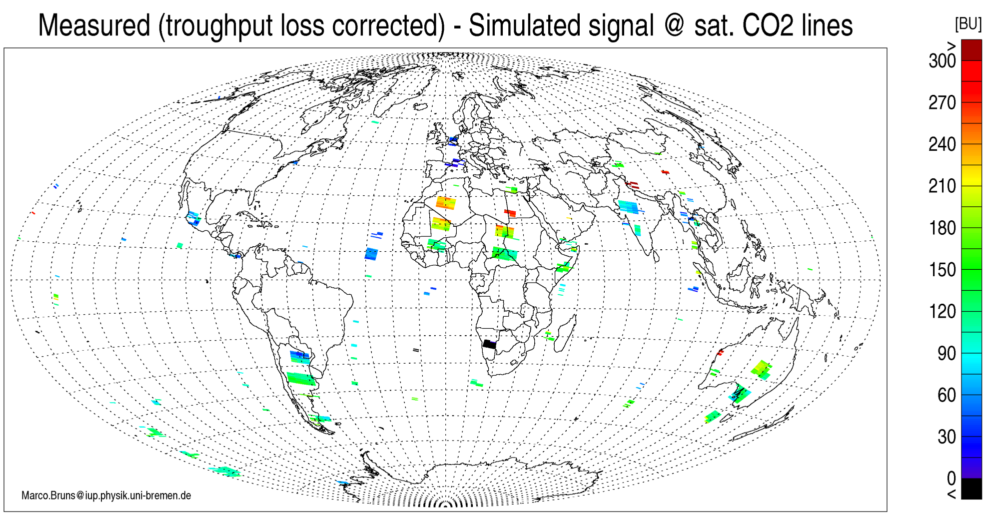

Figure 40: Determined light leak signal (signal of Fig. 39 subtracted from signal of Fig. 36). The accuracy still needs to be assessed. Obvious problems: Negative at some locations (min. about -100 BU over South Africa (high albedo, high surface elevation scene).

7.1.5 Light Leak Signal Algorithm

The purpose of this section is to provide a description of the algorithm used to calculate the light leak signal of SCIAMACHY's channel 7. This algorithm consists of several individual modules. Each module will be descriped seperately in a dedicated subsection. All steps combined represent the whole algorithm.

Step 1: Preprocessing of Light Leak Signal

directory: `create_LLSig/SCI_files`

The first step is to generate SCI-files using the IUP WFMD processor. The SCI-files contain the calibrated spectra measured by SCIAMACHY of a single orbit. To generate the light leak signal in photons/nm/cm^2/s/sr the sci-files have to be calibrated using options 0,1,2,3,4,5, and 7.

Step 2: Determine Light Leak Signal from SCIAMACHY Channel 7 Nadir Measurements

directory: `create_LLSig`

This step determines the signal including the light leak signal from SCIAMACHY channel 7 nadir measurements using the IDL-script `ll_sig_clus51_stat_CldMsk.pro`. This script reads the SCI-files of all desired orbits. In addition it reads the result files of an arbitrary CO_2 fit for the same orbits respectively in order to assign flag bytes for cloud situation, surface elevation, and scan mode to each ground segment of the orbit files since the SCI-files lack this information.

Then the script extracts the radiance measured by the center pixels of the three dedicated absorption lines from the spectrum of each ground segment and calculates an averaged radiance. The selection of the pixels used in this process has been described in the previous section.

Finally the averaged light leak radiance for each ground segment, the time, the geolocations of the ground segment, the scan mode, the cloud situation, and the surface elevation are being written into an new file. The file format is of the following: `hour min sec msec Orbit_Phase Lat1 Lat2 Lat3 Lat4 Lat Lon1 Lon2 Lon3 Lon4 Lon LLsigAvg LLsigMin ll_px1 ll_px2 ll_px3 SZA scan cloud elevation[km]`.

The frist 4 columns represent the time of the measurement, `Lat1` to `Lat4` and `Lon1` to `Lon4` represent the geolocations of the corners of the ground segment, `Lat` and `Lon` represent the geolocation of the center of the ground segment. `LLsigAv` and `LLsigMin` is the averaged and minimum radiance the light leak respectively. `ll_px1` to `ll_px3` is the radiance in the center of each of the dedicated absorption lines respectively, `SZA` is the solar zenith angle, `scan` is the scan mode (2 represents the back scan), `cloud` is the cloud situation (0 for cloud free and 1 for cloudy), and `elevation` is the surface elevation in km.

Step 3: Calculate Simulated Atmospheric Signal Due To Unsaturated CO_2 Lines

directory: `create_LLSig/sciatran_sim_SZA/parameter_files`
In the third step the atmospheric signal due to unsaturated CO_2 absorption lines is calculated for different scenarios (SZA, surface albedo, FWHM for convolution of simulated spectrum, and surface elevation) using SCIATRAN. The parameters are automatically changed using a set of bash-scripts. The main sript is the is called `scia_bat.scr`. It is basically a loop over all albedo values and calls the script `scia_bat_1.scr`. The main purpose of this script is to loop through all SZA values and calls the final script `scia_bat_2.scr`. This final script loops through all surface elevations and inserts the three parameter values for albedo, SZA, and surface elevation into SCIATRAN's `control.inp`-file accordingly using the tool sed. Finally this script calls SCIATRAN itself to perform the calculation.

Step 4: Format SCIATRAN Output

directory: `create_LLSig/sciatran_sim_SZA`

Format the SCIATRAN output using the IDL script `rad_satCO2lines.pro`. This script reads all output files of the simulation of the atmospheric signal including the variation of all parameters (SZA, surface albedo, FWHM for convolution of simulated spectrum, and surface elevation) and writes the data into one file for one SZA each. All these files contain the following columns: `altitude[km] albedo0.01 albedo0.05 albedo0.1 albedo0.15 albedo0.2 albedo0.25 albedo0.3 albedo0.35 albedo0.4 albedo0.45 albedo0.5 albedo0.55 albedo0.6 albedo0.65 albedo0.7`.

Step 5: Calculate Albedo from SCIAMACHY Channel 7 Radiance

directory: `create_LLSig/SCIA_albedo_files`

This step determines the surface albedo from SCIAMACHY channel 7 nadir measurements using the IDL-script `ll_sig_ch7_SCIAalb.pro`. This script works almost exactly like the script `ll_sig_clus51_stat_CldMsk.pro` except that it adds an additional column containing the surface albedo calculated from SCIAMACHY channel 7 radiance as described in subsection 7.1.4 "Light leak determination using saturated CO_2 lines" (see eq. (4)).

Step 6: Calculate Atmospheric Signal due to unsaturated CO_2 Lines

directory: `create_LLSig`

In this last step the IDL-script `calc_atmSig_from_SCIAalbedo.pro` calculates the atmospheric signal caused by unsaturated CO_2 absorption lines taking into account the specific SZA at the time of measurement, the surface albedo and the surface elevation of the ground scene. This script reads the output of the `ll_sig_clus51_stat_CldMsk.pro` script and adds another column containing the atmospheric signal due to unsaturated CO_2 lines for each ground scene. Thus, the output of this script has the same format as the output of the `ll_sig_clus51_stat_CldMsk.pro` script except that a column with the atmospheric signal is added.

7.2 Detector ice-layer issue

The ice-layer on the channel 7 detector results in a throughput (transmission) loss and changes of the slit function. According to Lichtenberg et al. (2005) a correction of the transmission is straight forward but not yet implemented. The impact of this correction procedure on DOAS-type retrieval algorithms is probably minor because DOAS-type retrievals are insensitive to spectrally slowly varying multiplication factors. Therefore, it is not expected that the transmission correction will result in improved CO_2.

An additional effect due to the ice layer is the widening of the slit function. This is a critical error source as it it expected to result in a time dependent (large) bias. Correction schemes using known (CO_2) columns for a certain location are presented in Buchwitz et al. (2005b) and Gloudemans et al. (2005). According to Lichtenberg et al. (2005), it is not possible to implement this algorithm in the operational processing. Even more important is that this approach has clear disadvantages: (i) it assumes that the CO_2 column is known over a certain location (which is not exactly true) and (ii) that the impact on the CO_2 column is assumed to be the same everywhere (as the information obtained at one location has to be extrapolated to the rest of the world).

Strictly speaking, a time dependent slit function needs to be determined. This can be done in various ways, for example by fitting slit functions to the SCIAMACHY solar spectra (using a high resolution solar reference spectrum), by analysing the spectra of the on-board line lamp (potential problem: the effective slit function for the lamp might not be appropriate for the nadir spectra), or by analysing the nadir spectra (using a similar approach as for the solar spectra; this is however difficult because of the variability of the nadir spectra; however one could do this over a location where CO_2 variability is expected to be small, e.g., over the Sahara). Determining the slit function using the nadir spectra is the preferred approach because it results in a slit function appropriate for the nadir spectra. Therefore, this approach will be investigated first.

First, however, a data set containing all CO_2 columns over the geolocation of 22.5° N, 2.5° E (Saharan Desert) and within a radius of 1000 km has to be processed by WFM-DOAS to see if the expected correlation of the CO_2 (bias) with the channel 7 throughput loss can be identified. Fig. 41 shows CO_2 columns above the Saharan Desert and the throughput loss curves of channel 7. As can be seen the troughput loss plotted with red symbols scaled to the CO_2 columns correlates quite well with the CO_2 columns retrieved from channel 7 nadir measurements. In this plot the same linear transformation has been used for all troughput loss data of the year 2003. Fig. 42 shows a transformed troughput loss (red symbols) using different linear transformation before and after day 100 resulting in a significantly higher correlation. This is expected from the experience with the troughput loss in channel 8 and the methane retrieval. The methane columns show a similar behaviour compared to the troughput loss data and the correlation is significantly higher when using different linear transformations for different periods of time. Fig. 43 shows the correlation of the RMS of the fit residuum with the troughput loss data. As can be seen from this plot that there is no significant correlation between the RMS and the troughput loss data meaning the fit results of the CO_2 columns cannot be used to develop an algorithm to correct for errors due to the ice layer issue.

To investigate the influence of the ice layer on the slit function the solar spectra of the several orbits have been analyzed. Fig. 44 shows the results of this investigation. This figure basically shows the dependence of the solar spectra on the troughput loss. The slit function dependence cannot be seen in this plot. This is because the variations in the slit functions are too small to be seen in such a broad spectral range. In the next step solar spectra convoluted with different slit functions are fitted to measured solar spectra. The RMS of these fits is used to determine the optimum slit function in the measured solar spectrum. Fig. 45 shows the results of these investigations. The orbits of the solar spectra used here are selected specificly to represent different stages of troughput loss. The hyperbolic slit function was used with two parameters (FWHM and an exponential factor EXP) being varied. The hyperbolic slit function can be calculated using the following equation:

$$SF = \frac{c}{1 + \left(2 \frac{\sqrt{(x-x_0)^2}}{FWHM} \right)^{EXP}} \qquad (5)$$

where c is a constant factor to normalize the slit function so that the area beneath the curve is 1, x is the distance from the center of slit function, x_0 is the center of the slit function, FWHM is the full width at half maximum, and EXP is the exponential factor determining the shape of the wings of the slit funtion. It can be seen in Fig. 45 the EXP factor is correlating with the troughput loss. This is preliminary evidence that the slit function is influenced by the characteristics of the ice layer but further investigation is necessary.

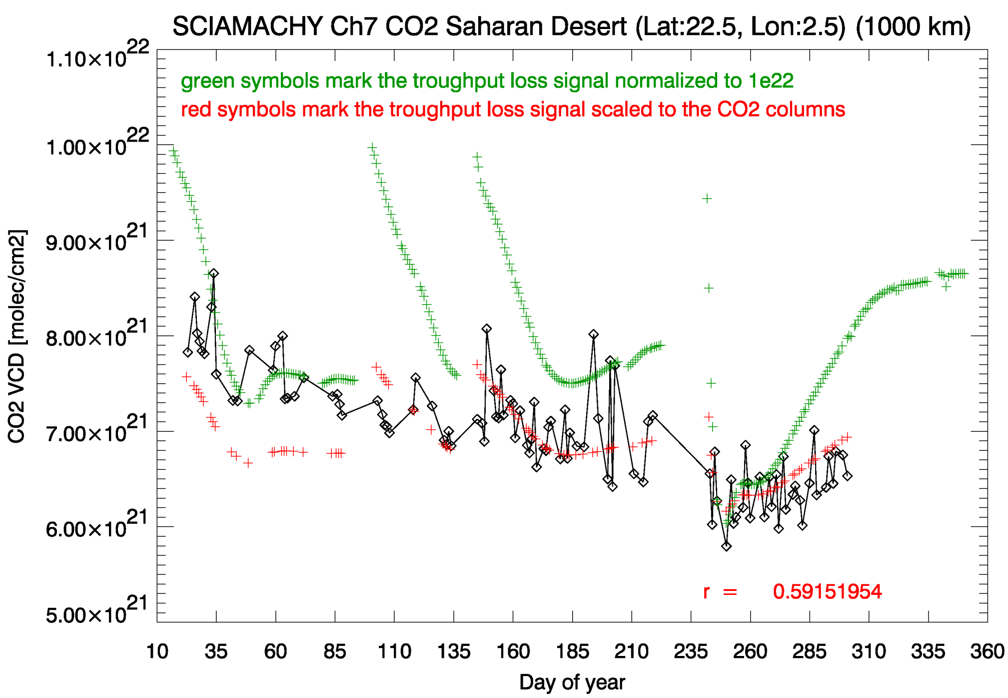

Figure 41: SCIAMACHY channel 7 WFM-DOAS CO_2 columns (black symbols; fitting window 2030 to 2040 nm) during 2003 over the Saharan Desert (22.5N, 2.5E, radius 1000 km). Also shown is the channel 7 throughput loss as provided by SOST (green crosses) normalized to 1e22 molec/cm^2, i.e., 1e22 molec/cm^2 corresponds to a troughput of 100% and 8e21 molec/cm^2 corresponds to a troughput of 80% (relative to the begin of the mission). Additionally the linear transformed troughput is shown in red for a better comparison with the retrieved CO_2 columns. The linear correlation coefficient between retrieved CO_2 and throughput is 0.59.

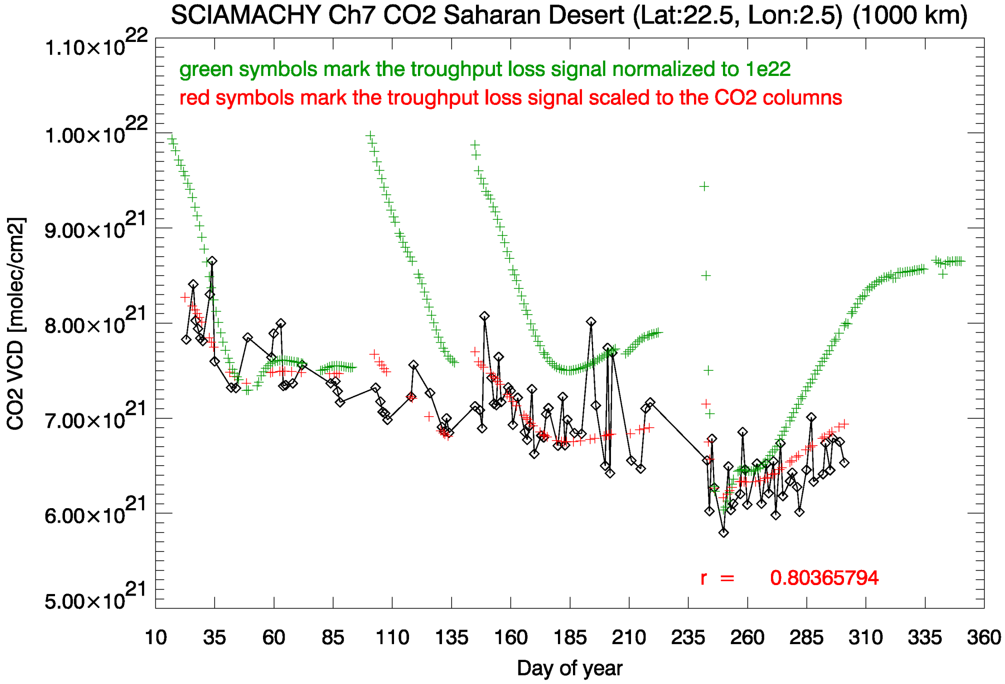

Figure 42: As Fig. 41 but using two separate linear transformations for the throughput, namely one for days earlier than day 100 and one for days later than day 100. This transformation results in a significantly higher correlation coefficient (0.80 compared to 0.59).

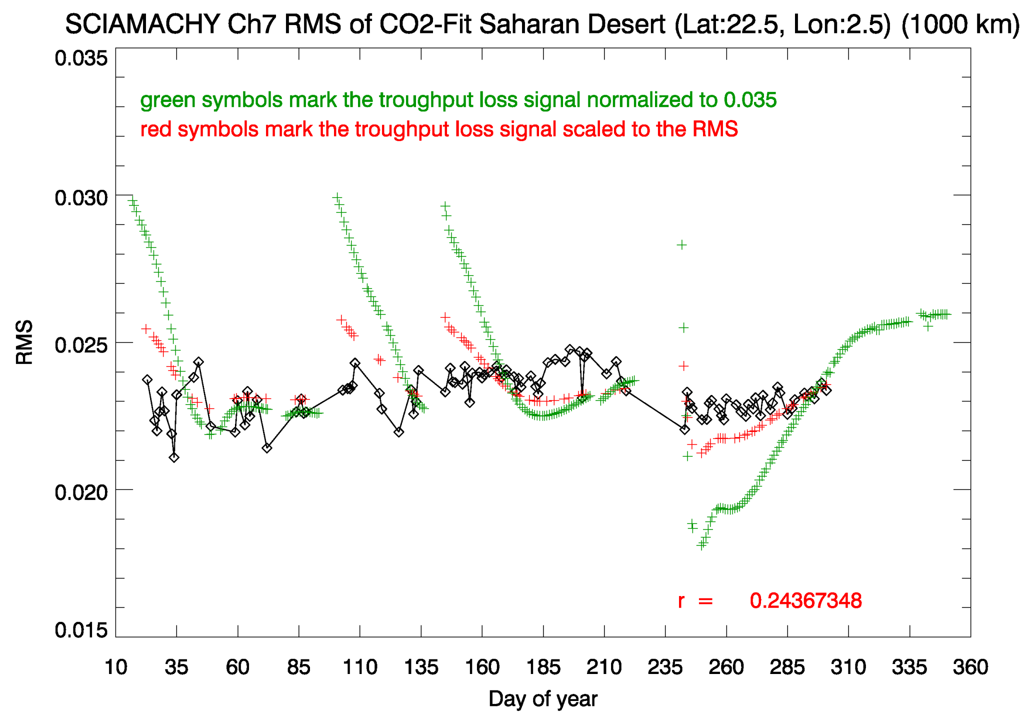

Figure 43: As Fig. 41 but for the RMS of the fit residuum (fitting window 2030 to 2040 nm).

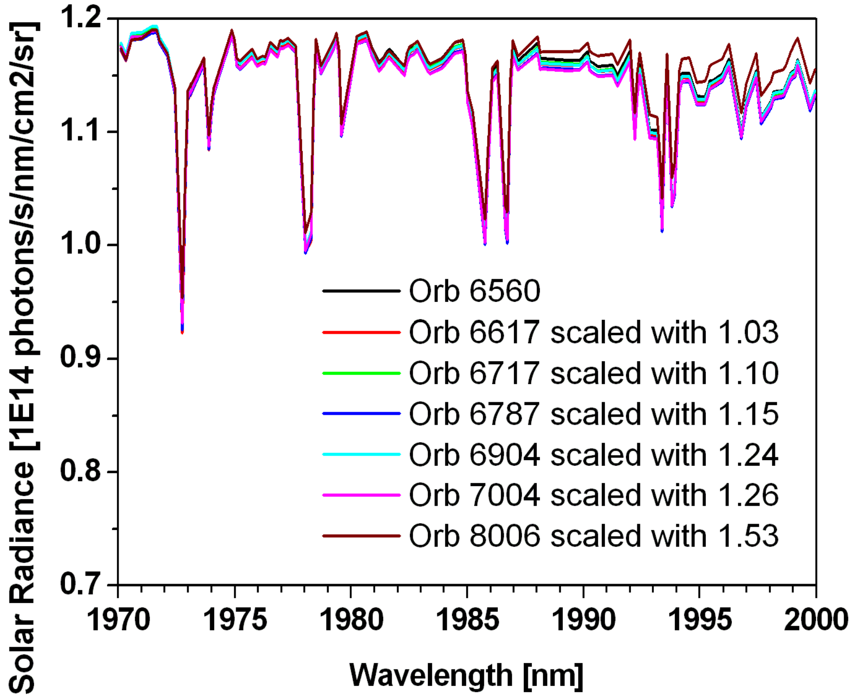

Figure 44: Various SCIAMACHY solar spectra basically ordered by throughput loss.

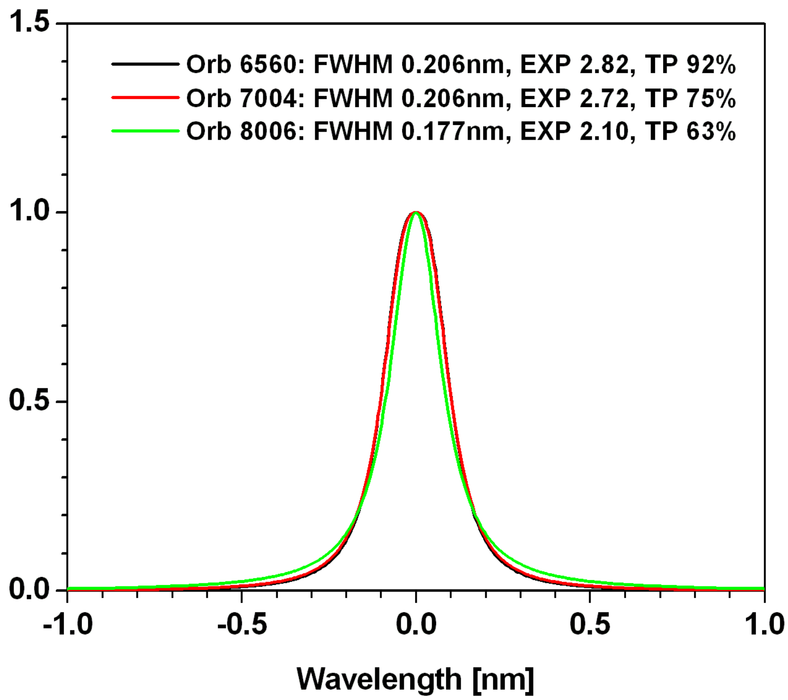

Figure 45: Parameters of a hyperbolic slit function determined by convolution of a high resolution solar spectrum and fit to SCIAMACHY solar spectra. Parameter EXP determines the broadening of the wings.

7.3 Dark signal calibration issue

For WFM-DOAS v0.4 processing of initial year 2003 channel 6 spectra it has been found that the quality of the dark signal calibration needs to be improved when using Level-1B version 4.00 and 4.03 (Buchwitz et al., 2005a). For channel 6 and channel 8 retrieval this has been done by "patching" the Level-1B data product. This means the dark signal measurement entries used by EnviView when converting Level 1b to Level 1c have been replaced by improved dark signals also contained in the Level-1B product but are not used for calibration so far.

In the nominal case, constant leakage current are stored in two arrays defined in the Level-1B product, one is containing time-independent dark signal (Fixed Pattern Noise, FPN), the other contains time dependent leakage current (called “Constant Leakage” within the product (!) to be distinguished from leakage variabilities during one orbit, the “Variable Leakage”). Both entries are originally determined during operational ground processing using the Instrument Engeneering Calibration Facility (IECF) module (ESA/ESRIN, Italy) applying a regression model through dedicated dark signal measurements, which are not necessarily from the same orbit, for three different Pixel Exposure Times (PET) , resulting in the above mentioned linear parameters.

The basic idea of the patching method is to use those darksignal measurements, which have the same PET as the nadir science measurements to be used for the tracegas retrieval and to avoid approximations as much as possible. Further more the dark signal measurements from the same orbit are used, which by definition should be contained in consolidated Level-1B. Currently for WFM-DOAS, there will be no processing if no or not enough dark signal measurements are found in the Level-1B product. However, this could be improved by using, e.g. dark signals from other near-by orbits. Also, instead of using consolidated Level-1B only, if these data are not available one could additionally use Near-Real-Time (NRT) data, which result from a kind of arbitrarally fragmented SCIAMACHY data stream, and puzzle together dark signal measurements (and probably other necessary calibration parameters) from near-by Level-1B. Both would significantly enhance the data budget especially for 2003. This could be future work...(?)

For the preparation of the patching step dark signal measurements have to be read out from Level-1B using S/W developed by S. Noel (IUP). Dark signals (ASCII output) are then analysed, selected and assigned to match the PET of the Nadir measurements for each nadir state ID. By the way, this software (R. de Beek, IUP) also performs the non-linearity-correction of the dark signal using a S/W tool provided by SRON (Q. Kleipool) via the internet. For each of 7 nadir state IDs one leakage current file is produced containing the matching dark signal measurements. Patching is done by a S/W tool developed by K. Bramstedt (IUP) which uses the leakage current files to produce seven Level-1B files, each for one nadir state ID. This is because there are only two entries in the Level-1B foreseen for dark signal entries and one (the FPN array) is used by the patcher. The second entry for time-dependent dark current is simply set to zero, as for the patching concept dark signal measurements are used directly containing both FPN and constant leackage contributions. The patcher S/W also does the non-linearity-correction of the nadir radiance measurements similar to the SRON tool. It also uses the SRON non-linearity database. Each of the seven Level-1B files is then converted into a WFM-DOAS specific ASCII format (sci-file) and, in a final step, the sci-files are merged together into one file containing all measurements in chronological order.

The patching software modules are not at all optimised and thus time consuming. However, patching was crusial in order to enable any usage of the near-infrared measurements in the first three years of operation as the ESA product quality was insufficient for any reasonable evaluation in this spectral range.

Figure 46 shows calibrated and uncalibrated spectra of channel 7, which illustrades the importance of dark signal calibration constituting the most dominant part of the instrument contributions to the measurements.

Figure 47 shows averaged dark signal contributions for one orbit as a function of latitude (left) and orbitphase. The orbitphase starts at zero which is the point of entering the eclipse in the southern hemisphere, i.e. sun-rise at the satellite is at about orbitphase 0.4.
It was a pleasure to learn from recent analysis of the SCIAMACHY near-infrared spectra for the years 2003-2005 data that for the most actual product version

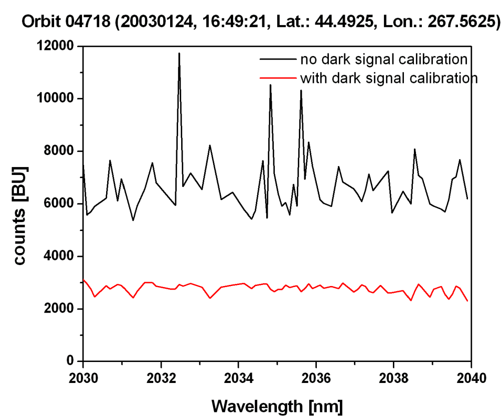

Figure 46: SCIAMACHY channel 7 nadir spectrum (CO_2 fitting window from 2030 to 2040 nm) from orbit 04718 near Park Falls, Wisconsin (USA). The uncalibrated spectrum is plotted in black and the spectrum with dark signal calibration is plotted in red. The initial pixel mask has been applied, i.e., dead pixels are not shown.

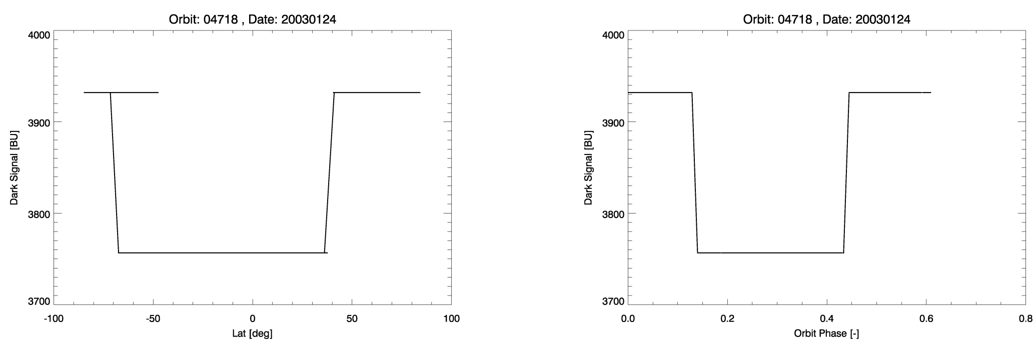

Figure 47: Left: SCIAMACHY channel 7 dark signal as a function of latitude for orbit 04718 (24 Jan 2003). The dark signal was averaged over the entire CO_2 fitting window from 2030 to 2040 nm after the application of the initial dead/bad pixel mask. Right: Same plotted as a function of orbit phase (more precisely: normalized time (zero means beginning of the orbit at entering the eclipse)).

(version 5.04) the quality of the calibration has been significantly improved, unfortunately for yet unknown reasons. However, patching of these product has not been necessary, i.e. the retrievals performed using patched and original data products are almost identical for channel 6 and at least very similar for channels 7 and 8.

Figure 48 gives an example of fitted channel 7 and 8 measurements using spectra detected in Orbit 8663 on 27. October 2003.

Outliers, i.e. larger discepancies between measurements and fitted model (red), can still be due to not yet identified dead/bad pixel, e.g. as seen for channel 7. Work to optimize the dead/bad pixel detection is in progress (see Section 7.4).

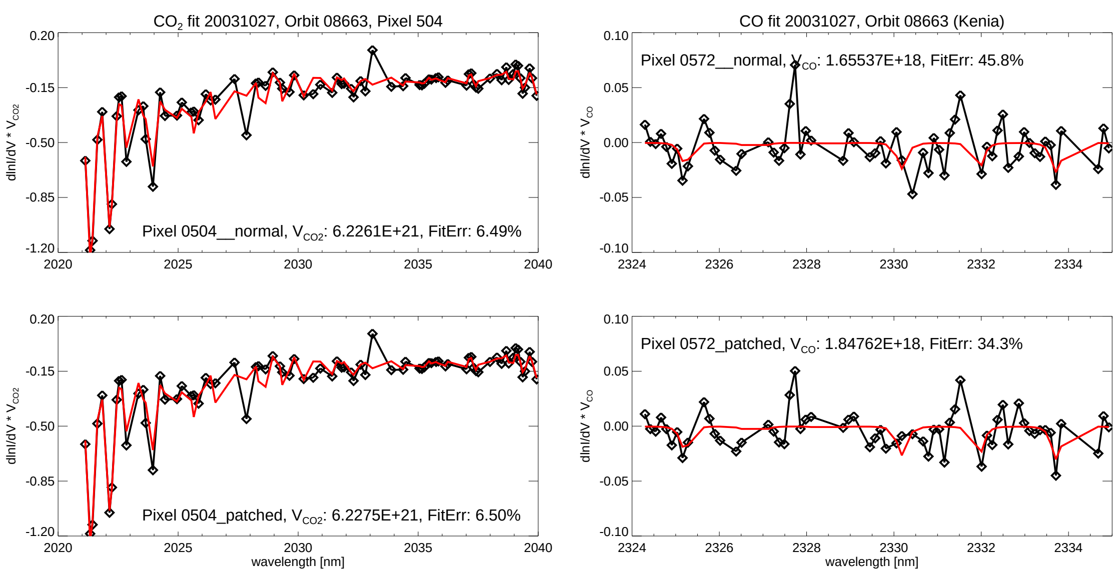

Figure 48: Example of fitted channel 7 (left) and 8 measurements using spectra detected in Orbit 8663 on 27. October 2003.

Figure 49 shows WFM-DOAS retrievals of CO_2 (Channel 7, left) and CO (Channel 8, right). Generally, for CO very small spectral changes already result in clear differences in the retrieved vertical columns, which are, however, not necessarily significant with respect to the retrieval precision.

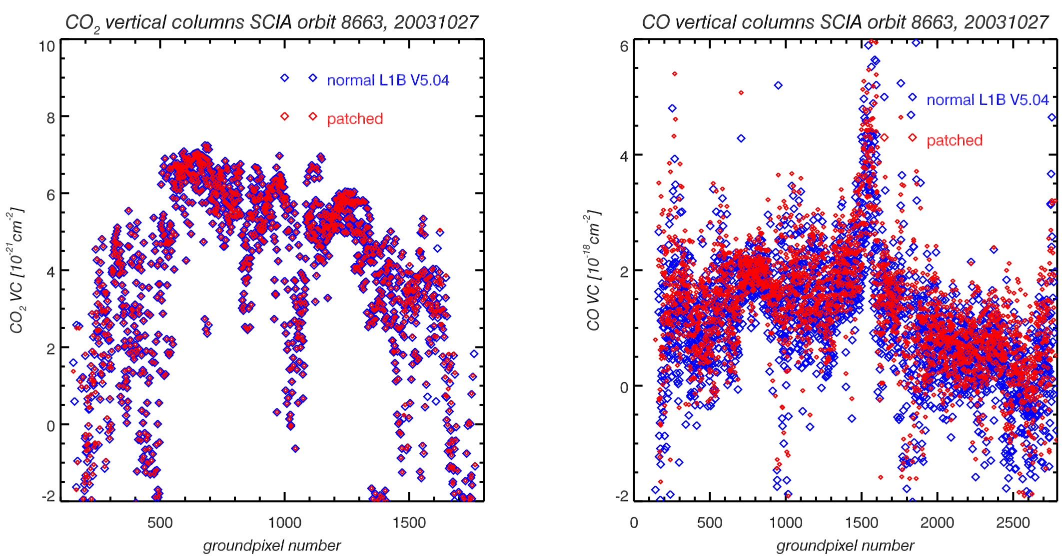

Figure 49: WFM-DOAS retrievals of CO_2 (Channel 7, left) and CO (Channel 8, right).

7.4 Dead/bad pixel mask issue

Accurate CO_2 retrieval requires a reliable identification of dead/bad pixels. A pixel mask has been defined (already pre-launch) where each pixel is classified as "good", "bad" or "dead" (Dead/Bad pixel Mask, DBM). It has been found in previous studies that the pre-launch pixel mask is not conservative enough. For WFM-DOAS v0.4 channel 6 CO_2 retrievals the (pre-launch defined) pixel mask has been modified manually to take into account additional "dead"(/bad) pixels, i.e., pixels that should not be used for retrieval as this would result in unreasonable results (e.g. negative vertical columns). For processing of years 2003 and 2005 channel 6 spectra two static pixel masks have been defined and the entire data sets have been processed using this masks.

In an earlier case study in the frame of the EU-ACCENT CO intercomparison workshop in April 2005 at SRON a DBM provided by IUP-Heidelberg has been successfully used for CO retrievals using orbit 8663 data (20031027) between 2324 nm and 2335 nm (channel 8). The same DBM turned out to be not sufficient anymore for the retrieval of CO from a spectrum about two years later (August 2005). CO retrievals using an updated DBM for this specific orbit provided by SRON (G. Lichtenberg, R. Jongma, priv. comm., (Kleipool, 2004)) also failed. For the particular case a significant hand-selected extension of the DBM has lead to the most reasonable results from channel 8, e.g. positive CO in the expected order of magnitude with higher values over biomass-burning, as expected.

In order to perform further analysis on this topic in the frame of CO_2 from channel 7 (i.e. this study) a DBM determination algorithm has been developed to provide DBMs for large sets of channel 7 data. It bases on an early rather simple approach developed within the ACCENT workshop activities. The algorithm, called ISDP (Initial Stochastics to Determine Pixels which... too long, simply “I See Dead Pixel”), uses dark signal data statistics obtained from Level-1B data.

7.4.1 Initial analysis

A channel 7 spectrum recorded in January 2003 is shown in Fig. 50 on top. The illustrated initial pixel mask has been determined by analyzing October 2003 spectra (dead/bad pixels which should not be used for retrieval are shown in red). The bottom panel of Figure 50 shows on the left a similar plot but for a spectrum recorded in March 2005 using the same initial pixel mask. As can be seen (e.g., black marked pixels with zero radiance) there are several dead/bad pixels in the 2005 spectrum which are not covered by the year 2003 pixel mask. This shows that the number of dead and bad pixels is increasing with time, which is consistent with the findings of SRON (Kleipool, 2004).

Figure 50 bottom right shows the same spectrum as shown on the left but with a pixel mask applied that has been generated automatically by analysing the dark signal files (including the dark signal statistics) contained in the Level-1B files (ISDP method, see below).

7.4.2 ISDP dead/bad pixel detection algorithm

For each dark signal state obtained during eclipse Level-1B files contain averages of all dark signal measurements determined over the dark signal state as calculated by the ground processor. For each mean value also the corresponding standard deviation is given. Five different dark states are defined with pixel exposure times from 0.0312s to 2.0s. Details as defined for Channel 7 are given in Table 10.

DarkStateId	PixelExposureTime [s]	CoAddingFactor
8	1.0	1
26	0.0312	16
46	0.0625	8
63	0.5	1
67	2.0	1

Table 10: Dark state parameters as defined for channel 7.

The basic idea of the ISDP method is to identify pixel which behave unexpected, e.g. non-linear, too variable or with no or saturated constant signals, as is typical for dead or bad pixels. Unwanted changes in the behaviour are detected by comparisons of the given signal level and standard deviation to the median of all pixel signal levels and standard deviations for a sub-channel spectral range (typically 102 pixels, i.e. 10 sub-channel regions per channel).

From experience with comparisons of ISDP results with a reference DBM empirical threshold parameters have been defined as upper and lower boundaries of the signal level and upper boundary of the standard deviation. As references for channel 8 the DBM according to the test orbit provided by SRON and also those developed by hand for the CO intercomparison workshop (IUP Heidelberg, IUP Bremen) have been used. It has been found out that for an optimized set of parameters most of the dead/bad pixels covered by the reference masks have been detected by ISDP. Similar parameters have then also been used for channel 7. As an example Figure 51 shows the DBM for the fitting window 2021 nm to 2040 nm (pixels 795 to 986) as derived for orbit 18111 on 17. August 2005.

Figure 52 shows fitted radiances when using the SRON DBM (top) and the ISDP DBM for the same orbit for an example ground scene with a mean surface elevation of 456m. Full DBMs are not shown, however, the green vertical lines illustrate the positions of additional dead pixels masked out by the DBMs compared to the initial on-ground generated OPTEC DBM, i.e. these pixels have been “good” from the outset and have “died” meanwhile!

The difference between using the SRON DBM and the ISDP DBM are about 5% in CO_2 vertical column. For this case the lower value after usage of the ISDP mask is plausible considering th mean surface elevation of about 456m, resulting in a decrease of about 5% compared to the expected CO_2 vertical column over sea level which is about $8E21\,cm^{-2}$. However, the results are very sensitive to modifications of the DBM and further investigations are needed to improve the DBM generation.

Up to now the main threshold parameters are the upper and lower boundaries for dark signal measurements of "good" spectral pixel given as factor with respect to the median of all signals in a specific spectral sub-window, e.g. 2.5 times the median of dark signal median is the upper threshold. A lower dark signal threshold is defined accordingly. Similarily the upper threshold for the standard deviation is defined relative to the median of all standard deviations in a given sub-window. For the deviation of a signal from the linear regression through all dark signal measurements for one pixel, i.e. for all different PETs, also an upper boundary is defined given in units of the standard deviation observed for the specific pixel. This means if the standard deviation of a pixel is below the standard deviation upper limit then the deviation from linearity can be of cause larger than for a pixel with low standard deviation. As an example, Figure ref illustrates the behaviour of pixel number 959 (orbit 18111, marked blue in Figure 51).

The bottom panel shows the differential (i.e. minus the model regression) to emphasize the small deviations. According to the described criteria the pixel has not been flagged dead, which is in contrast to the reference DBM.

Another criteria has been defined to filter out pixels having negative or too low leakage (e.g. if the darksignal measurement does hardly vary). A value of 2 binary units has been chosen as minimum value. In this respect it has been noticed, that for the case of the actual version 5.04 of Level-1B data for many pixels the leakage is indeed negative (acompanied with a very nice linear behaviour)! These pixels have not been flagged eventually as simply too many pixels are affected. The reason is yet unclear and has to be discussed with the data provider.

An overview of ISDP parameters to be set (see genDbm.inp) before running the program is given in Table 11.

Figure 54 shows the dark signal averages and standard deviations for the five dark signal measurement states. For the states 8, 63, 67 upper and lower thresholds are illustrated by red dashed lines. The transition from one sub-window to another can also be seen due to different thresholds. States 26 and 46 have not been used for the method. Again the example pixel number 959 is highlighted dashed blue (see Figure 53).

The ISDP method could be further improved first by making use of the history of each individual pixel to detect sudden changes. Secondly, one could for the signal level and standard deviation criteria focus on those states that match the science exposure time used for the nadir measurements. Then each nadir state would obtain its specific DBM depending on its PET. Background is that for some reason single pixel behave well for a certain PET but start failing for longer PETs. Both methods are part of future investigations.

The last Figure of this section shows the number of identified dead pixels as determined by SRON (Kleipool, 2004) for about orbit numbers 4500 to 13000 and as seen by the ISDP algorithm for orbit numbers 15000 to 19000 (2005). The SRON graphic shows deteced pixels depending on their individual selection criteria and the sum of all (upper curve). Although different years have been considered, the increasing number of dead pixels per time is similar for both methods at about 60 pixels per year. Also the 2005 curve follows well the thought extrapolation of the SRON curve.

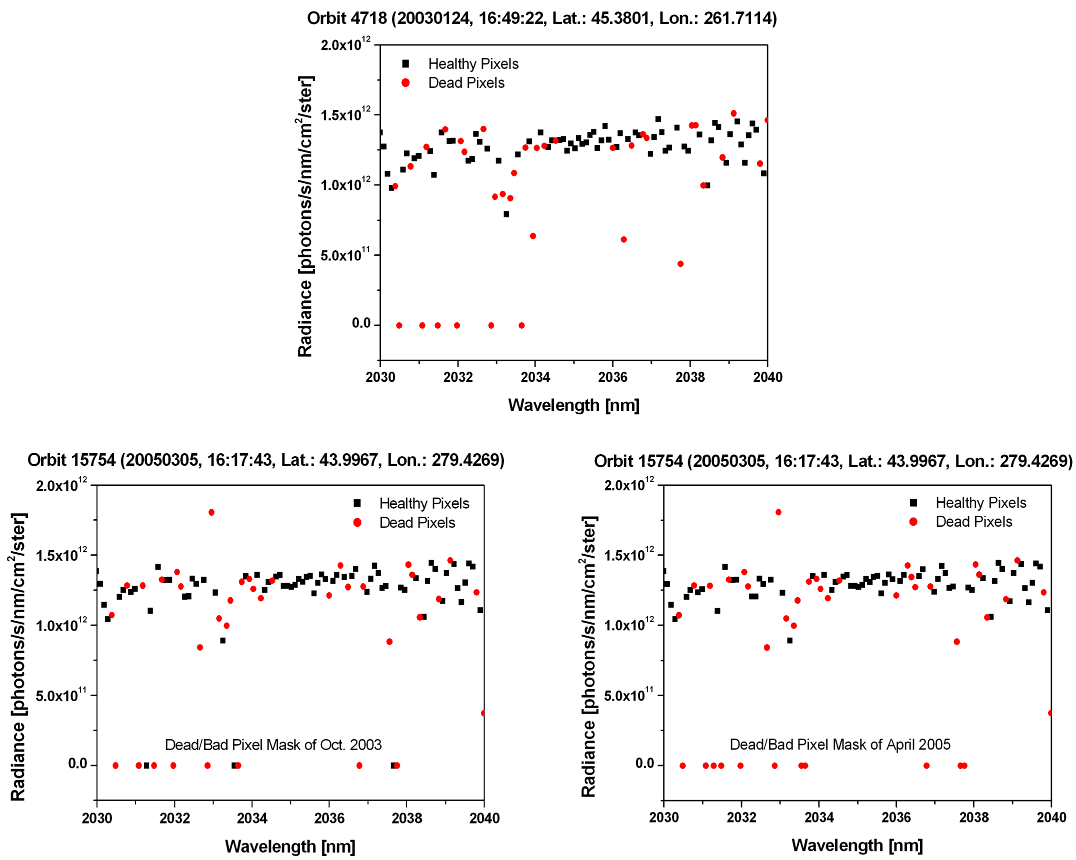

Figure 50: Top: SCIAMACHY channel 7 nadir spectrum (CO_2 fitting window 2030 to 2040 nm) from 24 Jan. 2003 (Orbit 04718) near Park Falls, Wisconsin (USA). An initial dead/bad pixel mask (= “Oct 2003 dmb” = “2003dbm”) has been used to mark the healthy pixels (the GOOD and BAD ones) with black squares and the DEAD pixels with red dots (the DEAD pixels are the pixels not used for retrieval). Only the pixels shown in black are used for retrieval. Bottom: Same ground scene as observed in orbit 15754, 5. March 2005. The same pixel mask has been used as for the top spectrum. As can be seen, the initial (year 2003) pixel mask is not appropriate for (all) measurements obtained later than 2003. Bottom right: Same spectrum but using a dynamically generated pixel mask obtained using the ISDP algorithm.

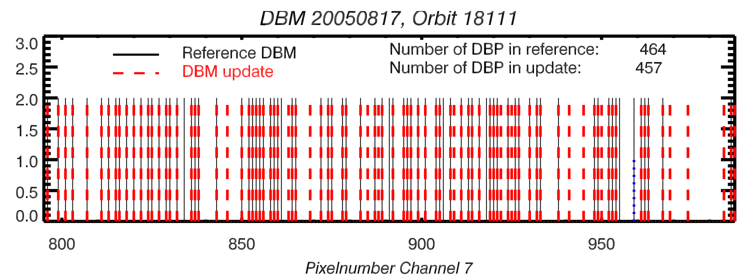

Figure 51: DBM for the fitting window 2021 nm to 2040 nm (pixels 795 to 986) as derived for orbit 18111 on 17. August 2005. SRONs DBM for this day has been used as a reference, the updated DBM is the ISDP output DBM (red vertical lines).

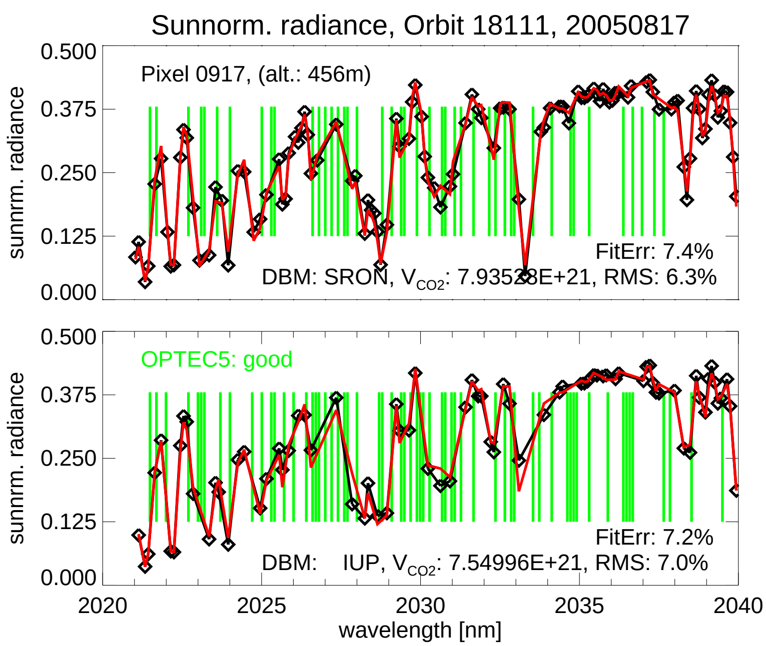

Figure 52: Effect of different pixel masks on the retrieved CO_2 column (top: SRON pixel mask, bottom: initial IUP-Bremen ISDP pixel mask). The green vertical lines denote pixels classified good in the pre-launch OPTEC 5 mask. The difference in the retrieved CO_2 column is 5%.

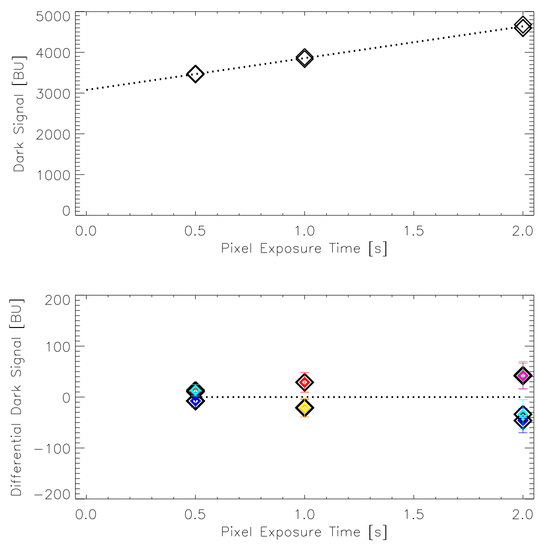

Figure 53: Behaviour of dark signal with increasing PET for pixel number 959 (orbit 18111, marked blue in Figure 51). Bottom: The differential (i.e. minus the model regression).

Parameter	Explanation	(Optimal) Threshold
nSpecStep	number of spectral sub-windows	10
specStep	number of spectral pixel per sub-window	102
fUp	upper boundary factor for dark signal measurements of "good" spectral pixel, i.e. 2.5 times the median of DsMsm is the upper threshold (the median is defined for each of nSpecStep spectral window of length specStep)	2.5
fLow	lower boundary factor, see above, i.e. 0.3 times the median of DsMsm is the lower threshold	0.3
maxStdDevFactor	maximum accepted dark signal standard deviation, i.e. 4.1 times the median of relative stdDev is the upper threshold	4.1
maxDev	maximum deviation from regression for one spectral pixel in units of its peticular given standard deviation	3.0
minLeakage	lower boundary for leakage signal to identify constant signal	2.0
viewWinStart	lower pixel number boundary for output graphics	e.g. 795 (for 2021 nm)
viewWinEnd	upper pixel number boundary for output graphics	e.g. 987 (for 2040 nm)

Table 11: ISDP dark signal threshold parameters and their values used for channel 7.

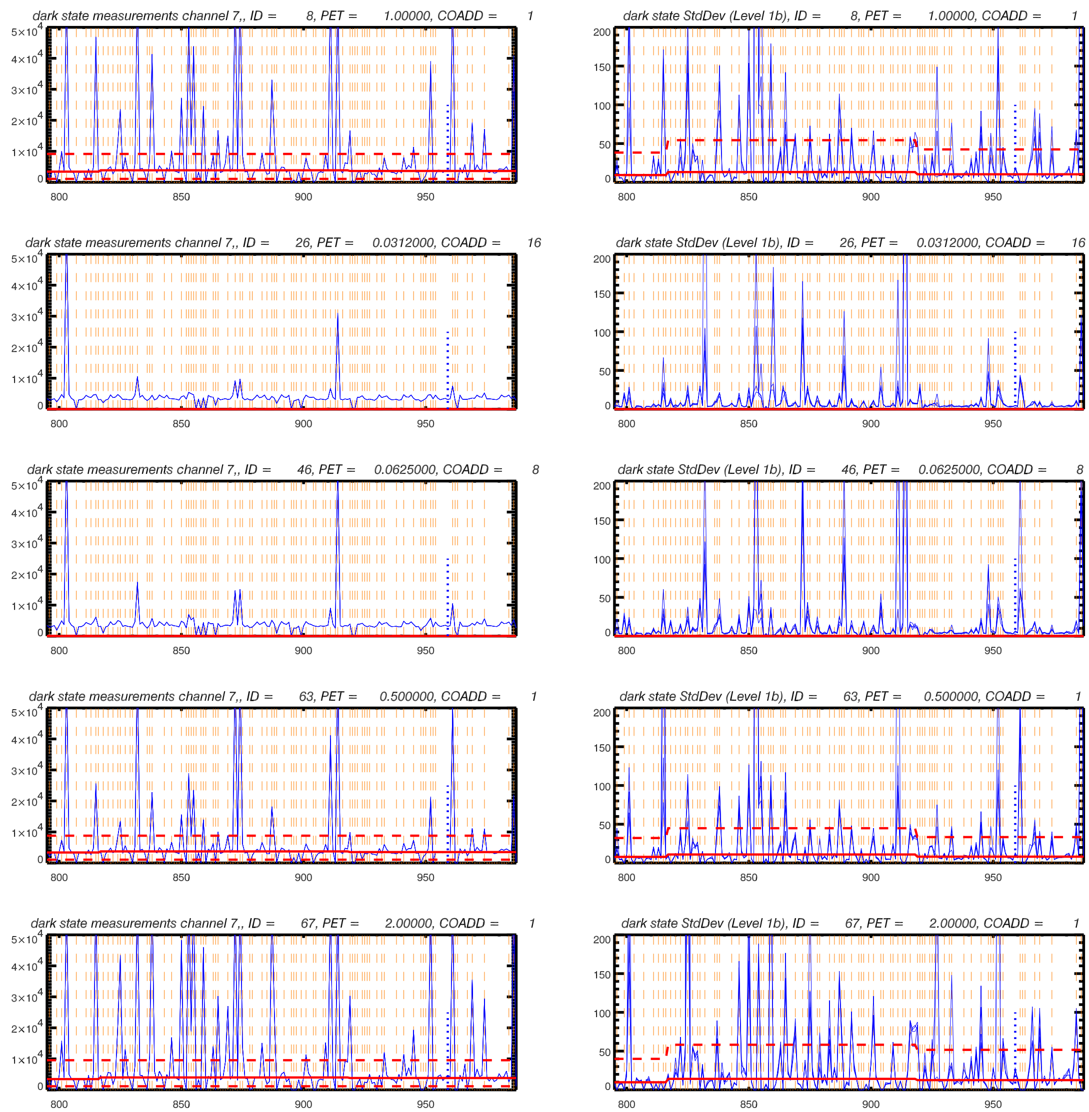

Figure 54: Dark signal averages (left panel) and standard deviations for the five dark signal measurement states. One measurement out of generally several for one state is shown. For the states 8, 63, 67 upper and lower thresholds are illustrated by red dashed lines. States 26 and 46 have not been used.

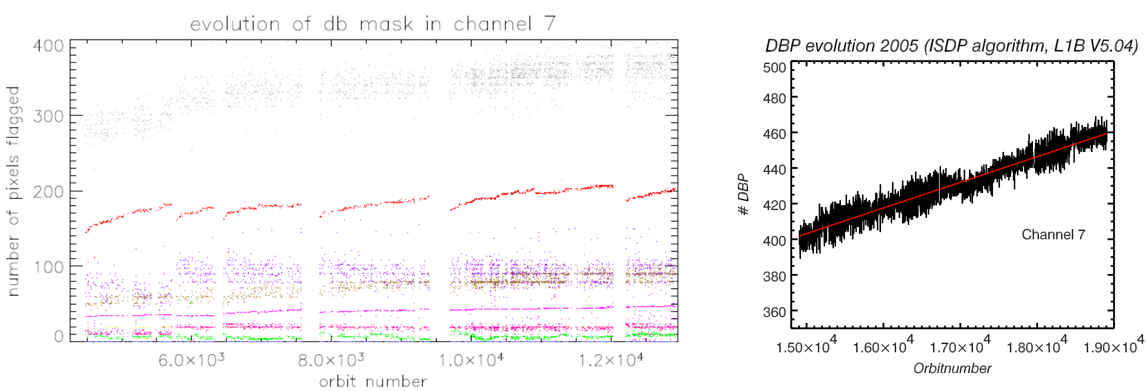

Figure 55: Number of dead/bad pixels for channel 7 as a function of time as given by SRON (Kleipool, 2004) and determined with the IUP pixel mask algorithm ISDP (PRELIMINARY) for orbits 5000 to 13000 and 15000 to 19000, resp.. The SRON graphic (left) shows deteced pixels depending on their individual selection criteria and the sum of all (upper dots).

7.5 Initial CO_2 restrievals for 2005

The 2005 dataset of consolidated Level-1B data (processor version5.04) has been used to retrieve CO_2 from channel 6 and channel 7 for May, July, and September 2005. Maps of gridded XCO_2 have been produced.

The main reason to produce a preliminary 2005 dataset from channel 6 CO_2 retrievals is to compare the data with results obtained from channel 7 for the same time range. For the new retrievals only 2005 data has been used as the icing effect in channel 7 is assumed to be low and, according to the throughput-loss monitoring, should be very constant for 2005. However, maps of XCO_2 for 2005 have also been produced in a similar manner to 2003 maps of WFM-DOAS version 0.4 products (Buchwitz et al., 2005b). There are in total five differences between the procedures, i.e. compared to the 2003 map...

1. Level-1B version 5.04 instead of version 4.00 and 4.03 have been used,
2. no patching of dark signals (original Level-1B used, see also Section 7.3),
3. no scaling of CO_2 (but still of O_2),
4. 4% maximum fit error instead of 10%,
5. well, data are of 2005, of cause.

As for WFM-DOAS product version0.4, for WFM-DOAS retrievals from channel 6 the fitting window 1558-1594 nm has been used.
As DBMs for 2005 two updated static DBMs were used for channel 6 and 7 one manually extended ISDP DBM of 20050930 (channel 6) and the other (for channel 7) determined by overlapping DBMs generated by ISDP (see Section 7.4) for all orbits between 1st February and 30th November 2005, which lead to a total number of 670 pixel masked out for the whole channel 7. In spite of information loss in contrast to using orbit-by-orbit DBM-updates (see Fig. 55), the advantage of a static DBM is that, if at all, a clear systematic error can be assumed from any undetected dead/bad pixel, i.e. variations in time and space can be related to any other remaining error sources and, hopefully of course, the atmospheric CO_2.

Figure 56 shows monthly mean XCO_2 on a $0.5° \times 0.5°$ latitude/longitude grid calculated for May, July, and September, on the left from WFM-DOAS product version 0.4 for 2003 (Buchwitz et al., 2005b) and on the rigth from new WFM-DOAS retrievals also using the same fitting window in channel 6 (static DBM as described above) for 2005.

Only cloud-free pixels over land are shown.
For channel 6 retrievals plumes of higher XCO_2 can be seen over desert regions for both, 2003 and 2005. There are less gaps in the 2005 map as compared to that of 2003. Most interestingly, the lower XCO_2 over the northern hemisphere in July compared to May and September are again evident as for 2003, which is as reported in-line with biological uptake during the growing seasons (Buchwitz et al., 2005b).

The results shown are preliminary, however, as they are not yet fully checked, and there is some more time and resources needed to do so!

For channel 7 retrievals, two fitwindows have been tried, 2030-2040 nm, still the actual operational approach, and 2021-2040 nm. However, using the to be admitted very conservative static DBM for channel 7 (2005) gives no reasonable results when using the smaller operational fitwindow (not shown).

Data of 2005 XCO_2 from channel 7 has been filtered as for channel 6 (version0.4 scheme), but using parameters adopted to the fit quality and also a more sophisticated method, which also introduces expected model values for O_2 and CO_2. A similar method has been applied for the production of CO and CH_4 maps from WFM-DOAS version 0.5 products (e.g. improved land filtering) (de Beek et al., 2006). The main difference to channel 6 data treatment is, however, a maximum fit error of 20% (instead of 4% for channel 6 CO_2 of 2005).

Figure 57 shows on the left the maps obtained from channel 6 retrievals, same as in Figure 56 on the right panel, but using a color scale consistent with that optimized for the results obtained from channel 7, and additionally showing also oceanic regions.

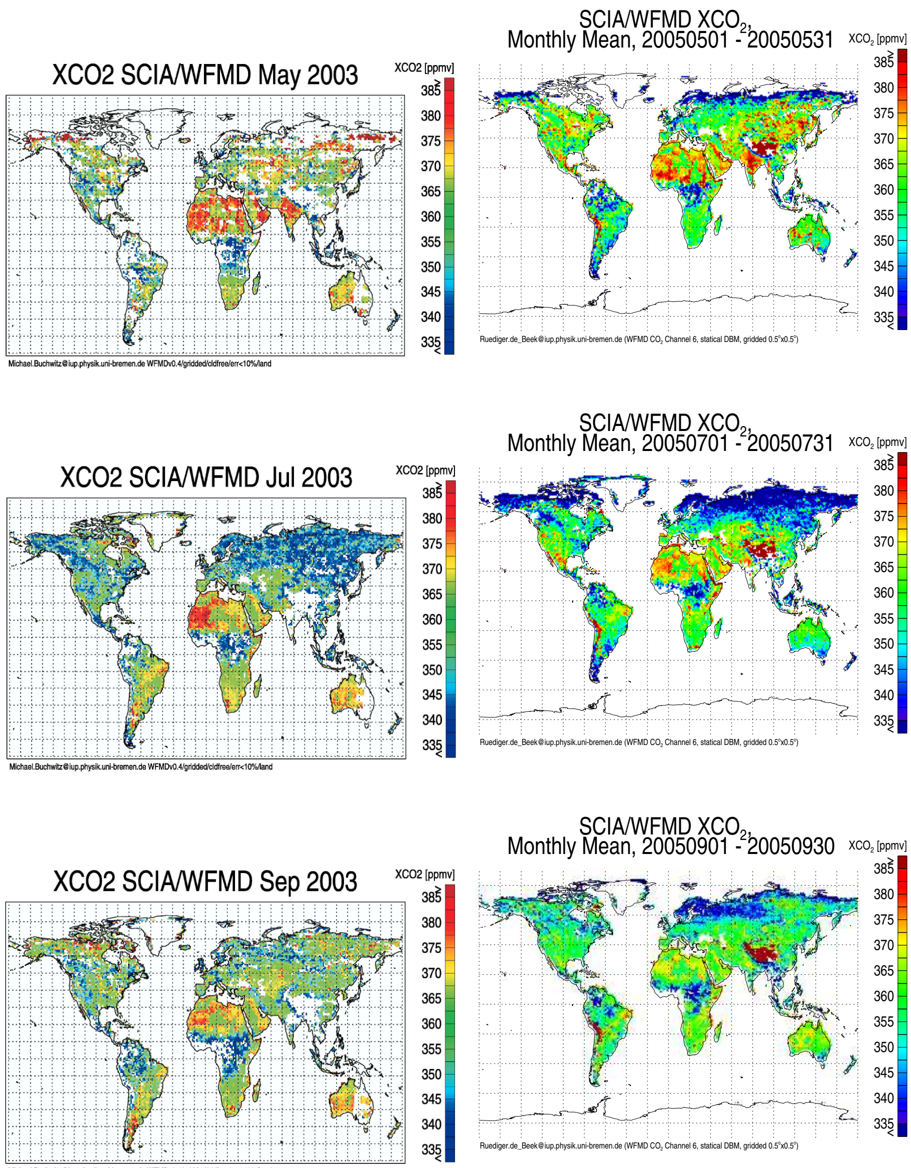

Figure 56: Monthly mean XCO_2 on a $0.5° \times 0.5°$ latitude/longitude grid calculated for May, July, and September, on the left from WFM-DOAS product version 0.4 for 2003 (Buchwitz et al., 2005b) and on the rigth from new WFM-DOAS retrievals also using the same fitting window in channel 6 (static DBM) for 2005. Only cloud-free pixels over land are shown.

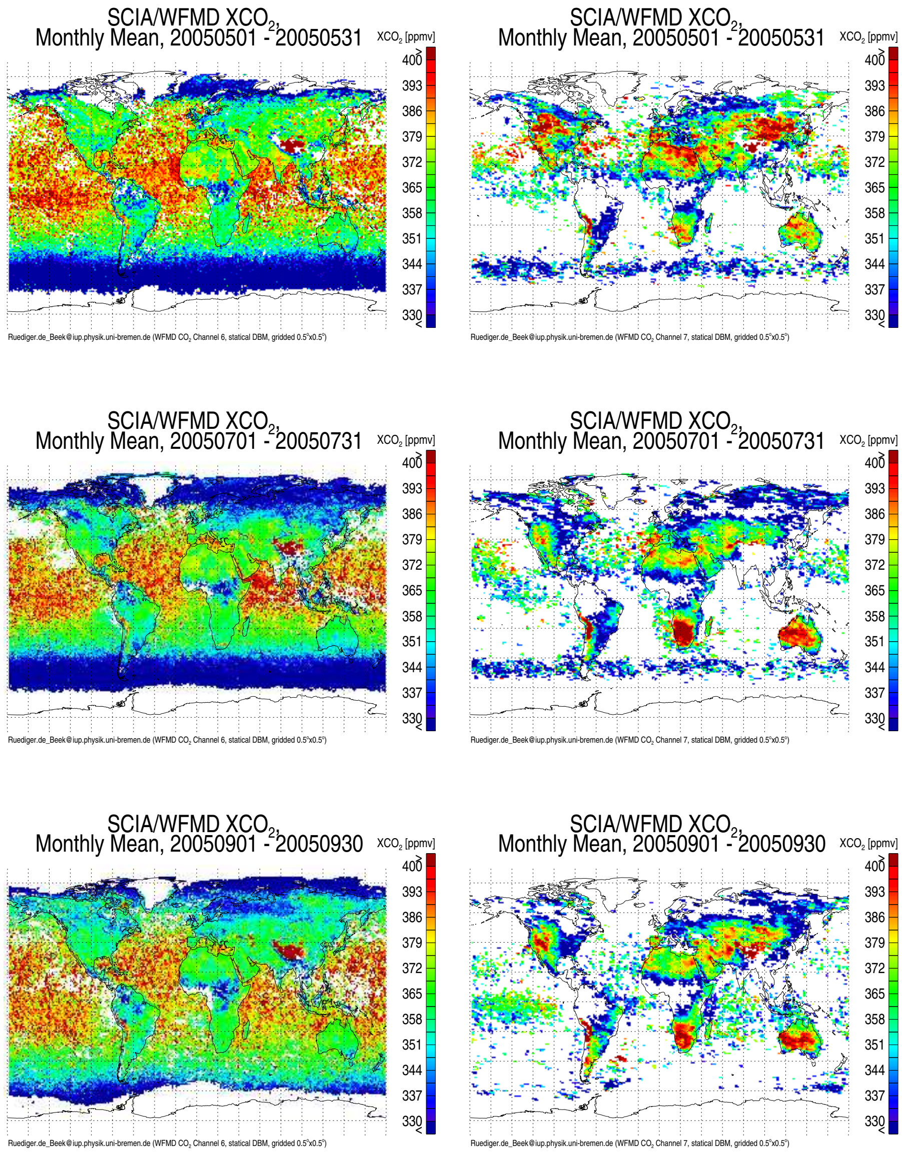

Figure 57: XCO_2 as in Figure 56, determined from SCIAMACHY Channel 6 (left, 1558-1594 nm) and Channel 7 (right, 2021-2040) using Level-1b Version5.04, statical DBM, no patching, no scaling! For Channel 6, parameters have been otherwise set similar as for WFM-DOAS 2003 Version0.4 (see text). Only cloud-free pixels are shown.

Otherwise, only cloud-free pixels are shown.

On the right panel of Figure 57 the results of channel 7 XCO_2 retrievals are shown. As can be seen there are similarities but also large differences in the patterns. Regions of strongly enhanced XCO_2 occur for channel 7 retrievals (2005). For version 0.4 this was mainly refered to high albedo and/or aerosol concentrations which would explain there occurence mainly over desert regions. Strongly elevated XCO_2 for channel 7 retrievals also occur over desert regions but at different locations (Northern Sahara and Arabic peninsula in May, South Africa, and Australia in July and September). The effect of aerosol loading on channel 7 retrieval together with aerosol index maps (TOMS) for the corresponding time ranges have to be considered in detail to allow further statements about channel 7 results in 2005. Elevated XCO_2 occurs also at locations in higher northern latitudes for channel 7 retrievals.

Low values occur in the tropics and over far-east regions, which are masked out in the maps from channel 7 retrievals. It is important to note that for channel 7 retrievals large gaps occur at least due to cloud filtering as the propability for cloud-free pixels is much lower due to the larger ground scene extensions (lower spatial resolution).

As for version 0.4 in 2003 and for channel 6 retrievals for 2005 lower values can be seen for channel 7 retrievals over the Nothern Hemisphere in July as compared to May and September. It has to be investigated how much this can be refered to biological uptake of CO_2 during the well corresponding growing seasons and how much any light leak effect is induced, e.g. by clouds surrounding the observed ground scene.

Partly high XCO_2 shows up over high mountains for 2005 both for channel 6 and 7 retrievals, which have been filtered out for version 0.4. At least for channel 7 a different and preliminary not yet optimised set of filter criteria has been used.

Again, the results for 2005 are still preliminary, also for channel 7 retrievals, of cause! The picture of channel 7 results gives raise for several interesting issues to be studied, which would certainly help to understand the aspects of CO_2 retrievals from SCIAMACHY either from channel 6, channel 7 or a to be developed scheme of both in combination similarely as being planned for OCO.

The last Figure of this section (Figure 58) shows an example spectrum of a fit of measurements over Sudan, 17. August 2005 over a desert region (16.16°N, 29.38°, west of Khartum), which was cloud-free according to the WFM-DOAS cloud detection.

In the sun-normalized radiance (top) a strong water absorption feature can be seen around 2028.5 nm. The fitted CO_2 in the mid panel is the scaled CO_2 weighting-function, where the scaling factor is the fitparameter, i.e. the vertical column difference to the reference. The fit is shown with and without residual added. The residual, i.e. the difference between measurement and fit, is shown in the bottom panel. The corresponding CO_2 vertical column is determined as 6.99e^{21}cm^{-2} with a fit error of 8.64%. The static DBM used is much more strikt as compared to Figure 52, where the same measurement has been used.

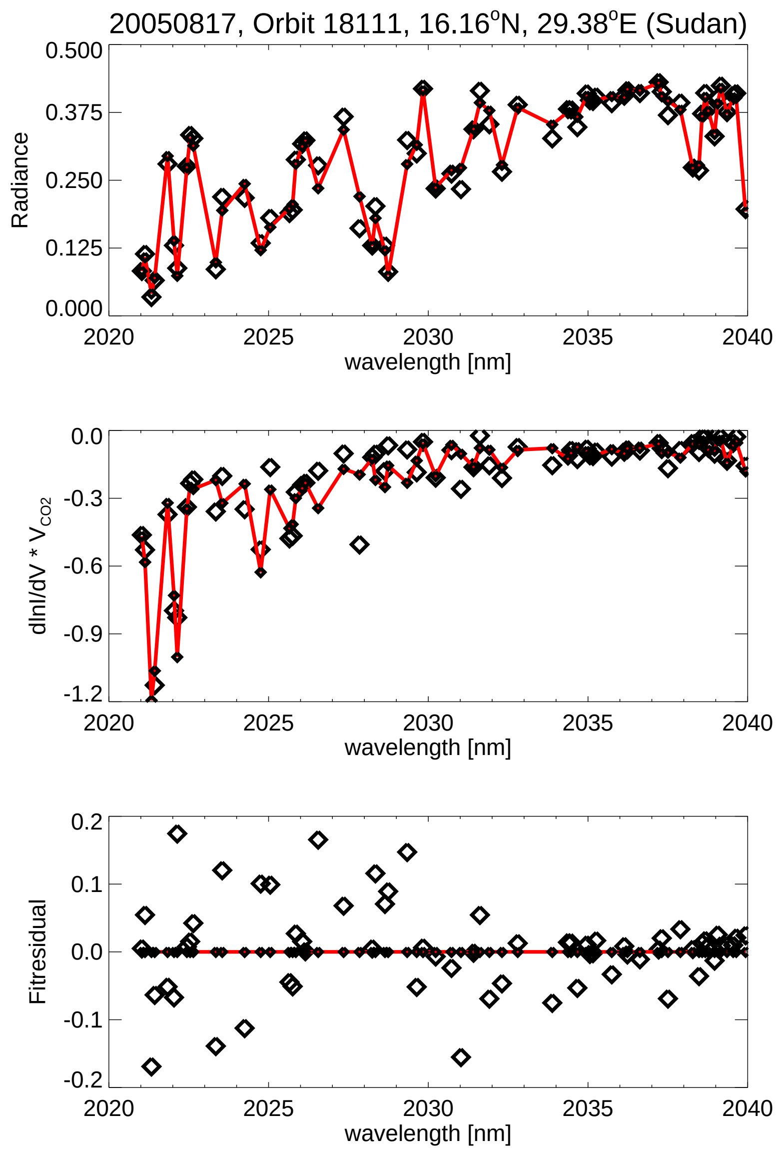

Figure 58: As an example a fit of a spectrum measured on 17. August 2005 over a desert region in Sudan (16.16°N, 29.38°, west of Khartum, cloud-free) is shown. The measurements are shown as open diamonds, the fitted model is in small diamonds and a red curve. The top panel shows the sun-normalized radiance, the middle the fitted CO_2 with and without residual added, and the bottom shows the residual. The CO_2 vertical column is determined as 6.99e^{21}cm^{-2} with a fit error of 8.64% (see also Figure 52, where the same measurement has been used).

References

de Beek, R., M. Buchwitz, S. Noël, et al., Atmospheric carbon gases retrieved from SCIAMACHY by WFM-DOAS: Improved global CO and CH_4 and initial verification of CO_2 over Park Falls (46°N, 90°W), *Atmospheric Chemistry and Physics Discussions*, **6**, 363–399, 2006.

Buchwitz, M., R. de Beek, J. P. Burrwos, et al., Atmospheric methane and carbon dioxide from SCIAMACHY satellite data: Initial comparison with chemistry and transport models, *Atmospheric Chemistry and Physics*, **5**, 941–962, 2005a.

Buchwitz, M., R. de Beek, S. Noël, et al., Carbon monoxide, methane and carbon dioxide columns retrieved from SCIAMACHY by WFM-DOAS: year 2003 initial data set, *Atmospheric Chemistry and Physics*, **5**, 3313–3329, 2005b.

Buchwitz, M. and J. Burrows, Retrieval of CH_4, CO, and CO_2 total column amounts from SCIAMACHY near–infrared nadir spectra: Retrieval algorithm and first results, in K. P. Schäfer (Editor), *Remote Sensing of Clouds and the Atmosphere VIII*, volume 5235 of *Proceedings of SPIE*, 375–388, 2004.

Buchwitz, M., V. Rozanov, and J. Burrows, A correlated-k distribution scheme for overlapping gases suitable for retrieval of atmospheric constituents from moderate resolution radiance measurements in the visible/near-infrared spectral region, *Journal of Geophysical Research*, **105**(D12), 15247–15262, 2000.

Gloudemans, A. M. S., H. Schrijver, Q. Kleipool, et al., The impact of SCIAMACHY near-infrared instrument calibration on CH_4 and CO total columns, *Atmospheric Chemistry and Physics*, **5**, 2369–2383, 2005.

Houweling, S., F.-M. Breon, I. Aben, et al., Inverse modeling of CO_2 sources and sinks using satellite data: A synthetic inter-comparison of measurement techniques and their performance as a function of space and time, *Atmospheric Chemistry and Physics*, **4**, 523–538, 2004.

Houweling, S., W. Hartmann, I. Aben, et al., Evidence of systematic errors in SCIAMACHY-observed CO_2 due to aerosols, *Atmospheric Chemistry and Physics Discussions*, **5**, 3313–3340, 2005.

Kleipool, Q., *SCIAMACHY: Recalculation of OPTEC5 Non-Linearity, SRON-SCIA-PhE-RP-013*, Technical report, SRON, 2003.

Kleipool, Q., *SCIAMACHY: Evolution of Dead and Bad Pixel Mask, SRON-SCIA-PhE-RP-021*, Technical report, SRON, 2004.

Lichtenberg, G., *Calibration status December '03, SRON-SCIA-PhE-RP-019*, Technical report, SRON, 2003.

Lichtenberg, G., *Some results on ice and the IR transmission in SCIA, SRON*, Technical report, SRON, 2003b.

Lichtenberg, G., Q. Kleipool, J. M. Krijger, et al., SCIAMACHY Level1 data: Calibration concept and in-flight calibration, *Atmospheric Chemistry and Physics Discussions*, **5**, 8925–8977, 2005.

Rayner, P. J. and D. M. O'Brian, The utility of remotely sensed CO_2 concentration data in surface inverions, *Geophysical Research Letters*, **28**, 175–178, 2001.

Skupin, J., *Possiblity of light leak in channel 7 of SCIAMACHY, Issue 1, 30-April-2003, IUP-SCIA-JS-20030403-LightLeakCh7*, Technical report, IUP, 2003.